TU Delft

Delft University of Technology

Document Version
Final published version

Citation (APA)
Vernaillen, T. (2026). *The Link Between the Rail Wear Rate and Rolling Contact Fatigue: From Bog Data Analysis to Lab Research*. [Dissertation (TU Delft), Delft University of Technology]. https://doi.org/10.4233/uuid:cef8b13c-1a5f-4dbf-8706-a0486013392b

Important note
To cite this publication, please use the final published version (if applicable).
Please check the document version above.

Copyright
In case the licence states “Dutch Copyright Act (Article 25fa)”, this publication was made available Green Open Access via the TU Delft Institutional Repository pursuant to Dutch Copyright Act (Article 25fa, the Taverne amendment). This provision does not affect copyright ownership.
Unless copyright is transferred by contract or statute, it remains with the copyright holder.

Sharing and reuse
Other than for strictly personal use, it is not permitted to download, forward or distribute the text or part of it, without the consent of the author(s) and/or copyright holder(s), unless the work is under an open content license such as Creative Commons.

Takedown policy
Please contact us and provide details if you believe this document breaches copyrights.
We will remove access to the work immediately and investigate your claim.

*This work is downloaded from Delft University of Technology.*

# The link between the rail wear rate and rolling contact fatigue

## From Big Data Analysis to Lab Research

Tim Vernaillen

# THE LINK BETWEEN THE RAIL WEAR RATE AND ROLLING CONTACT FATIGUE

FROM BIG DATA ANALYSIS TO LAB RESEARCH

# THE LINK BETWEEN THE RAIL WEAR RATE AND ROLLING CONTACT FATIGUE

FROM BIG DATA ANALYSIS TO LAB RESEARCH

## Dissertation

for the purpose of obtaining the degree of doctor
at Delft University of Technology
by the authority of the Rector Magnificus Prof. dr. ir. H. Bijl
Chair of the Board for Doctorates
to be defended publicly on
Wednesday 29 April 2026 at 10:00 o'clock

by


**Tim VERNAILLEN**

Master of Science in Civil Engineering
Master of Science in Management
Master of Science in Industrial Engineering

Vrije Universiteit Brussel VUB
Born in Aalst, Belgium

This dissertation has been approved by the promotors.

Composition of the doctoral committee:

| | |
|---|---|
| Rector Magnificus | chairperson |
| Prof. dr. ir. R.P.B.J. Dollevoet | Delft University of Technology, promotor |
| Prof. dr. Z. Li | Delft University of Technology, promotor |
| Assoc.Prof. Dr. A.A. Núñez Vicencio | Delft University of Technology, promotor |

*Independent members:*

| | |
|---|---|
| Prof. dr. M. Veljkovic | Delft University of Technology |
| Prof. dr. H. Li | University of Wollongong Australia |
| Prof. dr. D.J. Fletcher | Sheffield University |
| Dr. ir. B. Schotsman | Prorail |

This dissertation was financially supported by:

TU Delft Delft University of Technology

INFRABEL Right On Track

*Printed by:*

*Cover by:*

Copyright © 2026 by Tim Vernaillen

ISBN 978-94-6518-288-9
An electronic version of this dissertation is available at
http://repository.tudelft.nl/.

# CONTENTS

**Contents** vi

**Summary** ix

**Samenvatting** xiv

**Abbreviations** xix

**1. Introduction** 1
1.1. Balancing Wear and Rolling Contact Fatigue 2
1.2. Rail Asset Management in the Belgian Context: The Case of Infrabel 3
1.3. Rail Grinding as a Strategic Maintenance Tool 5
1.4. Research Goals and Future Directions 8
1.5. Research Questions 9
1.6. Dissertation Outline 11
References 13

**2. Rail wear rate on the Belgian railway network – a big-data analysis** 14
2.1. Introduction 15
2.2. Rail wear measurement 16
2.2.1. Description of the Belgian network and parameters to be analyzed 16
2.2.2. Definition of vertical wear and 45° Wear 18
2.2.3. Traffic Load 18
2.2.4. Description of the wear data 19
2.3. Data Analysis and discussions 23
2.3.1. Vertical wear versus tonnage of R260 rails from measurements in 2012 23
2.3.2. 45° wear versus tonnage of rails with R260 in 2012 25
2.3.3. Wear versus tonnage for R200 and R260 in 2012 27
2.3.4. Influence of preventive grinding 30
2.3.5. Vertical wear per year 33
2.4. Conclusions 35
References 37

**3. Statistical analysis and treatment method of head checks on the Belgian railway network** 39
3.1. Introduction 40
3.2. Field monitoring methods of HCs 41
3.2.1. Development phases and detection methods of HCs 42
3.2.2. HCs in the Belgian railway network 43
3.2.3. Assessment methods of HCs 46
3.3. Results and discussions of HC growth rates 48
3.3.1. HC growth rate versus track radius 48

3.3.2. HC growth versus annual train load and UIC class 50
3.3.3. HC growth per year 52
3.3.4. The relationship between HC growth and rail wear rate 53
3.4. Estimation of MWR for HC treatment 56
3.4.1. Evaluation of the effectiveness of the current grinding policy 56
3.4.2. MWR for HC treatment in Belgium 58
3.5. Conclusions 59
References 61

**4. grinding – good or bad for reduction of rolling contact fatigue–observations from in-service rails with white etching layer 65**
4.1. Introduction 66
4.2. Methodology 68
4.2.1. Rail samples on the Belgian railway network 68
4.2.2. Rail sample on the Swedish railway network 71
4.3. Results of Belgian rail samples 72
4.3.1. Sample R1-R260 with one grinding cycle on Line 130B 72
4.3.2. Sample R2-R260 without grinding on Line 130B 73
4.3.3. Sample R3-R350HT without grinding on Line 130B 74
4.3.4. Sample R4-R350HT with one grinding cycle on Line 130B 76
4.3.5. Sample R5-R350HT with one grinding cycle on Line 40 76
4.3.6. Sample R6-R350HT with two grinding cycles on Line 40 78
4.3.7. Summary of Samples R1-R6 79
4.4. Results of the Swedish rail sample 80
4.4.1. Microstructural features within the wheel-rail contact zone 80
4.4.2. Microstructural features of the non-contact zone 83
4.5. Discussions 84
4.6. Conclusions 87
References 89

**5. Conclusions and recommendations 95**
5.1. Conclusions 96
5.2. Synthesis of Principal Findings 99
5.2.1. Rail Wear and Influencing Factors (Chapter 2) 99
5.2.2. Head check growth and grinding strategy (Chapter 3) 100
5.2.3. Microstructural analysis of rail surfaces (Chapter 4) 101
5.3. Practical Recommendations 102
5.3.1. Maintenance Planning and Grinding Optimization 102
5.3.2. Asset Management and Procurement 102
5.3.3. Data and Technology Integration 103
5.4. Implications for Infrabel and European Rail Networks 103
5.4.1. Future Research Directions 104
5.5. Final Reflections 105

**Acknowledgments 108**

**Curriculum vitae** 111

**List of publications** 112

# SUMMARY

Railway infrastructure is a cornerstone of sustainable transportation, providing an energy-efficient and low-carbon alternative to road and air travel. At the heart of this system lies the rail, a high-value asset whose operational reliability and longevity are fundamental to safe and efficient train operations. Yet rails are subject to inevitable degradation, primarily wear and rolling contact fatigue (RCF). These degradation mechanisms are interdependent and often competitive: while moderate wear can delay or even suppress fatigue crack initiation, excessive wear undermines rail strength and shortens service life. Conversely, insufficient wear promotes RCF, particularly under modern high-traction rolling stock. This dissertation analyses the wear and RCF on the Belgium railway network, considering key factors including curve radius, annual traffic tonnage, steel grades and rail grinding, and explores how preventive maintenance strategies, most notably grinding, can be optimized by maintaining a dynamic balance between wear and RCF so as to extend rail life, reduce life-cycle costs, and sustain safe railway operations.

The thesis is situated within the Belgian railway context, where Infrabel, the national infrastructure manager, maintains approximately 6,400 km of track under high operational and financial constraints. Despite the introduction of higher-grade steels and the implementation of systematic grinding policies since 2012, the persistence of RCF, coupled with the capital-intensive nature of rail renewals, continues to challenge the infrastructure manager. The central research question guiding this thesis is therefore:

*How can the relationship between rail wear rate and rolling contact fatigue (RCF) be quantified and understood through big-data analysis of an entire national rail network, complemented by laboratory investigations on rail materials?*

To address this question, the dissertation integrates macro-scale big-data analytics with microstructural laboratory studies, supported by Infrabel's extensive monitoring infrastructure. The research is structured around three sub-questions, each targeting a specific dimension of the wear–RCF relationship: (i) the quantification of the rail wear rate

as a function of key operation parameters, (ii) the analysis of head check growth and its optimal treatment through the concept of a "Magic Wear Rate," and (iii) the role of White Etching Layers (WELs) after grinding.

The first part of the thesis develops a statistically validated big-data model for rail wear, drawing on measurement data across 5,000 km of the Belgian network. The analysis demonstrates that wear progression is strongly dependent on key factors like curve radius, steel grade, and traffic intensity, with R200 rails exhibiting 34% higher wear than R260 under comparable loads. Importantly, the results challenge traditional reliance on cumulative tonnage as a predictor of wear, showing that annual traffic and environmental exposure (particularly corrosion on low-traffic lines) exert greater influence. This model provides infrastructure managers with a predictive framework for planning rail renewals and optimizing grinding intervals based on local operating conditions, rather than relying on generic thresholds.

The second research component focuses on head check (HC) development as a manifestation of RCF. Statistical analysis of 212 curved track segments revealed that HC growth peaks in curves with radii of 750–1000 m and is counterintuitively faster in mm/100 million gross ton (MGT) under lower annual loads. This finding highlights the important role of time-dependent mechanisms in defect propagation, including corrosion processes and fluid-assisted crack growth driven by the pressurization of entrapped liquids under passing wheels. Moreover, the thesis confirms the competitive relationship between wear and RCF: in tight curves, high wear suppresses HC initiation, while in moderate curves with insufficient wear, RCF dominates. From these insights, the dissertation discusses the Magic Wear Rate (MWR), the optimal rate of artificial material removal through grinding that minimizes RCF without excessive rail consumption. By quantifying MWR values for different UIC traffic classes, the thesis demonstrates the inadequacy of uniform grinding schedules and provides an operationally relevant framework for targeted preventive maintenance.

The third component investigates the long-term effects (a minimum of 6 months in service after grinding) of rail grinding on material degradation by analysing seven in-service rail samples with different grinding histories, steel grades, and load conditions. Results show

that grinding does not introduce additional surface defects and that preventive grinding significantly reduces macrocrack formation by removing accumulated plastic deformation. Ratcheting is identified as the dominant crack-initiation mechanism and rails subjected to more grinding cycles display lower long-term surface hardness and smoother surfaces. Post-grinding load, rather than total accumulated load, is the key factor governing RCF development, and R260 steel exhibits better RCF resistance than R350HT under the examined conditions. The findings highlight the beneficial role of grinding in mitigating RCF, though larger datasets are needed to further validate these conclusions. Together, these findings provide a comprehensive, multi-scale understanding of the wear/RCF interplay. At the network scale, wear and fatigue were shown to be conditioned by geometry, traffic regime, and material properties, with environmental degradation emerging as a key driver on lightly loaded lines. At the microstructural scale, the presence of WELs underscores the need to integrate material science insights into maintenance planning. The dissertation's central contribution is in bringing the well-known concept of Magic Wear Rate into practice, for infrastructure managers, bridging the gap between empirical observation and actionable policy.

From a practical perspective, the research supports several recommendations. First, maintenance planning should adopt variable grinding intervals based on annual tonnage, curvature, and rail grade, rather than fixed thresholds based on cumulative tonnage. Second, asset procurement strategies should prioritize the use of R260, apply higher-grade steels only in the most heavily loaded track sections and curves, and progressively phase out older grades such as R200. Third, the integration of data and technology should be strengthened through predictive models for wear and RCF, developed based on extensive measurement systems and a systematic linkage of monitoring data.

The implications extend beyond Belgium. European infrastructure managers, facing similar challenges of growing traffic and constrained budgets, can benefit from the methodological framework developed in this thesis. By quantifying the competitive dynamics of wear and RCF and incorporating these insights into condition-based maintenance, the findings directly contribute to EU safety directives, UIC guidelines, and broader sustainability objectives. Furthermore, the thesis underscores the potential of academic–industry

collaboration, as exemplified by the Infrabel-TU Delft partnership, to generate actionable knowledge for infrastructure management.

Finally, the dissertation highlights several avenues for future research, including the need to investigate the origins and effects of Brown Etching Layers (BELs), quantify the contribution of corrosion under field conditions, and develop multiscale numerical models that couple contact mechanics with microstructural evolution. Integrating digital twin frameworks with full life-cycle environmental assessments enables a more sustainable and resilient approach to rail asset management by minimizing total $CO_2$ emissions, optimizing maintenance activities such as grinding and milling, and supporting data-driven decisions on when to repair or replace individual defects.

In conclusion, this thesis demonstrates that the effective management of rail wear and RCF requires an interdisciplinary, data-driven approach that links big-data analytics, microstructural science, and operational strategy. By articulating the concept of the Magic Wear Rate and validating it through both network-scale, field measurements and material analyses, the research provides infrastructure managers with a robust framework for extending rail life, reducing costs, and sustaining the safety and reliability of modern railway systems.

# SAMENVATTING

0

Spoorinfrastructuur vormt een essentiële pijler van duurzaam vervoer en biedt een energie-efficiënt en koolstofarm alternatief voor weg- en luchtverkeer. Centraal binnen dit systeem staat de spoorstaaf, een hoogwaardig kapitaalgoed waarvan de betrouwbaarheid en levensduur cruciaal zijn voor veilige en efficiënte treinoperaties. Spoorstaven zijn echter onvermijdelijk onderhevig aan degradatie, voornamelijk door slijtage en rolling contact fatigue (RCF). Deze degradatiemechanismen zijn onderling afhankelijk en vaak competitief: terwijl een matige slijtage de initiatie van vermoeiingsscheuren kan vertragen of zelfs onderdrukken, leidt overmatige slijtage tot een verminderde spoorsterkte en een verkorte levensduur. Omgekeerd bevordert onvoldoende slijtage de ontwikkeling van RCF, in het bijzonder onder modern rollend materieel met hoge tractiekrachten. Dit proefschrift analyseert slijtage en RCF op het Belgische spoornet, rekening houdend met factoren zoals boogstraal, jaarlijkse verkeersbelasting, staalsoort en slijpstrategieën, en onderzoekt hoe preventief onderhoud, met name slijpen, kan worden geoptimaliseerd door een dynamisch evenwicht tussen slijtage en RCF te handhaven.

Het onderzoek is gesitueerd binnen de Belgische spoorcontext, waar Infrabel, de nationale infrastructuurbeheerder, circa 6.400 km spoor onderhoudt onder aanzienlijke operationele en financiële druk. Ondanks de invoering van hoogwaardigere staalsoorten en de systematische toepassing van slijpstrategieën sinds 2012, blijft RCF een belangrijke oorzaak van spoorvernieuwing, mede door de kapitaalintensieve aard van railvervangingen. De centrale onderzoeksvraag van dit proefschrift luidt daarom:

*Hoe kan de relatie tussen slijtagegraad en rolling contact fatigue (RCF) van spoorstaven worden gekwantificeerd en begrepen via big-data-analyse van een volledig nationaal spoornetwerk, aangevuld met laboratoriumonderzoek op spoormaterialen?*

Om deze vraag te beantwoorden combineert het proefschrift grootschalige big-data-analyse met microstructureel laboratoriumonderzoek, ondersteund door de uitgebreide meetinfrastructuur van Infrabel. Het onderzoek is opgebouwd rond drie deelvragen, elk gericht op een specifieke dimensie van de slijtage–RCF-relatie: (i) de kwantificering van

de slijtagegraad als functie van operationele parameters, (ii) de analyse van head check-groei en de optimalisatie ervan via het concept van de *Magic Wear Rate*, en (iii) de rol van White Etching Layers (WELs) in relatie tot slijpen.

Het eerste deel ontwikkelt een statistisch gevalideerd big-data-model voor spoorstaafslijtage, gebaseerd op meetgegevens over 5.000 km van het Belgische netwerk. De resultaten tonen aan dat slijtage sterk wordt beïnvloed door boogstraal, staalsoort en verkeersintensiteit, waarbij R200-spoorstaven ongeveer 34% sneller slijten dan R260 onder vergelijkbare belasting. De studie stelt bovendien het klassieke gebruik van gecumuleerd tonnage als primaire voorspeller van slijtage in vraag: jaarlijkse verkeersbelasting en omgevingsinvloeden, met name corrosie op weinig bereden lijnen, blijken doorslaggevender. Het ontwikkelde model biedt infrastructuurbeheerders een voorspellend kader om spoorvernieuwingen en slijpintervallen af te stemmen op lokale bedrijfsomstandigheden in plaats van generieke drempelwaarden.

Het tweede onderzoeksdeel richt zich op de ontwikkeling van head checks als uiting van RCF. Statistische analyse van 212 bochten toont aan dat de HC-groei maximaal is in bochten met een straal tussen 750 en 1000 m en, tegen de intuïtie in, sneller verloopt (uitgedrukt in mm per 100 MGT) bij lagere jaarlijkse verkeersbelasting. Dit onderstreept het belang van tijdsafhankelijke mechanismen in defectgroei, waaronder corrosie en vloeistof geassisteerde scheurgroei door drukopbouw van ingesloten vloeistoffen onder passerende wielen. De resultaten bevestigen bovendien de competitieve relatie tussen slijtage en RCF: in scherpe bogen onderdrukt hoge slijtage de initiatie van head checks, terwijl in middelgrote bogen met onvoldoende slijtage RCF domineert. Vanuit deze inzichten wordt het concept van de *Magic Wear Rate* (MWR) besproken: de optimale snelheid van kunstmatige materiaalafname via slijpen die RCF minimaliseert zonder overmatige railconsumptie. Door MWR-waarden te kwantificeren voor verschillende UIC-verkeersklassen toont het onderzoek aan dat uniforme slijpschema's onvoldoende zijn en biedt het een praktisch toepasbaar kader voor doelgericht preventief onderhoud.

Het derde deel onderzoekt de langetermijneffecten van slijpen op spoorstaafdegradatie via laboratoriumanalyse van zeven in dienst zijnde spoorstaven met verschillende slijphistorieken, staalsoorten en belastingen (minstens zes maanden na slijpen). De

resultaten tonen aan dat slijpen geen bijkomende oppervlaktedefecten introduceert en dat preventief slijpen de vorming van macroscheuren significant vermindert door opgebouwde plastische vervorming te verwijderen. Ratcheting wordt geïdentificeerd als het dominante initiatiemechanisme voor scheurvorming. Spoorstaven die vaker werden geslepen vertonen op lange termijn een lagere oppervlakhardheid en gladdere loopvlakken. Niet de totale gecumuleerde belasting, maar de belasting na het laatste slijpmoment blijkt bepalend voor RCF-ontwikkeling. Daarnaast vertoont R260 staal onder de onderzochte omstandigheden een betere RCF-weerstand dan R350HT. Hoewel grotere datasets nodig zijn voor verdere validatie, bevestigen de resultaten de gunstige rol van slijpen in het beheersen van RCF.

Gezamenlijk bieden deze bevindingen een geïntegreerd, multischalig inzicht in de interactie tussen slijtage en RCF. Op netwerkniveau worden slijtage en vermoeiing bepaald door geometrie, verkeersregime en materiaaleigenschappen, met omgevingsdegradatie als belangrijke factor op licht belaste lijnen. Op microstructureel niveau benadrukt de aanwezigheid van WELs de noodzaak om materiaalwetenschappelijke inzichten expliciet te integreren in onderhoudsstrategieën. De centrale bijdrage van dit proefschrift ligt in het operationeel toepasbaar maken van het bekende concept *Magic Wear Rate*, waarmee de kloof wordt overbrugd tussen empirische observaties en praktisch onderhoudsbeleid.

Vanuit praktisch oogpunt leidt het onderzoek tot meerdere aanbevelingen. Onderhoudsplanning zou variabele slijpintervallen moeten hanteren op basis van jaarlijkse tonnage, boogstraal en staalsoort, in plaats van vaste drempels op basis van gecumuleerd tonnage. Bij spoorstaafaankoop verdient R260 prioriteit, terwijl hardere staalsoorten selectief worden toegepast in zwaar belaste secties en oudere kwaliteiten zoals R200 geleidelijk worden uitgefaseerd. Daarnaast is een verdere integratie van data en technologie noodzakelijk via voorspellende modellen voor slijtage en RCF, gebaseerd op uitgebreide meetsystemen en een systematische koppeling van monitoringdata.

De relevantie van dit onderzoek reikt verder dan België. Europese infrastructuurbeheerders, geconfronteerd met toenemend verkeer en beperkte budgetten, kunnen profiteren van het methodologische kader dat in dit proefschrift is ontwikkeld. Door de competitieve dynamiek tussen slijtage en RCF te kwantificeren en deze inzichten te integreren in conditiegebaseerd onderhoud, draagt het onderzoek bij aan EU-veiligheidsrichtlijnen, UIC-

aanbevelingen en bredere duurzaamheidsdoelstellingen. Bovendien onderstreept de studie het belang van samenwerking tussen academie en industrie, zoals geïllustreerd door het partnerschap tussen Infrabel en TU Delft.

Tot slot identificeert het proefschrift verschillende pistes voor toekomstig onderzoek, waaronder de oorsprong en impact van Brown Etching Layers (BELs), de kwantificering van corrosie onder praktijkomstandigheden en de ontwikkeling van multischalige numerieke modellen die contactmechanica koppelen aan microstructurele evolutie. De integratie van digital twins met levenscyclusanalyses biedt hierbij een veelbelovende weg naar duurzaam en veerkrachtig assetmanagement.

Dit proefschrift toont aan dat effectief beheer van slijtage en RCF een interdisciplinaire, datagedreven aanpak vereist die big-data-analyse, microstructurele wetenschap en operationele strategie met elkaar verbindt. Door het concept van de *Magic Wear Rate* te concretiseren en te valideren via zowel netwerkanalyses als laboratoriumonderzoek, biedt dit werk infrastructuurbeheerders een robuust kader om de levensduur van spoorstaven te verlengen, kosten te verlagen en de veiligheid en betrouwbaarheid van moderne spoorwegsystemen te waarborgen.

# ABBREVIATIONS



| | |
|---|---|
| **AL** | Annual Load |
| **BEL** | Brown Etching Layer |
| **C** | Carbon |
| **CEN** | Comité Européen de Normalisation |
| **ECT** | Eddy Current Testing |
| **EM130** | Infrabel Measuring Train ($v_{max}$ = 130km/h) |
| **EN** | European Norm |
| **HC** | Head check |
| **MGT** | Million Gross Tons |
| **Mn** | Manganese |
| **MPa** | Megapascal |
| **MWR** | Magic Wear Rate |
| **NV** | Naamloze Vennootschap |
| **R200/260/350HT** | Rail steel grades (EN13674-1) |
| **RCF** | Rolling Contact Fatigue |
| **RM** | Tensile Strength |
| **Si** | Silicium |
| **TL** | Traffic Load |
| **UIC** | Union Internationale des Chemins de fer |
| **UIC60E1/50E2** | Rail profile designation (EN13674-1) |
| **UT** | Ultrasonic Testing |
| **WEL** | White Etching Layer |

0

# 1

# INTRODUCTION

# 1. INTRODUCTION

## 1.1. BALANCING WEAR AND ROLLING CONTACT FATIGUE

Railway infrastructure plays a pivotal role in sustainable transportation, offering a reliable and energy-efficient alternative to road and air travel. With low $CO_2$ emissions, rail transport is a key component in global efforts to combat climate change [1-3]. This thesis focuses on the rail asset, a crucial element of the infrastructure that ensures safe and efficient train operations. However, maintaining the safety and reliability of rails remains a challenge due to their inevitable degradation over time. Rails are subjected to various stressors, including dynamic loads, environmental conditions, and the cumulative impact of repeated train passages, all of which contribute to wear and the formation of surface and subsurface defects. According to the International Union of Railways (UIC), railway infrastructure asset management is a structured framework designed to optimize asset performance, reduce risks, and control expenditures, thereby supporting business objectives while minimizing life cycle costs [4].

One of the most pressing issues in rail maintenance is managing rolling contact fatigue (RCF), a phenomenon characterized by the initiation and propagation of cracks due to the cyclic loading of rail surfaces. Left unchecked, RCF can lead to rail fractures, posing significant safety risks and increasing operational costs. Simultaneously, rail wear—the gradual loss of material from the rail surface—further complicates maintenance efforts. While some degree of wear can mitigate RCF by removing surface defects, excessive wear compromises the rail's structural strength and reduces its service life. Balancing these competing factors is a core challenge in rail maintenance [5][7][8][9][10][11]. This thesis addresses the complex interplay between wear, rolling contact fatigue (RCF), and preventive grinding in modern railway networks, integrating insights from three extensive studies conducted across the Belgian and Swedish rail systems. Together, these works examine long-term rail degradation mechanisms, quantify wear and head-check development across thousands of kilometres of track, and analyse the microstructural consequences of grinding under real operating conditions. Although wear, RCF, and grinding are traditionally studied as separate disciplinary domains (each with its own models, test methods, and monitoring strategies), this integrated analysis demonstrates that

they are deeply interdependent phenomena governed by shared mechanical, microstructural, and operational drivers.

To address these issues, rail grinding has emerged as a critical maintenance strategy. By reshaping the rail profile and removing surface imperfections, grinding not only extends the service life of rails but also enhances the interaction between wheels and rails, improving overall track performance. Modern grinding trains are equipped with advanced technologies that enable precise material removal, making them indispensable tools for managing wear and RCF. However, the effectiveness of grinding depends on a deep understanding of the complex interplay between rail wear, RCF, and other influencing factors such as axle loads, traffic volume, and environmental conditions [12].

This thesis focuses on providing new insights into rail maintenance strategies that utilise grinding technology to manage wear and RCF effectively. By analysing the mechanisms of rail degradation and leveraging data-driven approaches, this research aims to provide insights into the conditions under which grinding can best mitigate RCF while maintaining acceptable wear levels. Additionally, the thesis examines the long-term effects of grinding on rail durability and performance, providing recommendations for sustainable maintenance practices that ensure safety, reliability, and cost-effectiveness in railway operations.

Through a combination of field data analysis, laboratory investigations, and predictive modelling, this research contributes to the advancement of rail maintenance methodologies. By addressing the dual challenges of wear and RCF, this work supports the development of a more robust and sustainable railway infrastructure, aligning with the broader goals of sustainable transportation.

## 1.2. Rail Asset Management in the Belgian Context: The Case of Infrabel

Infrabel NV, Belgium's railway infrastructure manager, plays a central role in ensuring the safety, performance, and longevity of the national rail network. Since its establishment as an autonomous public company in 2005, following the EU's railway liberalisation, Infrabel has assumed responsibility for the maintenance, modernisation, and strategic development

of approximately 6,400 kilometres of main tracks. Headquartered in Brussels and operating similarly to its Dutch counterpart ProRail, Infrabel oversees a critical component of the nation's transport infrastructure.

The rail asset lies at the heart of Infrabel's operations, with an average lifespan of 43 years. However, this figure illustrates the complexity of rail longevity, which is influenced by an interplay of technical specifications, traffic intensity, environmental exposure, and operational dynamics. Sustaining safety and managing costs within such a demanding environment requires a nuanced and data-driven approach to rail monitoring and maintenance.

To this end, Infrabel employs a multi-layered inspection regime. Measurement trains equipped with visual, ultrasonic, and eddy current technologies systematically assess rail health across the network (9,000 km of track annually). Complementary manual inspections (performed annually at 1,000 km) and laser-based profile measurements (performed annually at 14,000 km) provide further insight into rail condition. These inspection strategies inform maintenance decisions that balance preventive grinding and milling with reactive interventions, such as replacing short rail segments affected by critical defects.

A key challenge in rail management has emerged with the growing prevalence of Rolling Contact Fatigue (RCF). This defect type, linked to cyclic mechanical stresses and intensified by the performance characteristics of modern rolling stock, has reshaped maintenance priorities over the past two decades. Despite the introduction of new steel grades intended to address fatigue, RCF has proven persistent, prompting the adoption of an updated maintenance strategy in 2012 [10]. This approach draws on internal operational experience, international standards, and collaboration with European infrastructure managers.

Understanding the fatigue behaviour of rails requires attention to both their historical composition and the evolving mechanical demands placed upon them. Older rails, particularly those manufactured before 1982, exhibit vulnerability due to internal impurities, while new-generation trains amplify surface stresses that accelerate wear and fatigue. In response, Infrabel applies a structured strategy built on three pillars: systematic

inspection, preventive maintenance through grinding (3,500 km annually) and milling (50 km annually), and corrective interventions when critical defects arise.

Investment in rail renewal remains a cornerstone of long-term asset management. Lifespan expectations vary significantly across the network, influenced by track usage categories defined by UIC classification. While lightly used lines may retain rails for several decades, high-load corridors require more frequent renewal cycles. Financial planning reflects these priorities, with approximately €55 million annually invested in renewing 200 kilometres of track and approximately €5 million in rail maintenance, such as grinding and milling. This commitment has helped reduce rail fracture incidents from nearly 200 per year in the early 2000s to fewer than 15 in recent years.

However, the economic sustainability of this model hinges on optimising the timing and scope of renewals. Rails represent one of the most capital-intensive components of the network. With replacement costs nearing €275,000 per kilometre (Average cost per kilometre in 2024 to replace 1 km of double rail - materials and labour cost), premature renewals, often triggered by RCF, can significantly impact long-term budgets. Although higher-performance steel grades were introduced to extend lifespan, the increasing wear rate associated with high-traction rolling stock continues to challenge these assumptions.

A central aim of this research is to clarify the relationship between rail wear, material properties, and the development of RCF defects. By enhancing our understanding of how these factors interact under various operational conditions, this thesis aims to support more strategic decisions regarding material selection, maintenance planning, and investment timing. Given the long-term implications of rail infrastructure choices, such insights are essential for ensuring that today's decisions support a sustainable and resilient railway system for decades to come [7].

## 1.3. RAIL GRINDING AS A STRATEGIC MAINTENANCE TOOL

Rail grinding plays a central role in the preservation and performance of railway infrastructure. As rails represent both a high-value and long-lifespan asset, effective maintenance strategies are critical for ensuring their safe operation and maximising their economic life. Among available techniques, grinding offers a unique advantage: it enables

defect management and profile correction without necessitating partial or complete rail replacement.

At its core, grinding involves the controlled removal of a thin layer of metal from the rail head using high-speed rotating stones, typically at 3,600 rpm. These abrasive stones, driven by electric motors, remove surface material to restore the intended rail profile and eliminate emerging defects. What began in the 1930s as a basic solution to surface defects and corrugation has since evolved into a precise and automated process, adapting to modern demands in speed, load, and infrastructure performance [6].

The evolution of rail grinding technology reflects the growing complexity and demands of modern railway systems. Initial grinding trains, introduced in the late 1930s, were relatively rudimentary and deployed primarily on freight and metro lines. Their primary objective was to eliminate surface defects and delay the need for costly rail replacements. However, as rail operations intensified and train speeds increased, especially from the 1980s onward, grinding transitioned from a reactive measure to a standard, periodic maintenance practice aimed at both preserving optimal rail profiles and removing defects. Grinding technology also began to incorporate features such as automatic adjustment of stone angles, enabling more consistent and efficient material removal. Today, grinding trains are highly automated and engineered to deliver precise rail profile corrections within tight tolerances, enhancing both safety and the long-term performance of the track. A wide range of grinding equipment is available, with configurations varying from compact units equipped with eight motors to large-scale trains featuring up to 120 grinding motors, each typically providing 22 kW of power [7].

In modern railway operations, maintaining the geometric and structural integrity of rails is crucial, not only for ensuring safety and ride quality but also for managing wear and controlling noise and vibration. Surface damage, such as squats, head checks, ballast imprinting and corrugation, compromises this integrity, often originating from dynamic loading, material fatigue, and contact stress at the wheel-rail interface. If left unaddressed, these defects propagate and threaten the overall reliability of the track system [8].

Grinding addresses these issues by restoring the rail's transverse profile and removing shallow defects before they evolve into deeper structural problems. In this context, Infrabel employs a structured grinding strategy built on three pillars: preventive, corrective, and cyclic grinding. Preventive grinding is conducted shortly after rail installation. Its purpose is to remove the decarburized surface layer formed during manufacturing, a layer known to be more brittle and crack-prone, and to refine the rail's profile, especially around welded joints. This early intervention improves the mechanical behaviour of the rail under loading and contributes to long-term durability, with minimal material removal. Corrective grinding, on the other hand, is applied in response to more pronounced issues such as profile distortion, severe corrugation, or localised surface damage. It enables Infrabel to restore the functional integrity of areas exhibiting advanced degradation, often in curves or transition zones where dynamic forces are higher. The material removal depends on the size of the defect, and in severe cases, it can exceed several millimetres. This form of grinding also helps mitigate noise, vibrations, and excessive wear on rolling stock. Cyclic grinding represents a more proactive, scheduled intervention. Introduced in Belgium in 2012, this approach is based on predefined traffic thresholds and targets rail segments with known susceptibility to rolling contact fatigue (RCF). The aim is not only to maintain rail geometry but to remove incipient cracks before they propagate systematically. The success of this strategy was clearly observed on high-speed line 1 (Brussels–Paris), where regular grinding significantly reduced RCF damage. In contrast, sections that were excluded from the grinding program exhibited extensive fatigue-related defects. To ensure the efficacy of cyclic grinding, certain baseline conditions must be met: the rail must have a correct transverse profile and be free of critical surface damage. If these conditions are not satisfied, corrective grinding or even rail replacement may be required before the track can enter a cyclic maintenance cycle.

Rail networks are increasingly challenged by rolling contact fatigue (RCF), manifesting in defects such as squats and head checks. The growing traction power of modern locomotives aggravates these issues. The concentrated forces transmitted through the small contact patch between wheel and rail, approximately 2 $cm^2$, play a critical role in the initiation and propagation of RCF. As illustrated in Figure 1(b), the otherwise uniform running band is disrupted by multiple surface defects.

(a) (b)

Figure 1.1: (a) HC on L37 - 2014 (b) Squats on L2 – 2015

Infrabel's grinding policy is thus adaptive and condition-based, aligning maintenance efforts with the operational characteristics of the track. In Belgium, grinding intervals are determined based on accumulated tonnage, typically set at 60 million tons for mainline track classes and 25 million tons for curves with a history of head checking. This study shows that a strategy based on fixed cumulative tonnage–based grinding periodicities is not successful in all situations. Other EU railway infrastructure managers that implement cyclic grinding use similar, though not always identical, intervals. Through a combination of inspection data, the current rail profile, and visual assessments, Infrabel determines the most appropriate grinding intervention—whether preventive, corrective, or cyclic.

Ultimately, the integration of rail grinding into a comprehensive asset management strategy enables Infrabel to extend rail service life, reduce lifecycle costs, and enhance the overall reliability of the rail network. The careful balance between defect mitigation and material preservation reflects the broader objective of ensuring long-term infrastructure sustainability in the face of evolving mechanical and environmental demands.

## 1.4. RESEARCH GOALS AND FUTURE DIRECTIONS

This thesis aims to develop an integrated framework, validated with extensive empirical data, to identify the primary factors governing rail wear behaviour and the initiation and growth of Rolling Contact Fatigue (RCF). By gaining a clearer understanding of how wheel–rail contact conditions, material properties, traffic loading, and maintenance

interventions interact, the work will support in refining predictive maintenance strategies, optimising renewal planning, and improving both cost efficiency and rail longevity. Given the central role of grinding in rail maintenance, the thesis will further investigate the White Etching Layer (WEL) formation and assess its contribution to RCF development. This will help address long-standing concerns that grinding may, under certain circumstances, induce microstructural features that accelerate fatigue damage.

Building on Infrabel's large-scale measurement infrastructure, the research seeks to derive rail-profile-specific wear laws, quantify optimal grinding intervals, and validate concepts such as the Magic Wear Rate across different traffic classes and operational environments. Future work will expand microstructural datasets and integrate them with network-scale statistical models, enabling a unified view of the competition between natural wear, plastic deformation, WEL formation, and fatigue crack propagation. The collaboration between Infrabel and TU Delft provides essential access to specialised expertise and to a unique nationwide dataset of raw and processed measurements, strengthening both partners' capacity to advance rail degradation science. Ultimately, this research aims to establish adaptive, data-driven maintenance frameworks that optimise steel grade selection, grinding parameters, and intervention schedules, thereby enhancing network safety, extending rail service life, and reducing long-term maintenance costs.

## 1.5. RESEARCH QUESTIONS

The primary objective of this thesis is to equip infrastructure managers with valuable insights to extend the lifespan of rail infrastructure and minimise life cycle costs through effective preventive maintenance strategies. The intensified and more aggressive use of rails by modern rolling stock implements a preventive maintenance approach essential for maintaining cost efficiency throughout the rail life cycle. Furthermore, the findings of this thesis aim to support informed decision-making in track maintenance at the network level.

The central research question guiding this thesis is as follows:

***How can the relationship between rail wear rate and rolling contact fatigue (RCF) be quantified and understood through big data analysis encompassing an entire country's rail infrastructure, combined with laboratory research on rails?***

The following sub-research questions are formulated to address the main research question comprehensively.

**Sub-question 1:** ***What are the key parameters influencing rail wear rates, and how can a big data-validated model be developed to predict this phenomenon?***

This sub-question is addressed in Chapter 2, which presents a big-data analysis of rail wear on the Belgian railway network. This chapter focuses on analysing rail wear by leveraging data collected across the Belgian railway network since 2012. Key factors influencing wear are examined, including accumulated tonnage, rail age, curve radius, rail grades, differences in wear between high and low rails, and the impact of preventive grinding.

**Sub-question 2:** ***How can the analysis of head check growth, considering factors such as wear development, curve radius, annual train traffic, and accumulated tonnage, inform the optimisation of preventive rail maintenance strategies, including the determination of an ideal "magic wear rate"?***

This sub-question is addressed in Chapter 3, "Analysis of Head Checks on the Belgian Railway Network." This chapter examines the growth of head check defects in railway rails, with a focus on the influence of wear development, curve radius, annual train traffic, and accumulated tonnage. The analysis is based on 212 curves in the Belgian railway network using R260 rail steel, with data collected from eddy current measurements.

**Sub-question 3: Is the artificial wear by grinding to remove RCF beneficial to rail service life, and what is the impact of white etching layers on rail performance and durability?**

This sub-question is addressed in Chapter 4, "Grinding – good or bad for reduction of rolling contact fatigue – observations from in-service rails with white Etching Layers ." In this chapter, the formation of White Etching Layers in rails was analysed, comparing ground and non-ground samples after at least 6 months in service to ensure that no transient phenomena affected the results.. Six rail samples from the Belgian railway network and one sample from the Swedish railway network were used.

## 1.6. DISSERTATION OUTLINE



This dissertation examines the relationship between rail wear rates and rolling contact fatigue (RCF) through a combination of big data analysis and laboratory research, organised into five chapters. The background and motivation for the thesis are introduced in Chapter 1, which outlines the challenges in rail maintenance and highlights the importance of data-driven approaches in improving durability. Chapter 2 presents an analysis of large-scale rail wear data from the Belgian railway network collected since 2012. This analysis identifies key factors such as accumulated tonnage, rail age, curve radius, and the impact of preventive grinding, providing insights that support the development of predictive wear models and maintenance strategies tailored to varying railway conditions. Insights into the growth of head check defects are provided in Chapter 3, which focuses on R260 rail steel across 212 curves. The thesis highlights the more decisive influence of annual tonnage compared to accumulated tonnage on defect progression, challenging traditional maintenance schedules. This chapter also introduces a framework for optimising grinding and milling operations, including the concept of a "magic wear rate" to enhance preventive maintenance. Chapter 4 investigates the formation of White Etching Layers (WEL) in rails through laboratory research. By comparing ground and unground samples, the thesis reveals that WEL formation is primarily driven by mechanical stress and thermal effects from train traffic rather than grinding. These findings underscore the need to address stress-induced material fatigue in maintenance strategies to improve rail durability. The dissertation concludes with a synthesis of findings in Chapter 5, offering practical recommendations for rail maintenance strategies and future research directions. This work contributes to the optimisation of rail maintenance practices and the sustainable management of railway infrastructure. An overview is given in Figure 1.2.

1

**CHAPTER 1**

**INTRODUCTION**

**CHAPTER 2**

**Rail wear rate on the Belgian railway network – A big-data analysis**

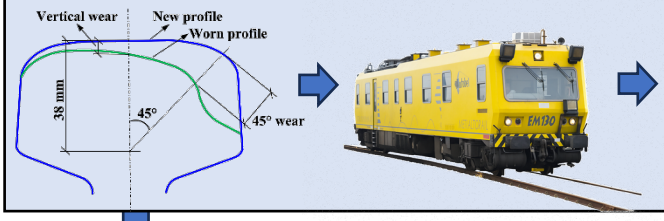


- 4,409km in 2012
- 5,338km in 2019

Calculated and influence Curve radius/steel grade/UIC class/ grinding assessed & discussed

**CHAPTER 3**

**Statistical analysis and treatment method of head checks – BE network**

212 Curves with head checks

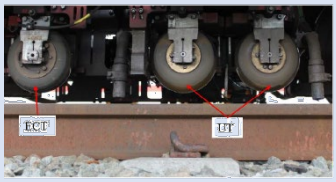


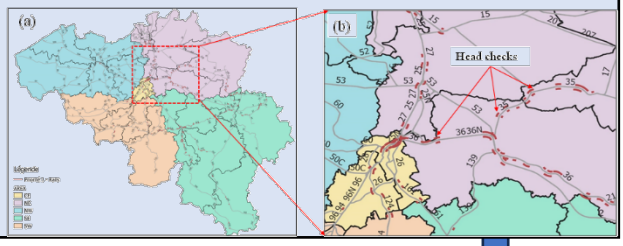


**CHAPTER 4**

**Grinding – good or bad for reduction of rolling contact fatigue – observations from in-service rails with white Etching Layers**

6 samples on Belgian & 1 on Swedish network

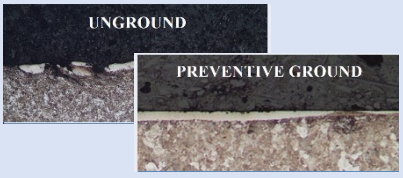


**CHAPTER 5**

**CONCLUSIONS AND RECOMMENDATIONS**

Figure 1.2: Structure of this dissertation

## REFERENCES


[1] International Union of Railways (UIC), 2022 Global rail sustainability report, 2023.

[2] N. Epicoco, M. Falagario, Decision support tools for developing sustainable transportation systems in the EU: a review of research needs, barriers, and trends, Research in Transportation Business & Management 43 (2022) 100819.

[3] M. Dotoli, N. Epicoco, M. Falagario, C. Seatzu, B. Turchiano, A decision support system for optimizing operations at intermodal railroad terminals, IEEE Transactions on Systems, Man, and Cybernetics: Systems 47 (2017) 487–501.

[4] International Union of Railways (UIC), Guidelines for the application of asset management in railway infrastructure organisations, 2010.

[5] Krause H, Poll G. Wear of wheel–rail surfaces. Wear. 1986; 113: 103-122.

[6] A. M. Zarembski, "The Evolution and Application of Rail Profile Grinding," Bulletin of the American Railway Engineering Association, Bulletin 718, Vol. 89, December 1988.

[7] Zoeteman A, Dollevoet R, Li Z. Dutch research results on wheel/rail interface management: 2001-2013 and beyond. Proceedings of the Institution of Mechanical Engineers, Part F: Journal of Rail and Rapid Transit. 2014; 228(6): 642-651.

[8] Li Z. Wheel-rail rolling contact and its application to wear simulation. PhD thesis, Delft University of Technology, 2002.

[9] Li Z, Kalker J. Simulation of severe wheel-rail wear. Transactions on the Built Environment. 1998; 34: 393-402.

[10] Christoforou P, Fletcher D, Lewis R. Benchmarking of premium rail material wear. Wear. 2019; 436-437, 202990.

[11] Lewis R, Olofsson U. Mapping rail wear regimes and transitions. Wear. 2004; 257: 721-729.

[12] Lichtberger B. Track compendium: track system, substructure, maintenance, economics. Hamburg: DVV Media Group GmbH Eurailpress; 2011.

[13] Stock R, Pippan R. RCF and wear in theory and practice-The influence of rail grade on wear and RCF. Wear. 2011; 471: 125-133.

# 2

# Rail wear rate on the Belgian railway network – a big-data analysis

*This chapter presents a big data-based analysis of the rail wear of the whole Belgian railway network measured in 2012 and 2019. Wear rates are reported, discussed, and quantitatively formulated as functions of critical factors in terms of curve radius, annual tonnage (rail age), high rail in curves, an average from both rails in straight tracks at rail top (vertical wear) and gauge corner (45° wear) and for steel grade R200 and R260. The influence of preventive grinding is also analyzed. The wear rates are derived in an aggregated manner for the whole network. The wear rates do not show significant change with changes in rolling stock over the years, implying that the wear rates could also hold for other networks. It is found that R200 shows, on average, a 34% higher wear rate than R260. Also, the wear rate per tonnage is lower for high-loaded tracks. Thus, time is a relevant factor in explaining the wear evolution of low-loaded tracks; for instance, the effect of corrosion may have an important role. The paper provides statistically significant information that can be used for wear modeling, understanding and treating rolling contact fatigue based on the wear rate and developing tailored rail maintenance strategies.*

Apart from minor updates, this chapter has been published as: Tim Vernaillen, Li Wang, Alfredo Núñez, Rolf Dollevoet, Zili Li (2024). Rail wear rate on the Belgian railway network – a big-data analysis. International Journal Of Rail Transportation 2024, Vol.12, NO.5, 765-780.

## 2.1. INTRODUCTION



An important challenge for railway infrastructure managers is to avoid or minimize the changes in rail and wheel contact surfaces due to wear [1]. New technologies and methods to control wear are needed to maintain train stability and passenger comfort, decrease rail and track system degradation and reduce the risk of derailment. Rail wear is a complex phenomenon that depends on the local conditions of the infrastructure, the rolling stock, and the exogenous variables such as the environment and weather conditions at the track location. Rail wear varies by location because of the many stochasticities in the involved parameters that can change with time and space [2]. Wear is usually assumed to be proportional to frictional work [3]. The proportionality and frictional work are functions of the rail steel grade (such as R260 and R200), wheel steel grade (such as ER6 and ER7), pairing between rail material and wheel material, normal contact stress, coefficient of friction, and relative slip [4]. Rail wear is also influenced by the design, construction, and maintenance of the vehicles (primary yaw stiffness, braking and traction control, etc.), tracks (radii of curves, cant, etc.), the rail and wheel profiles, the surface treatments such as coating or lubrication, the interaction between the vehicles and the tracks, and the environment (humidity, corrosion, etc.) [5, 6]. A discussion of the influence of some of the design parameters for certain material pairings is given in [1].

The many influencing parameters and uncertainties hinder deriving simple mathematical laws for wear behavior. Wear mapping of materials is a common research practice [7]. Various assumptions are usually considered when determining the wear behavior in laboratories. In [8], the relations between rail wear rate regimes and transitions obtained from twin disc tests, pin-on-disc machines, and field measurements are discussed. The normal stress and relative slip can be controlled in a laboratory environment and small-scale field tests [9]. Managing the relative slip becomes difficult for large-scale field operational conditions. Although many small-scale field data are available for standard rail grades, a systematic analysis of rail wear over a long period and on a country-wide network is rare [8, 10]. Numerical models are also essential for exploring wheel and rail wear. Many numerical models have been developed, and the modeling strategy varies from a single wear calculation to iteration of dynamic simulations [11-14]. In practice, rail wear and

rolling contact fatigue (RCF) develop simultaneously. The competitive effects between wear and RCF should be treated carefully in the simulations [15, 16].

This chapter analyzes the wear behavior of rails from long-term monitoring measurements of the whole Belgian railway network. The wear rates are derived and analyzed based on the rail steel grades, the curve radius, the UIC classes of annual traffic load, and the accumulated million gross tons (MGT). Wear data from two measuring campaigns, conducted in 2012 on 4,409 km tracks and in 2019 on 5,338 km tracks, are analyzed.

The chapter is organized as follows. In Section 2.2, the wear measurement data is described. Section 2.3. analyzes the data and presents the results and discussions. Section 2.4. shows conclusions and further research.

## 2.2. RAIL WEAR MEASUREMENT

### 2.2.1. DESCRIPTION OF THE BELGIAN NETWORK AND PARAMETERS TO BE ANALYZED

Since the late 1990s, the Belgian railway infrastructure manager Infrabel has been using an automatic train-borne measuring system to monitor the rail parameters mounted on the EM130 measurement train. The recorded rail parameters include vertical wear, horizontal wear, wear at 45° and inclination of the rails. The railway network is typically divided into homogenous sections of 50 m for analysis. A requirement for a track section to be homogenous is that the rails (age, profile, and steel grade) and annual train tonnage are the same. The measurements are matched with a technical inventory that includes the detailed status of the track asset, which the local track managers constantly update. All relevant data are then averaged in each of the 50 m sections following the technical inventory.

By 2020, the Belgian railway network consisted of 422 km of high-speed lines, 222 km of freight lines, and 5,853 km of conventional lines with mixed passenger and freight traffic. In this paper, only the conventional lines with mixed passenger and freight traffic are considered. The rails are installed with an inward inclination of 1:20. The nominal gauge is 1435 mm, and two rail profiles are used in the plain track: the UIC60E1 profile

and the Belgian 50E2 profile [17]. These two profiles have different geometrical dimensions, but the widths of the railhead and the profiles are equal. The most commonly utilized rail materials are pearlitic steels. In 1982, Infrabel started replacing steel grade 700 (chemical composition, % by mass: C 0.4/0.6, Si 0.05/0.35, Mn 0.8/1.25 and RM 680/830MPa) according to UIC leaflet 860-0 with R260 (EN13674-1) steel grade (chemical composition, % by mass: C 0.62/0.8, Si 0.15/0.58, Mn 0.7/1.20 and RM ≥880MPa). The steel grade 700 (UIC 860-0) is referred in the rest of the document as R200 (EN13674-1) because the chemical composition is closest (chemical composition, % by mass: C 0.4/0.6, Si 0.15/0.58, Mn 0.7/1.20 and RM ≥680MPa). This steel grade corresponded no longer to the needs in track, due to its greater sensitivity to wear. Both steel grades R200 and R260 are not heat treated. Over the years, the steel manufacturing process has been improved, reducing the occurrence of internal defects. However, regarding surface defects, experiences on the Belgian and French railway networks indicate that these changes decreased the wear but might trigger more surface defects. Approximately 66%, 32% and 2% of the network consist of R260 rails, R200 rails installed before 1982, and R350HT rails or rails with high hardness, respectively. This paper will focus on R200 and R260, as the number of rails of R350HT and higher hardness is small.

Wear calculation is influenced by many in-service parameters and production tolerance. The rails used in Belgium conform to the standard EN 13674-1. The tolerance for the rail height is +0.5/-1.0 mm for height <165 mm (50E2) and +0.6/-1.1 mm for height ≥ 165 mm (UIC60E1). This tolerance can influence the calculation of the average wear rate, especially for newly installed rails. Thus, measurements from individual track sections are not applied in this analysis. Individual cases are more sensitive to local variables and manufacturing tolerances. Instead, all measurements for the thesis are divided into three groups according to the three most significant parameters, i.e., curve radius, rail grade, and load (UIC class), and the analysis is performed on these aggregated data.

### 2.2.2. DEFINITION OF VERTICAL WEAR AND 45° WEAR

In this paper, we focus the analysis on vertical wear and 45° wear. Vertical wear is calculated by subtracting the measured rail height from the designed rail height, and the 45° wear is calculated by subtracting the measured length from the reference length of the new profiles at 38 mm below the rail surface on the center axis of the rail, as illustrated in Figure 2.1 In tangent tracks, the vertical wear is computed as the average of both rails. In the curves, the high and low rails are separately analyzed. On the high rail in curved tracks, wear mainly occurs at the gauge corner, with substantial vertical wear [18]. One of the main types of rolling contact fatigue, head checks, mainly occur in the gauge corner, where 45° wear is measured.

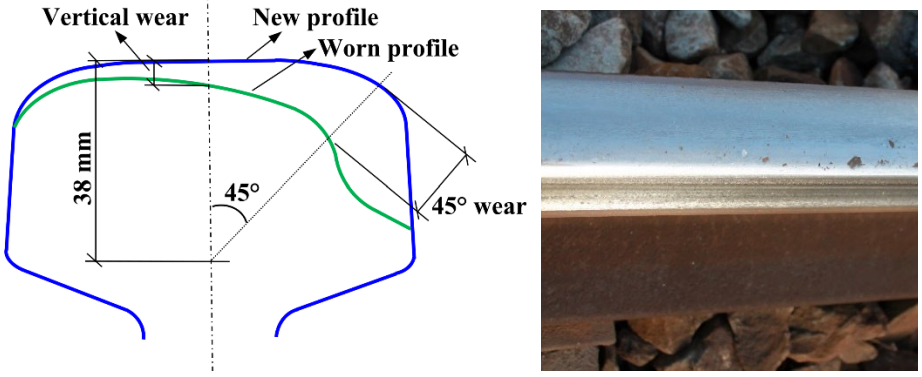


(a) (b)

**Figure 2.1: Measurements of vertical wear and 45 wear on the railhead (a) Definitions of vertical wear and 45° wear (b) Typical in situ rail wear**

### 2.2.3. TRAFFIC LOAD

The traffic load is defined in terms of UIC class. In the UIC714R leaflet [19], six groups are defined:

$$\mathrm{UIC}_i = \begin{cases} \mathrm{UIC1} & \text{if } 130000[\mathrm{ton/day}] < \mathrm{TL}_i \\ \mathrm{UIC2} & \text{if } 80000[\mathrm{ton/day}] < \mathrm{TL}_i \leq 130000[\mathrm{ton/day}] \\ \mathrm{UIC3} & \text{if } 40000[\mathrm{ton/day}] < \mathrm{TL}_i \leq 80000[\mathrm{ton/day}] \\ \mathrm{UIC4} & \text{if } 20000[\mathrm{ton/day}] < \mathrm{TL}_i \leq 40000[\mathrm{ton/day}] \\ \mathrm{UIC5} & \text{if } 5000[\mathrm{ton/day}] < \mathrm{TL}_i \leq 20000[\mathrm{ton/day}] \\ \mathrm{UIC6} & \text{if } \mathrm{TL}_i \leq 5000[\mathrm{ton/day}] \end{cases} \quad (1)$$

where UICi is the UIC class of track Section i, and TLi is the measured traffic load for track Section i. All track sections are given a specific UIC class depending on the annual MGT, as shown in Figure 2.2.

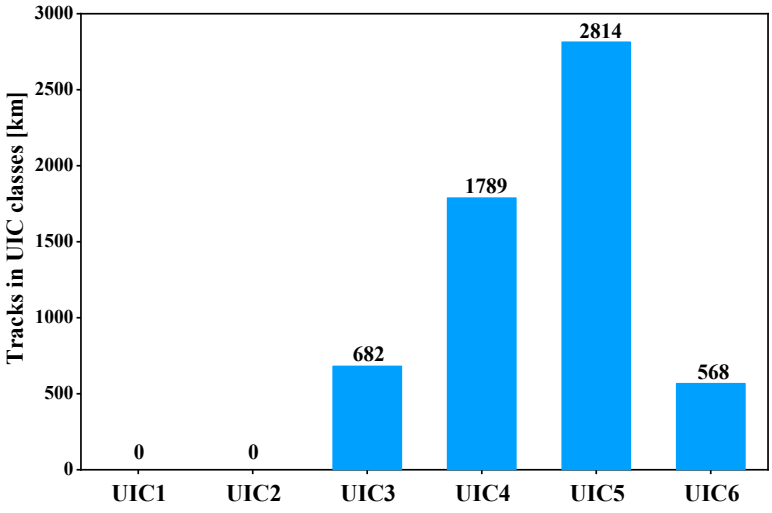


**Figure 2.2: Division of the network in UIC classes considered in this paper**

Given the negligible track length in the UIC1 and UIC2 classes, they are not considered in this analysis. The total traffic load in 2011 is used for the wear measurement in 2012 and that in 2018 is employed for the wear measurement in 2019.

### 2.2.4. DESCRIPTION OF THE WEAR DATA

The complete network is measured twice a year with the EM130, and the rail profiles are measured every 25 cm along the track. Wear is recorded as mm/MGT or mm/year. The start time of the wear calculation is the installation date of the rails, and the endpoint of the wear calculation is the moment of measuring the wear.

The measurements for 2012 and 2019 are analyzed in this paper. The reason for choosing these two years is that before 2012, negligible preventive grinding was performed. A preventive cyclic grinding program has been in force since 2012. Thus, in 2019, rail wear consisted of natural wear due to train traffic, as well as corrosion and artificial wear due to grinding. In this paper, wear refers to mechanical wear due to both wheel-rail contact and natural wear due to corrosion unless otherwise indicated. A comparison between the wear measurements in 2012 and 2019 allows the evaluation of the effects of preventive grinding. The Infrabel policy states that grinding is performed at a location only when no rolling contact fatigue (RCF) is reported there. If RCF is reported for a track, that track should not be ground before the rail is replaced. There could, however, be situations where RCF defects were present while the rail was still ground. The data analysis shown indicates that these small inconsistencies between execution and policy do not influence the analysis primarily because the data show good consistency, as will be seen below. The situations of 2012 and 2019 are compared by examining the following data:

(a) The wear rate derived from the 2012 measurement relative to the dates when the rails were installed.

(b) The wear rate derived from the 2019 measurement relative to the dates when the rails were installed. The rails considered for the 2019 measurement were installed before and after 2012.

In total, measurements for the 4,409 km and 5,338 km tracks are used for 2012 and 2019, respectively. The complete batch of 5,853 km of tracks is not employed because not all the tracks were measured (due to track works and missing data), and not all the measurements were valid. Data were considered invalid when considerable deviations were observed and extreme values were obtained, e.g.:

(1) Compared with the nominal rail profile, a recently installed rail will have almost no wear, but it may have a manufacturing deviation of 0.6/-1.1mm, as illustrated in Figure 2.3. This deviation can erroneously produce a very high wear rate.

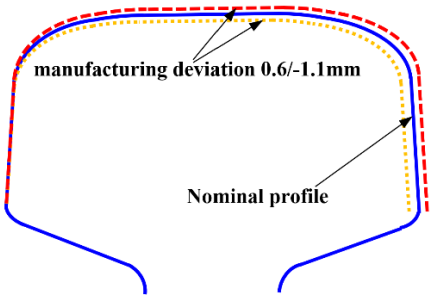


**Figure 2.3: Illustration of manufacturing deviation**

(2) On some lines, re-used rails were installed. The age of the rail used for the wear calculation is the installation date, but the rail can be many years older, which generates wear rates that are too high.

(3) The technical inventory was not updated after rail renewal. The measuring system will measure a low wear rate, but the age of the old rail is used for the calculation, which produces very low wear rates.

(4) The profile recognition system does not always work correctly, e.g., a UIC50E2 profile is taken as UIC60E1. An incorrect profile detection yields extreme values for the wear rate.

(5) Measurement conditions at different track locations might affect the measurement due to the dynamics of the measurement vehicle, particularly at a point with drastic track geometry changes, such as transitions to bridges and level crossings.

In Figure 2.4, data of the vertical wear (average of the left and right rails) is shown for the measurements in 2019 for the R260 rail, UIC4 load and tangent tracks. The average vertical wear is 1.20 mm/100 MGT with a standard deviation of 3.50 mm for the complete dataset, i.e., 100% of the data. The data showed extremely high wear rates of up to 60 mm/100 MGT. Such a wear rate is physically impossible and has an important influence on the overall average wear. Thus, data with these large deviations will be removed from the analysis. In Figure 4, the average and standard deviation of the vertical wear are presented when 100%, 95%, 92%, 90% and 85% of the data points are employed for the 5,338 km of tracks in 2019 (0%, 2.5%, 4%, 5% and 7.5% of the data points that are the highest and

lowest are removed from the measurements). Based on the 90% dataset, the average vertical wear is 0.82 mm with a standard deviation of 0.62 mm. This 90% dataset will be employed in further analysis, i.e., the 5% highest values and 5% lowest values are not considered in further research.

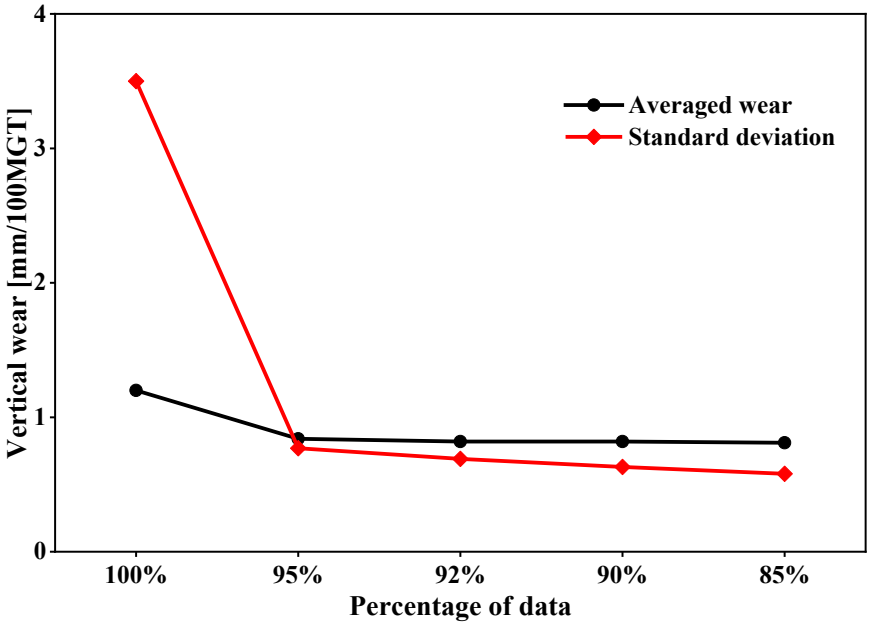


**Figure 2.4: Vertical wear at tangent tracks shows that 5% of the data contains large deviations (2019, R260)**

Thus, the analysis will consider the load categories UIC3, UIC4, UIC5 and UIC6. The rail grades are R200 and R260. The curve radius is divided into the following groups:

$$R_i = \begin{cases} 1 \text{ if } & R \leq 500[\text{m}] \\ 2 \text{ if } & 500[\text{m}] < R \leq 750[\text{m}] \\ 3 \text{ if } & 750[\text{m}] < R \leq 1000[\text{m}] \\ 4 \text{ if } & 1000[\text{m}] < R \leq 1250[\text{m}] \\ 5 \text{ if } & 1250[\text{m}] < R \leq 1500[\text{m}] \\ 6 \text{ if } & 1500[\text{m}] < R \leq 2000[\text{m}] \\ 7 \text{ if } & 2000[\text{m}] < R \leq 2500[\text{m}] \\ 8 \text{ if } & 2500[\text{m}] < R \leq 3000[\text{m}] \\ 9 \text{ if } & 3000[\text{m}] < R \end{cases} \quad (2)$$

where Ri is the number of a curve radius group where track segment i belongs and R is the measured radius. Note that tangent tracks are included in the 9th group where R > 3000[m]. All the measurements are averaged per 50m and for transition curves also the average curve radius per 50m is used.

## 2.3. DATA ANALYSIS AND DISCUSSIONS

### 2.3.1. VERTICAL WEAR VERSUS TONNAGE OF R260 RAILS FROM MEASUREMENTS IN 2012

A railway track consists of tangent and curved parts. The rail will wear differently in these two parts. The rail-wheel contact point is located at the top of the rail in a tangent line, and the vertical wear will thus be the most important. The average vertical wear of both rails is utilized for the analysis of this part. For a curved track, the investigation will be separated for vertical wear and 45° wear at the high rail.

The wear rate is defined as

$$\Delta w_{vertical}^{traffic} = \frac{w_t}{AL_t(t-t_0)} \times 100 \tag{3}$$

where $\Delta w_{vertical}^{traffic}$ is the wear rate per 100 MGT in mm/100MGT measured in year t, wt in mm is the wear measured in year t, ALt is the annual traffic load in MGT measured in year t, and t0 is the year of the rail installation.

Table 2.1 lists the vertical wear on straight tracks with R260 in terms of the UIC classes. It can be seen in Table 1 that the wear is quite different on tracks under different traffic loads. The rails on heavily loaded lines wore at a slower rate as a function of tonnage, with a smaller standard deviation, while those on less loaded lines wore at a quicker rate, with a larger standard deviation. Usually, rail wear happens because of three main reasons: traffic loads, natural corrosion, and grinding. The data in Table 2.1 does not include grinding effects. Therefore, the reason behind the faster wear rate on less loaded lines is probably because of natural corrosion. Less loaded tracks have more time per tonnage for corrosion. The effect of natural corrosion is considerable because a factor of 12.7 is observed: on UIC-

Class 6 it was 4.2 mm/100MGT, whereas on UIC-Class 3, it was 0.33 mm/100MGT. UIC-Class 4 tracks had a wear rate that is nearest to that of [20].

**Table 2.1: Vertical wear (average of both rails) on straight track in relation to UIC Class (2012 - R260)**

| UIC-Class | # km | Vertical wear [mm/100MGT] | Standard deviation [mm/100MGT] |
|---|---|---|---|
| UIC3 | 700 | 0.33 | 0.21 |
| UIC4 | 809 | 0.78 | 0.46 |
| UIC5 | 564 | 1.57 | 1.22 |
| UIC6 | 67 | 4.20 | 3.48 |
| Total | 2140 | 0.93 | 0.67 |

**Figure 2.5: shows the vertical wear rate with respect to track radius and UIC class.**

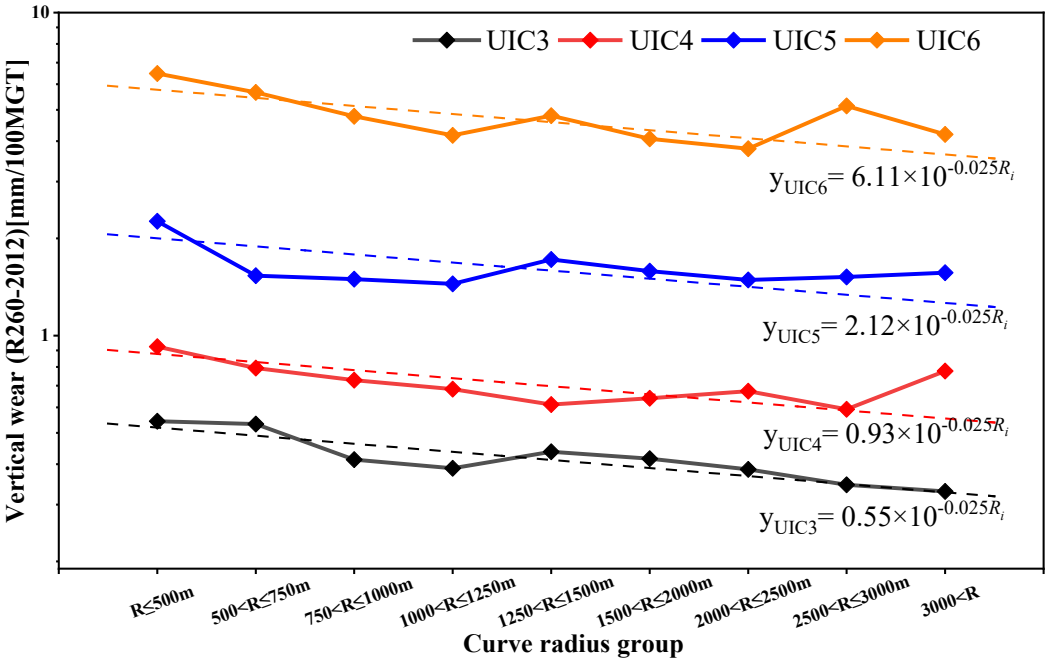


Figure 2.5: Vertical wear of high rail with R260 in 2012 in relation to UIC class and curve radius. (Wears of high and low rails are averaged at each tangent track, i.e. R>3000m; The R-Squared values of the fittings for UIC3, UIC4, UIC5 and UIC6 are 0.784, 0.343, 0.240 and 0.453, respectively).

In Figure 2.5, the horizontal axis is the track radius, Ri = 1, 2, …, 9 as defined in (2), and the vertical axis is the vertical wear rate (high rail in curves and average of both rails in straight tracks). The wear rate in logarithm is a linear function of the radius, i.e.,

$$\lg(yUICj) = k \cdot Ri + \lg(y0) \tag{4}$$

where y0 is the vertical wear extrapolated to radius = 0; they are 0.554, 0.926, 2.115 and 6.117 for UICj, j = 3, 4, 5 and 6, respectively.

Note that (4) is equivalent to

$$yUICj = y0 \cdot 10k \cdot Ri \tag{5}$$

The four curves in Figure 2.5 are approximately parallel to each other, meaning that in (4) they have approximately the same k value. This k equals -0.025.

Thus, the vertical wear rate in mm/100 MGT of R260 is, on the Belgium network, as a function of curve radius and traffic load, including corrosion:

$$yR260_2012_vertical\ wear = y0(j) \cdot 10\text{-}0.025Ri,$$
$$Ri = 1,2,\ldots 9 \text{ and } j \in \{3, 4, 5, 6\} \tag{6}$$

with y0(j) = 0.55, 0.93, 2.12 and 6.11 for j = 3, 4, 5, 6, respectively.

### 2.3.2. 45° WEAR VERSUS TONNAGE OF RAILS WITH R260 IN 2012

With a decrease in the curve radius, the rail-wheel contact at the high rail shifts toward the gauge corner. The narrower the curve is, the more pronounced this phenomenon will be. Wear in curves is therefore characterized by wear at an angle of 45°. Figure 2.5 shows the wear at 45° for all radius groups. The logarithmic wear rate roughly linearly increased with decreasing curve radius. The influence of the daily load of the track is important, similar to the vertical wear rate in Section 3.1. The lower the daily tonnage was, the faster the wear per tonnage. In narrow curves with a radius of less than 500 m, the wear evolves on average 2 to 3 times as fast as in a tangent section of the track; the wear rate of UIC3 is, for example, 0.4 for R > 3000 and 0.96 for R < 500m in Figure 6. Also, Figure 6 shows a high wear rate with low tonnage due to corrosion.

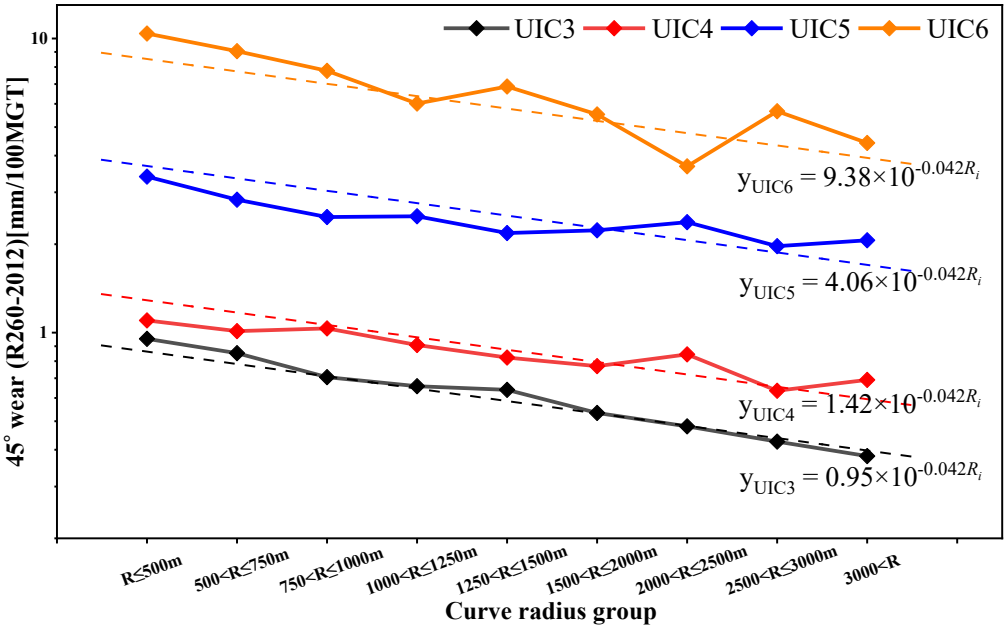


Figure 2.6: 45° wear of high rail with R260 in 2012 in relation to UIC-class and curve radius. (Wears of high and low rails are averaged at each tangent track, i.e. R>3000m; The R-Squared values of the fittings for UIC3, UIC4, UIC5 and UIC6 are 0.968, 0.892, 0.755 and 0.811, respectively)

Following the same way of deriving (4) – (6), the 45° wear rate rail in mm/100MGT of an R260 high rail is, on the Belgium network, as a function of curve radius and traffic load, including corrosion:

$$\text{yR260_2012_45° wear} = y0(j)\cdot 10\text{-}0.042Ri,$$
$$Ri = 1,2,\ldots 9 \text{ and } j \in \{3, 4, 5, 6\} \quad (7)$$

with y0(j) = 0.95, 1.42, 4.06 and 9.38 for j = 3, 4, 5, 6, respectively.

### 2.3.3. WEAR VERSUS TONNAGE FOR R200 AND R260 IN 2012

#### 2.3.3.1. VERTICAL WEAR AT TANGENT TRACKS

The 2012 wear rates of R200 and R260 are compared in Table 2.2.

**Table 2.2: Comparison between R200 and R260 in terms of vertical wear at tangent tracks in 2012**

| UIC-Class | Vertical wear [mm/100MGT] | | Difference |
|---|---|---|---|
| | R260 | R200 | |
| UIC3 | 0.33 | 0.44 | 33% |
| UIC4 | 0.78 | 0.80 | 3% |
| UIC5 | 1.57 | 1.93 | 23% |
| UIC6 | 4.20 | 9.94 | 137% |
| **Average*** | **0.95** | **1.27** | **34%** |

*** The average is calculated based on the kilometers in each UIC class in Table 1.**

On average, the R200 rail will wear 34% faster than the R260 rail in a tangent section of the track. Low tonnage lines show high wear rates per tonnage, which is the effect of corrosion. The wear rate is higher for the R200 steel grade compared to R260. UIC4 seems to be the load with which the 2 grades behave the most similarly, considering the effect of corrosion.

#### 2.3.3.2. 45° WEAR AT CURVES

Most of the R200 rails are present in the low-loaded lines, as these are also the oldest rails. Thus, UIC6 is chosen for comparison in figures 2.7 and 2.8. Figure 2.7 shows the wear at 45° in the curves for R200 and R260 in 2012.

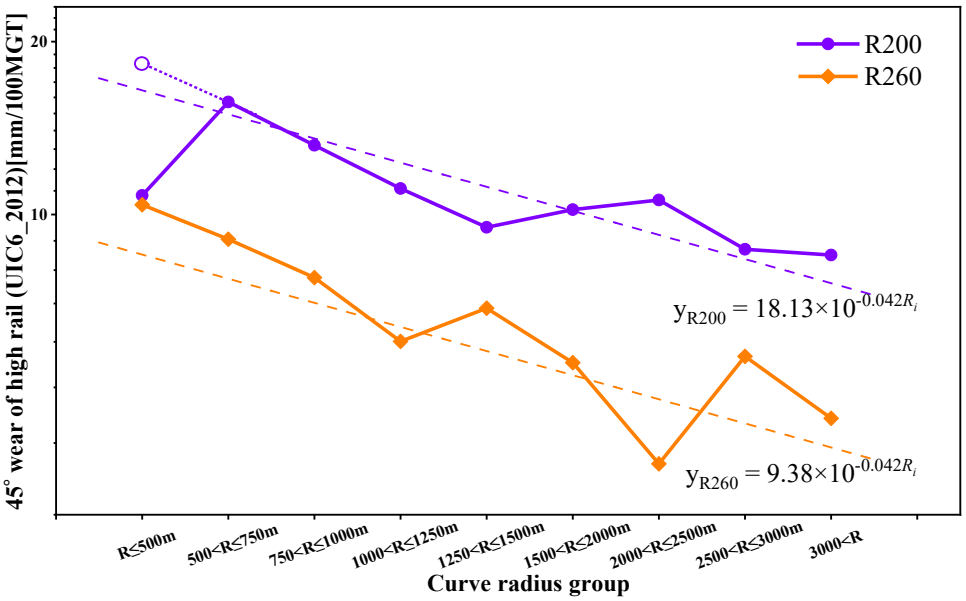


**Figure 2.7: 45° wear of high rail with R200 or R260 in 2012 for UIC6 in relation to curve radius (The R-Squared values of the fittings for R200 and R260 are 0.529 and 0.811, respectively)**

As shown in Figure 2.7, there is an approximate constant difference, with a scale of about 1.93, between the wear rates of R200 and R260, i.e., the wear rate of R200 is proportional to and 1.93 times as high as that of R260. The average difference between R200 and R260 at 45° is comparable with the literature, i.e., R260 has 34% less wear (table 2.2) [21].

Figure 2.8 shows the comparison between 2012 and 2019 in terms of 45° wear of high rail for UIC6 in relation to the curve radius for R200.

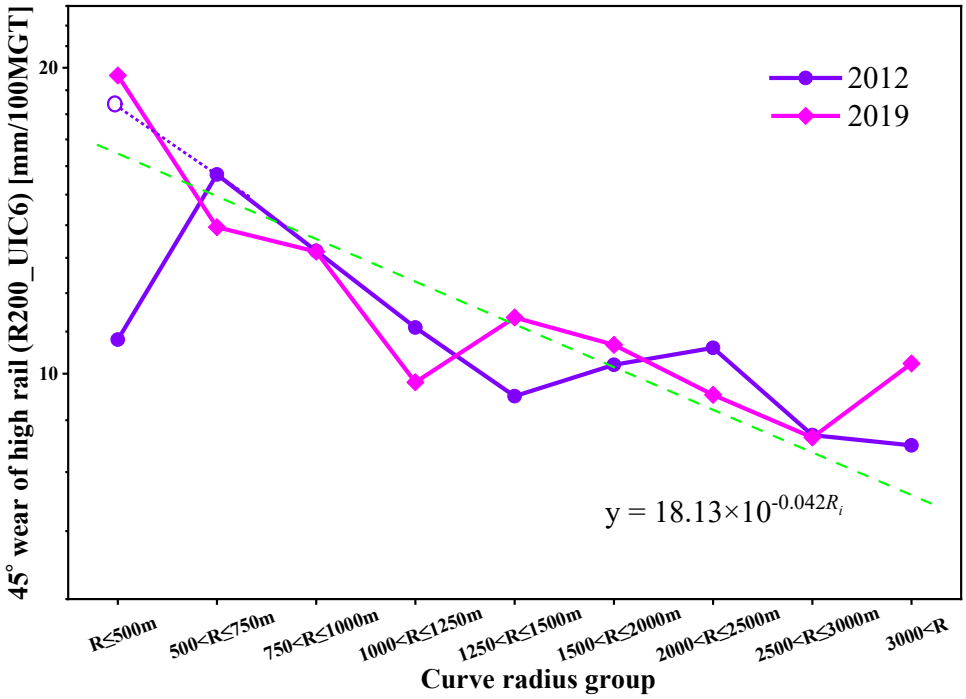


**Figure 2.8: 45° wear of high rail with R200 in 2012 and 2019 for UIC6 in relation to curve radius (The R-Squared values of the fittings for 2012 and 2019 are 0.529 and 0.658, respectively)**

A deviation is nevertheless noted in figures 2.7 and 2.8 for R≤500m. The wear seems to be much less than expected for R200 in curves with a radius of less than 500 m. A more detailed analysis attributes this deviation to the technical inventory not being updated. Due to the high wear rates, the high rail was more frequently replaced, sometimes without updating the technical inventory.

This inconsistency is not observed with either R260 in 2012 (Figure 2.7) or R200 in 2019 (Figure 2.8), because there has been much emphasis on keeping the technical inventory data up to date in recent years. The 2019 measurements are more consistent in the curves with a small radius (Figure 2.8). If extrapolating the 2012 R200 wear rate to a

radius of less than 500 m, as indicated by the dotted line in figures 2.7 and 2.8, it can be seen in Figure 2.8 that the wear rate of R200 has a good agreement between 2012 and 2019.

### 2.3.4. INFLUENCE OF PREVENTIVE GRINDING

Since 2012, Infrabel has introduced a preventive maintenance strategy in which the rails are periodically ground to remove shallow cracks in the rail surface. This strategy should influence rail wear because grinding creates artificial wear. The wear data from 2012 and 2019 are compared to investigate whether this preventive maintenance is visible in the data.

For the R200 rails, there should be no pronounced difference in the wear rate between 2012 and 2019 because the preventive grinding strategy focuses on recently installed rails on important, high-loaded lines. Usually, these lines are equipped with R260, installed after 1982. Between 2012 (the start of the preventive grinding strategy) and 2018, a total of 10.536 km of tracks were ground with two or more grinding passes.

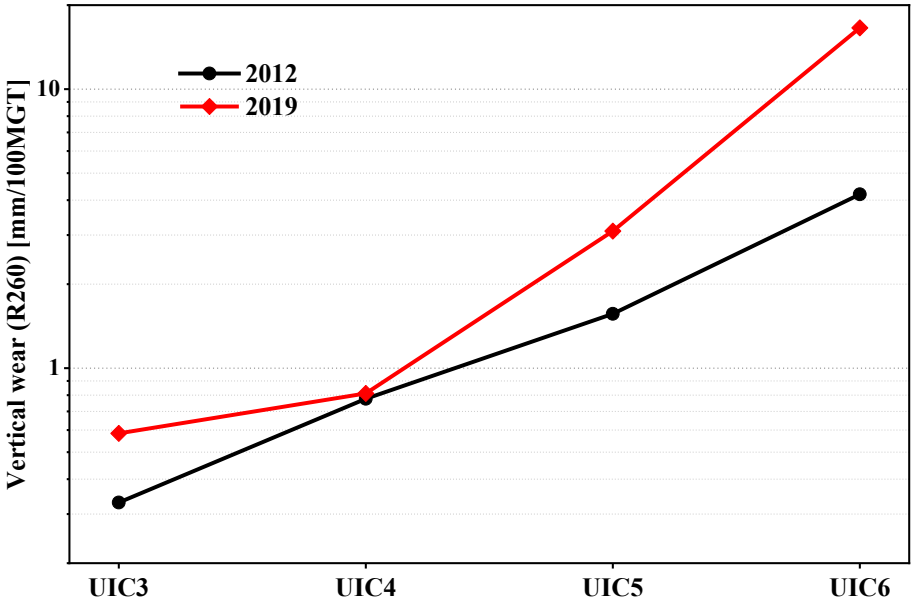


**Figure 2.9: Vertical wear at tangent tracks (average of high and low rails) in 2012 and 2019 for R260**

Figure 2.9 shows that in tangent tracks, the wear of R260 was higher in 2019 than in 2012 due to preventive grinding, except for UIC class 4. For UIC4, the wear in 2012 and 2019 are equal, meaning there was a lack of grinding for UIC4 tracks, assuming that the mechanical wear rate due to wheel-rail contact is the same, as was argued in Section 3.3.2.

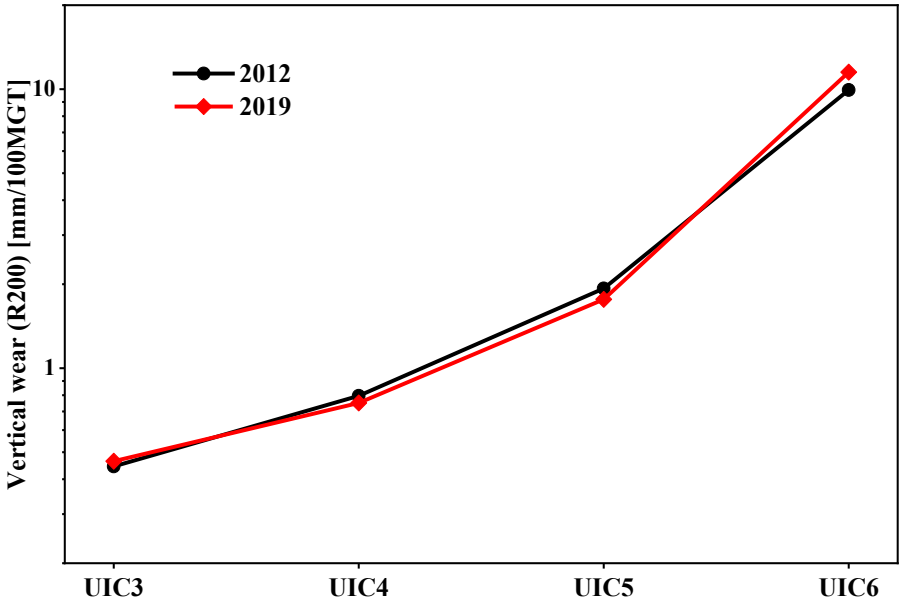


**Figure 2.10: Vertical wear at tangent tracks (average of high and low rails) in 2012 and 2019 for R200**

Figure 2.10 shows that the wear in R200 was equal in 2019 and 2012. This can be explained by the fact that the preventive grinding campaigns were focused on recent rails (R260). Figure 2.10 shows the curves overlay with each other almost perfectly, indicating a very good consistency and, thus, reliability of the measurement data. Since this consistency is observed in the entire network for each load class (UIC3, 4, 5, 6) (Figure 10) and each radius group (Figure 2.8), it is reasonable to believe that the other data shown in this paper are also consistent and reliable, as they are collected in the same way on the same network in the same period.

In 2019, the wear rate of R260 rails in tangent tracks was higher than that of R200 due to preventive grinding (compare figures 2.9 and 2.10). Taking the R260 natural wear rates of 2012 and 2019 being equal, the artificial wear can be calculated. With UIC3 in

Figure 2.9, the mechanical and natural wear was 0.33 mm/100MGT, and the artificial vertical wear was 0.25 mm/100MGT on average between 2012 and 2019 for tangent tracks (i.e., R > 3000 m). The artificial wear combined with the natural wear made the total wear of R260 higher than the total wear of R200, which was natural wear only.

The difference between 2012 and 2019 is even more pronounced in the curves, as shown in Figure 2.11 below, taking UIC3 as an example. The artificial wear in curves is higher compared with tangent tracks mainly because curves need more preventive maintenance. Between 2012 and 2016, the grinding interval was 80 MGT for both curved and tangent tracks. Since 2016, the grinding interval is 25 MGT in curves and 60 MGT in tangent tracks.

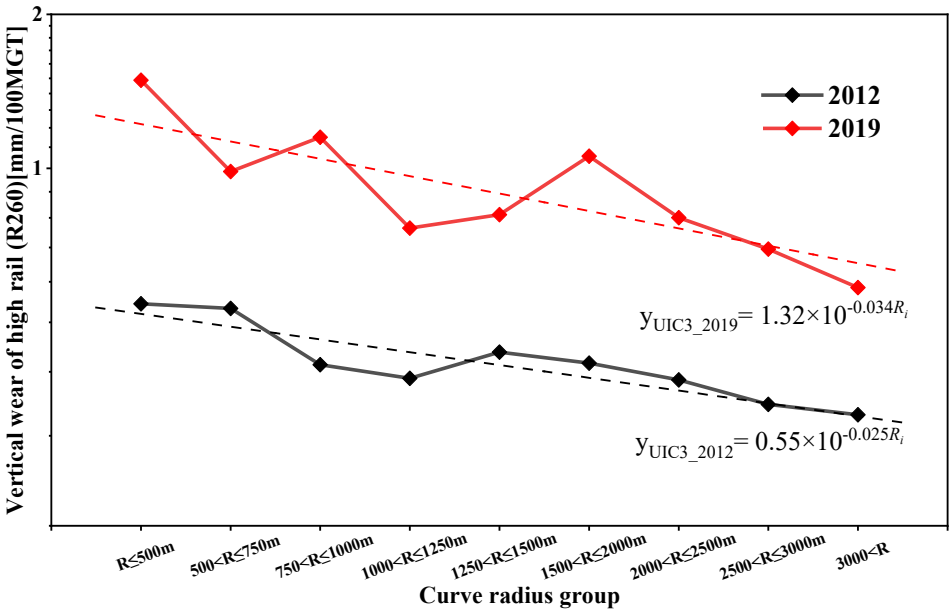


**Figure 2.11: Vertical wear (high rail in curves and average both rails in straight track) in mm/MGT in relation to curve radius – comparison of 2012 and 2019 (R260 – UIC3) (The R-Squared values of the fittings for 2012 and 2019 are 0.787 and 0.652, respectively)**

Figure 2.12 shows the average vertical wear rates of 2019 for the 4 UIC load classes.

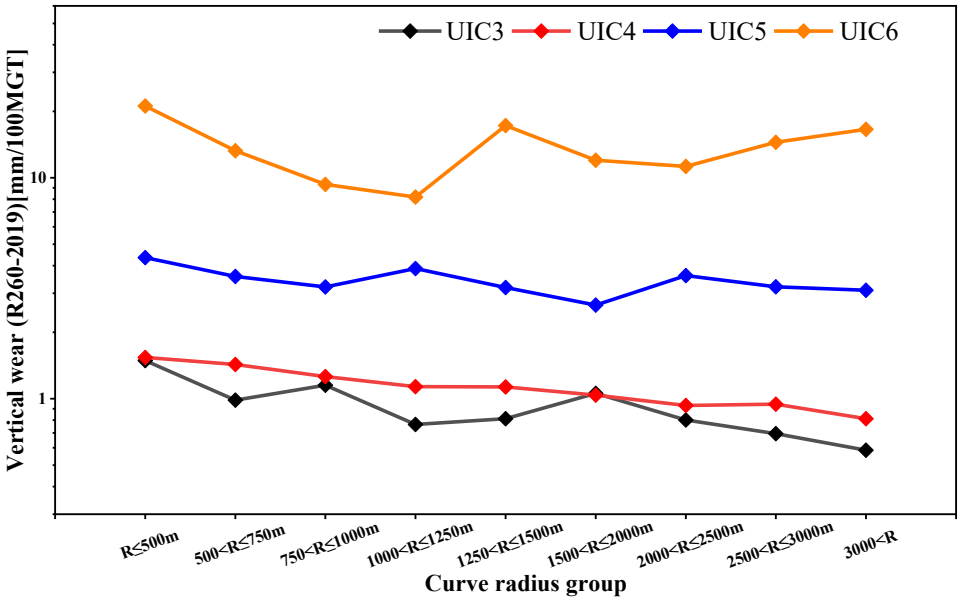


**Figure 2.12: Vertical wear (high rail in curves and average both rails in straight track) in relation to curve radius in 2019 (R260)**

Comparing Figure 2.12 with Figure 5, all the measurements show higher wear rates in 2019 than in 2012 due to the preventive grinding. Figure 2.12 also shows that the UIC4 curve almost overlaps with that of UIC3, meaning that the UIC4 rail had the least grinding, in line with what can be seen in Figure 2.9.

### 2.3.5. VERTICAL WEAR PER YEAR

In previous analyses, wear was expressed in mm/100MGT. In this section, wear will be expressed in mm/per year since the installation of the rails, calculated as follows:

$$\Delta w_{vertical}^{yearly} = \frac{w_t}{t - t_0} \tag{8}$$

where $\Delta w_{vertical}^{yearly}$ is the wear rate per year in mm/year measured in year t, wt [mm] is the wear measured in year t, and t0 is the year of the rail installation.

Figure 2.13 shows the vertical wear per UIC group in relation to the curve radius based on the measurements performed in 2012.

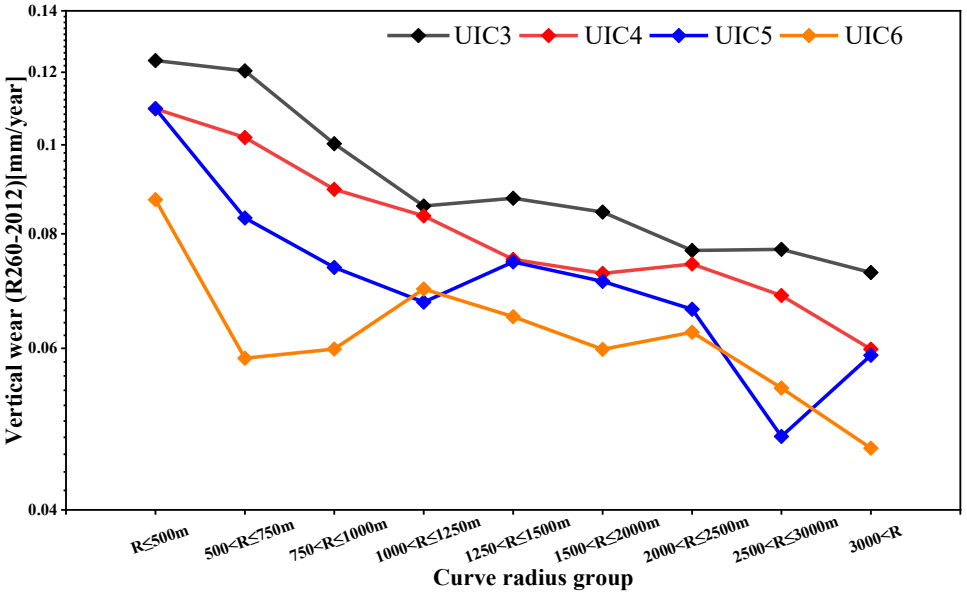


**Figure 2.13: Vertical wear rate in mm/year in relation to UIC class and curve radius in 2012 (R260)**

The wear increased when the curve radius was narrower. The wear rate per year also increased when the daily load was increased, contrasting the trend of the wear rate per tonnage. A higher daily load produces more wear per year. Corrosion is time-related and most likely causes fewer differences between the UIC classes compared with the analysis in mm/100MGT, where the influence of time is less important. Steel without any protection will corrode under atmospheric conditions, and time becomes an important parameter for the lower tonnage tracks.

## 2.4. CONCLUSIONS



Rail wear rate of the whole Belgian network from 2 measuring campaigns (2012–4,409 km and 2019–5,338 km) has been calculated and analyzed. The effects on the wear rate of the curve radius, steel grade, UIC class, and grinding influence has been assessed and discussed. The following conclusions are drawn:

(1) for both vertical wear and 45° wear, the rail wear rate (mm/100MGT) in the logarithm scale is found to be an approximately linear function of curve radius. The gradient can be considered the same for different UIC classes.

(2) the wear rate for rails with grade R200 is proportional to and 1.93 times as high as that for rails with grade R260.

(3) the artificial wear due to rail grinding makes the rail wear rate not a linear function of curve radius in the logarithm scale (as is the case for natural wear. Comparing the wear data between 2012 and 2019, the effect of the preventive grinding strategy in Belgium is clearly shown.

(4) when the rail wear rate is calculated in mm/100MGT, the rail wear shows to be much faster in less busy traffic lines. However, when the rail wear rate is calculated in mm/year, the higher the tonnage, the higher the rail wear rate. Wear rate analyses are recommended per UIC class, thus for better-guided maintenance.

(5) the rail wear rates do not show significant variations with changes in rolling stock over the years, which implies that the estimated wear rates in this paper could also possibly hold for other networks.

There are still gaps in the current knowledge of rail steel wear data and wear mechanisms. For example, in further research, the role of corrosion in low-loaded lines is to be quantified and analyzed, including its influences on wear and its possible consequences on rolling contact fatigue. Further research can also be done to derive the wear laws for each point of the rail profile by simulating the wear process of the Belgium railway network [22]. Such simulation can be done with vehicle dynamic modeling considering detailed wheel-rail contact solution [3]. The wear can be assumed to be

proportional to the local frictional work in the contact patch [3, 23]. The simulated worn profile should match the measured profiles. Such wear laws can then be used for predicting the evolution of the rail profiles and for optimizing monitoring and maintenance procedures of rail [24]. Many railway networks have rolled out a preventive grinding strategy in recent decades. The magic wear rate needed to control preventive maintenance depends on the annual tonnage. Further research on how RCF evolves (mm/ton and mm/year) in lines with different annual tonnages, including the findings on wear behavior obtained in this paper, is needed.

# REFERENCES



[1] Krause H, Poll G. Wear of wheel–rail surfaces. Wear. 1986; 113: 103-122.

[2] Zoeteman A, Dollevoet R, Li Z. Dutch research results on wheel/rail interface management: 2001-2013 and beyond. Proceedings of the Institution of Mechanical Engineers, Part F: Journal of Rail and Rapid Transit. 2014; 228(6): 642-651.

[3] Li Z. Wheel-rail rolling contact and its application to wear simulation. PhD thesis, Delft University of Technology, 2002.

[4] Li Z, Kalker J. Simulation of severe wheel-rail wear. Transactions on the Built Environment. 1998; 34: 393-402.

[5] Enblom R. Berg M. Proposed procedure and trial simulation of rail profile evolution due to uniform wear. Proceedings of the Institution of Mechanical Engineers, Part F: Journal of Rail and Rapid Transit. 2008; 222(1): 15-25.

[6] Ranjha S, Mutton P, Kapoor A. Effect of head wear and lateral forces on underhead radius crack propagation. Proceedings of the Institution of Mechanical Engineers, Part F: Journal of Rail and Rapid Transit. 2014; 228(6): 620-630.

[7] Christoforou P, Fletcher D, Lewis R. Benchmarking of premium rail material wear. Wear. 2019; 436-437, 202990.

[8] Lewis R, Olofsson U. Mapping rail wear regimes and transitions. Wear. 2004; 257: 721-729.

[9] Olofsson U, Nilsson R. Surface cracks and wear of rail: a full-scale test on a commuter train track. Proceedings of the Institution of Mechanical Engineers, Part F: Journal of Rail and Rapid Transit. 2002; 216: 249-264.

[10] Olofsson U, Terriskivi T. Wear, plastic deformation and friction of two rail steels-a full-scale test and a laboratory study. Wear. 2003; 254 (1-2): 80–93.

[11] Li W, Wang P, Wang S, et al. Wheel–rail wear simulation and rail cant optimization based on railway vehicle dynamics. International Journal of Vehicle Performance. 2021; 7(1–2) 4–20.

[12] Chang C, Wang C, Chen B, et al. A Study of a numerical analysis method for the wheel–rail wear of a heavy haul train. Proceedings of the Institution of Mechanical Engineers, Part F: Journal of Rail and Rapid Transit. 2010; 224(5) 473–482.

[13] Ignesti M, Malvezzi M, Marini L, et al. Development of a wear model for the prediction of wheel and rail profile evolution in railway systems. Wear. 2012; 284–285:1–17.

[14] Innocenti A, Marini L, Meli E, et al. Development of a wear model for the analysis of complex railway networks. Wear. 2014; 309(1):174–191.

[15] Butini E, Marini L, Meacci M, et al. An innovative model for the prediction of wheel–rail wear and rolling contact fatigue. Wear. 2019; 436–437:203025.

[16] Wang H, Wang W, Han Z, et al. Wear and rolling contact fatigue competition mechanism of different types of rail steels under various slip ratios. Wear. 2023; 522, 204721.

[17] EN13674-1. Railway applications - Track - Rail Part 1: Vignole railway rails 46 kg/m and above. 2011.

[18] Wei K, Chen R, Xu Y. Rail profile wear on curve and its effect on wheel-rail contact geometry. Advanced Materials Research. 2013; 779-780: 655-659.

[19] UIC (International Union of Railways). Classification of lines for the purpose of track maintenance. Paris: Leaflet 714 R, International Union of Railways; 1989.

[20] Lichtberger B. Track compendium: track system, substructure, maintenance, economics. Hamburg: DVV Media Group GmbH Eurailpress; 2011.

[21] Stock R, Pippan R. RCF and wear in theory and practice-The influence of rail grade on wear and RCF. Wear. 2011; 471: 125-133.

[22] Zobory I. Prediction of wheel/rail wear. Vehicle System Dynamics. 1997; 28: 221–259.

[23] Ignesti M, Innocenti A, Marini L, et al. Development of a wear model for the wheel profile optimization on railway vehicles. Vehicle System Dynamics. 2013; 51(9):1363–1402.

[24] Bosso N, Magelli M, Zampieri N. Simulation of wheel and rail profile wear: a review of numerical models. Railway Engineering Science. 2022; 30, 403–436.

# 3

# STATISTICAL ANALYSIS AND TREATMENT METHOD OF HEAD CHECKS ON THE BELGIAN RAILWAY NETWORK

*This chapter investigates the growth and treatment of a major type of rail rolling contact fatigue (RCF) known as head checks (HCs). The analysis is based on extensive field data of 212 curved tracks made of R260 steel across the entire Belgian railway network. The HC crack depth was mainly measured by eddy current testing. The growth rates of HCs are analyzed in relation to the curve radius, annual traffic load, and rail wear. The key findings are as follows: 1) Tracks with radii between 750 and 1000 m exhibit the highest HC growth rate of about 1.5 mm per 100 million gross tons (MGT) and the largest occurrence probability of about 25%; 2) A counterintuitive result is found that both the HC growth and rail wear rates per MGT are higher on lines with lower annual traffic loads; 3) The artificial wear method to control RCF, such as preventive grinding, should consider annual traffic load and service time, rather than solely on accumulated tonnage as is current practice. Based on these findings, a new method is proposed to estimate the magic wear rate for the Belgian railways, which can serve as input for optimising grinding operations to mitigate HCs.*

Apart from minor updates, this chapter has been published as: Tim Vernaillen, Pan Zhang, Alfredo Núñez, Rolf Dollevoet, Zili Li. Statistical analysis and treatment method of head checks on the Belgian rail network. International Journal of Fatigue, Volume 203, February 2026, 109349

3

## 3.1. INTRODUCTION

Rail defects caused by rolling contact fatigue (RCF) pose an increasing challenge to the railway industry worldwide [1-3]. They are a significant factor driving the cost of rail maintenance and renewal, and are expected to occur more frequently due to growing demands for rail services. Head checks (HCs) are a major type of RCF defect, characterised by clusters of inclined, closely spaced cracks in the rail shoulder or gauge corner [4, 5]. Infra managers of railway networks worldwide have implemented various strategies to detect [6], assess [7], mitigate, and prevent HCs [8-10]. Since 2015, Infrabel, the Belgian rail infrastructure manager, has experienced a steady annual rise in maintenance costs related to HCs, including the need for additional testing, preventive grinding, corrective milling, and rail renewal. To better control the life cycle cost for rails, there is an urgent need to develop more effective treatment methods for HCs, on the basis of a deeper understanding of the HC development.

HCs typically occur on the outer rails of curves with radii between 500 m and 3000 m [11]. Previous studies have investigated the initiation and growth of HCs through numerical simulations [12-15], laboratory tests [16-18] and field monitoring [19-21]. On curved tracks, the wheel flange frequently contacts the shoulder or gauge corner of the outer rail due to the angle of attack and centrifugal forces of the train. The resulting lateral and spin creepages, combined with the possible longitudinal creepage from traction or braking, generate high shear stresses at the wheel-rail interface. These stresses cause cyclic plastic deformation of rail materials, triggering the initiation of HCs [12, 22, 23]. Once initiated, cracks can propagate deeper into the rail material, a process accelerated by tractive forces [14] and fluid entrapment within cracks [24-26], although this mechanism remain subject of ongoing debate. While existing research predominantly investigates HC formation under specific loading conditions on particular track sections, large-scale statistical analyses of HC growth across entire railway networks remain scarce.

Several countermeasures have been applied to mitigate HCs, such as anti-stress rail profile [11, 27], lubrication [28], and rail grinding [29]. Among these, preventive grinding is widely used in practice, with grinding intervals often based on accumulated

tonnage. However, the growth of HCs is influenced not only by total accumulated tonnage but also by various parameters, including curve radius, steel grade, and wear [21]. Therefore, effective preventive grinding strategies must account for these operational complexities and diverse track parameters and conditions. The optimal grinding interval should achieve a balance between adequately preventing RCF defects and avoiding excessive grinding that can shorten rail life. This concept aligns with the concept of the 'magic' wear rate (MWR), which represents the practical balance between wear and RCF damage on rails [30, 31]. The MWR represents an optimal combination of natural and artificial material removal that effectively controls rolling contact fatigue without unnecessarily accelerating rail degradation. To the best knowledge of the authors, the MWR for HCs treatment has not yet been defined quantitatively, highlighting the need for large-scale comprehensive analyses of entire railway networks to account for the different HC growth rates under complex operational conditions.

This paper aims to enhance the understanding of HC growth by a statistical analysis. To achieve this goal, an extensive investigation was carried out on HCs from 212 curved track sections across the whole Belgian railway network, covering various track curvatures and train loading conditions. Based on this analysis, a more effective HC treatment approach using preventive grinding and MWR is proposed. The structure of this paper is organised as follows. Section 2 describes the field conditions, development phases, and assessment methods of HCs. Section 3 presents and discusses the HC growth rates in relation to the curve radius, accumulated tonnage, annual traffic, and rail wear. Section 4 evaluates the effectiveness of the current grinding policy on controlling HCs and proposes an optimal grinding strategy, i.e., an MWR for the Belgian network. The main conclusions are summarised in Section 5.

## 3.2. FIELD MONITORING METHODS OF HCS

This section first introduces the typical development phases of HCs and the nondestructive testing methods used for their detection. Afterwards, we take the HCs in the Belgian railway network for the case study and describe the quantitative assessment methods of HC growth rates.

### 3.2.1. DEVELOPMENT PHASES AND DETECTION METHODS OF HCS

In general, the development of HCs can be divided into three phases, following the empirical approach proposed in [21]. Fig. 3.1 shows some typical HC cracks observed in the Belgian railway network. Phase I is the initial crack formation with depths smaller than 0.1 mm, typically during the first 5–10 MGT of traffic. In Phase II (depth between 0.1 and 5.0 mm), HCs show a relatively low and uniform crack growth into the rail at a shallow angle of approximately 15–30°, with a typical rate of around 1.0 mm/100 MGT in the vertical direction [21]. In this phase, corrective maintenance by grinding or milling could be performed for HC treatment. In Phase III (depth larger than 5.0 mm), cracks develop horizontally with vertical branches at a considerably fast growth rate up to 1 mm/ 1 MGT [21], and thus, they are rather short-duration events. In this phase, corrective maintenance is not possible, and rail replacement is almost inevitable to avoid rail breakage. Figs. 1e and 1f show two examples of the further rail degradation due to HCs. It is important to note that this empirical classification is derived from a large field database and intended to reflect general trends in HC development. It may not capture the full complexity of individual crack formation processes.

Two nondestructive testing methods are usually used to detect the rail cracks: the eddy current testing (ECT) and the ultrasonic testing (UT) methods. The ECT is sensitive to the conditions at the rail surface [32], and is suitable to detect clusters of HC cracks in Phase II with depths from 0.1 to 5.0 mm. The UT mainly detects local and deep cracks, which can be used to measure the dangerous transverse defects of HC cracks in Phase III above 5.0 mm. The HC cracks in Phase I may begin to appear visually to the naked eye, but they are below the detection threshold of both ECT and UT systems.

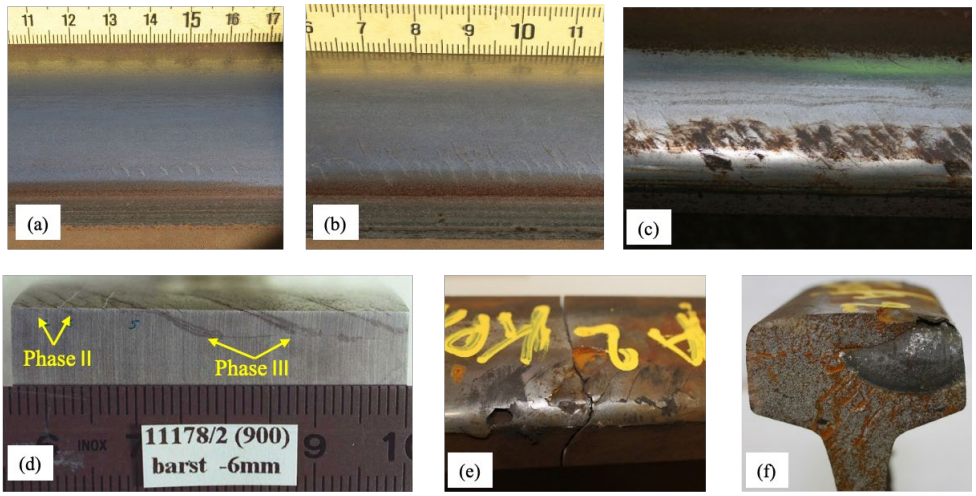


**Fig. 3.2**. Different development phases of HCs in the Belgian railway network. (a) Phase I: initial crack formation; (b) Phase II: uniform crack growth into the rail; (c) Phase III: cracks develop horizontally with vertical branches, with a significant rise in the crack growth rate; (d) a cross-section of Phases II and III HCs along the middle of the running band (not the same rail as in (c)); (e) Rail surface breakage due to HCs; (f) Transverse HC fatigue crack of Phase III.

### 3.2.2. HCS IN THE BELGIAN RAILWAY NETWORK

By 2000, HCs were registered by visual inspection on the Belgian rail network. Afterwards, UT on a dedicated test vehicle was employed in the entire network for HC detection, as shown in Fig. 2a. However, UT mainly measures moderate and severe cracks, e.g., with depths more than 5.0 mm, and cannot identify the small HCs in the early stage. It is reported that the number of rail breaks due to HCs increased from 0 in 2010 to 12 in 2014. Therefore, since 2014, the ECT system has been installed in the test vehicle to detect HCs. This system consists of ten vertical spring-loaded probes across the full width of the rail head (see Fig. 2b), to detect vertical crack depth (see Fig. 3.2c) ranging from 0.1 to 5.0 mm. Data collected from all ten probes were at 1mm intervals along the track, with a depth resolution of 0.1 mm. The ECT and UT in Belgium used a commercial system provided by Sperry, operating at speeds of up to 50 km/h. This system is designed to operate reliably across a wide range of environmental and operational conditions, and has been widely deployed in many

countries including Belgium, the UK, Germany, the United States, and China. The reported inspection accuracy ranges between 85% and 95%, depending on track conditions and refers to defect detection performance (i.e., the correct identification of defect presence).

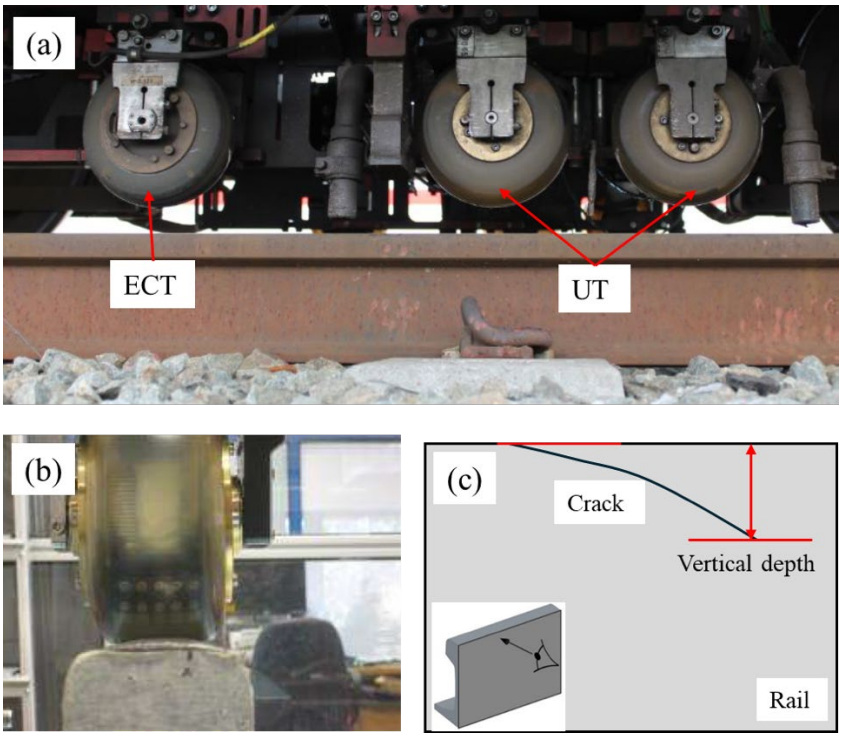


**Fig. 3.2**. Field ECT and UC systems in a dedicated test vehicle in Belgium. (a) The test vehicle; (b) the ECT system; (c) a schematic drawing of the HC depth measurement by ECT.

To prevent HCs, Infrabel launched a cyclic grinding program on UIC classes 1 to 4 lines (defined below in Equation (1) [33], $TL_i$ refers to the measured traffic load for track Section *i*) in 2012, which implied a rail removal of 0.25 mm per 80 MGT on both curves and tangent tracks. This was found to be insufficient to avoid HCs. Since 2016, the grinding strategy has been changed to 0.25 mm per 60 MGT on tangent tracks and 0.25 mm per 25 MGT in curves for all UIC classes 1 to 6. This program results in a decrease in HCs of both Phase II (375 km with HCs in 2016 compared to 125 km in 2023) and Phase III (411 new

individual cracks from UT in 2014 compared to 38 in 2022). We also observe a significant reduction in the number of rail breaks caused by HCs, which is 12 in total from April 2014 to March 2015, compared to 1 from April 2022 to March 2023.

$$\mathrm{UIC}_i = \begin{cases} \mathrm{UIC1} & \text{if } 130000[\mathrm{ton/day}] < \mathrm{TL}_i \\ \mathrm{UIC2} & \text{if } 80000[\mathrm{ton/day}] < \mathrm{TL}_i \leq 130000[\mathrm{ton/day}] \\ \mathrm{UIC3} & \text{if } 40000[\mathrm{ton/day}] < \mathrm{TL}_i \leq 80000[\mathrm{ton/day}] \\ \mathrm{UIC4} & \text{if } 20000[\mathrm{ton/day}] < \mathrm{TL}_i \leq 40000[\mathrm{ton/day}] \\ \mathrm{UIC5} & \text{if } 5000[\mathrm{ton/day}] < \mathrm{TL}_i \leq 20000[\mathrm{ton/day}] \\ \mathrm{UIC6} & \text{if } \mathrm{TL}_i \leq 5000[\mathrm{ton/day}] \end{cases} \quad (1)$$

The analysis in this work was mainly based on the extensive field data across the entire Belgian network in 2019. The curves of R260 rails with radii smaller than 3000 m were considered, amounting to a total of 1429 km among the 3113 km of measured tracks. For these curves, the grinding interval was 0.25 mm/80 MGT between 2012 and 2016, and has been 0.25 mm/25 MGT since 2016. It is worth noting that from 2012 to 2019, some lines might have undergone less grinding than others in practice, due to the initial trial and implementation of preventive grinding programs during these periods, such as for UIC 4 lines [33]. Only HCs in Phase II, as detected by ECT, were analysed, since their slow and uniform crack growth makes it reasonable to define an average growth rate for them. This analysis covered 212 curves with a total length of 172 km. These rails are on conventional railway lines with mixed passenger and freight traffic, excluding high-speed and freight lines. Two rail profiles are used: the UIC60E1 profile and the Belgian 50E2 profile according to the standard EN 13,674–1 [33]. These two profiles have different geometrical dimensions, but the same nominal curvature across the rail head, including gage corner and the same rail head width, and thus the same wheel-rail contact geometries. The rail inclinations were both 1:20, with a nominal track gauge of 1435 mm. The complete network was measured twice a year with the vehicle EM130 to record the track parameters every 25 cm, such as the longitudinal and vertical profiles and rail cant. Another dedicated vehicle equipped with UT and ECT measurement systems was used to detect cracks twice a year.

### 3.2.3. ASSESSMENT METHODS OF HCS

This work mainly analyses the influence of the track radius and annual tonnage on the growth rates of HCs. Fig. 3a shows the locations of the 212 curves with HCs across the Belgian railway network, indicated by the red lines. The average HC depth $h_{t,c}$ in each is defined as follows,

$$h_{t,c} = \frac{1}{x_{t,c}^{\text{end}} - x_{t,c}^{\text{ini}}} \sum_{j=x_{t,c}^{\text{ini}}}^{x_{t,c}^{\text{end}}} \max_{p\in\{1,\ldots,P\}} d_{t,c,j,p} \tag{2}$$

where $d_{t,c,j,p}$ is the vertical depth measured by probe $p$ at kilometre position point $j$ of the curve $c$ ($c$ = 1, 2,…., 212) in year $t$. $P$ is the total number of probes ($P$ =10), and $x_{t,c}^{\text{ini}}$ and $x_{t,c}^{\text{end}}$ are the kilometre position points in curve $c$ where the head check defect is first detected and where it ends in the measurement campaign conducted in year $t$.

The HC growth rate per 100 MGT is defined as follows,

$$\Delta h_{t,c}^{\text{T}} = \frac{100 h_{t,c}}{A_t \left(t - t_0\right)} \tag{3}$$

where $\Delta h_{t,c}^{\text{T}}$ is the HC growth rate of curve $c$ per 100 MGT (mm/100 MGT) in year $t$, $h_{t,c}$ in mm is the average defect depth of curve $c$ measured in year $t$, $A_t$ is the average annual traffic load in MGT in the years between $t_0$ and $t$, and $t_0$ is the year of the rail installation. It is worth noting that the measured HC growth rate represents the residual or net crack growth, i.e., the portion of crack growth that remains after accounting for the rail wear. Mathematically, the total crack growth would be approximately the sum of the measured crack growth and the material removed through wear.

The HC growth rate per year since the installation of the rails is calculated as follows:

$$\Delta h_{t,c}^{\mathrm{Y}} = \frac{h_{t,c}}{t - t_0} \tag{4}$$

where $\Delta h_{t,c}^{\mathrm{Y}}$ is the HC growth rate per year in mm/year measured in year *t*.

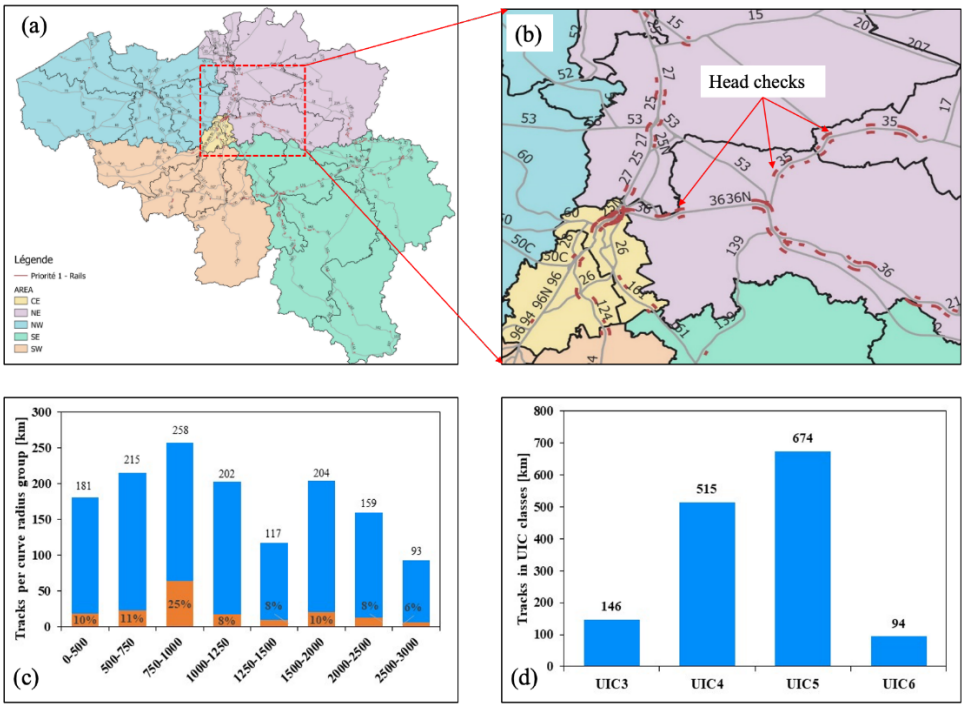


**Fig. 3.3.** Statistical data of HCs in the Belgian rail network. (a) The analysed curved tracks with HCs across the entire Belgian rail network; (b) zoom-in of a certain area of (a); (c) the total mileage of tracks per curve radius group in blue, with the percentage of tracks with HCs in orange. (d) division of the analysed curves into UIC classes.

The track curve radius is divided into the following eight groups:

$$R_i = \begin{cases} 1 & \text{if} \quad R \le 500\text{m} \\ 2 & \text{if} \quad 500\text{m} \le R \le 750\text{m} \\ 3 & \text{if} \quad 750\text{m} \le R \le 1000\text{m} \\ 4 & \text{if} \quad 1000\text{m} \le R \le 1250\text{m} \\ 5 & \text{if} \quad 1250\text{m} \le R \le 1500\text{m} \\ 6 & \text{if} \quad 1500\text{m} \le R \le 2000\text{m} \\ 7 & \text{if} \quad 2000\text{m} \le R \le 2500\text{m} \\ 8 & \text{if} \quad 2500\text{m} \le R \le 3000\text{m} \end{cases} \tag{5}$$

where $R_i$ is the number of a curve radius group where track segment $i$ belongs, and $R$ is the measured radius. Fig. 3.3b presents the total mileages of tracks per curve radius group (in blue) and the percentage of tracks with HCs (in orange). All track sections are also assigned to a specific UIC class depending on the annual MGT, as shown in Fig. 3.3c. Given the negligible track length in the UIC1 and UIC2 classes, they are not considered in this analysis. All the measurements from different databases and measuring vehicles were merged into a single data set and averaged per 50 m, for the same rail grade, profile, curve radius and annual tonnage. The transition curves are also included and averaged per 50 m.

## 3.3. RESULTS AND DISCUSSIONS OF HC GROWTH RATES

In this section, the growth rate of HCs in Phase II is analysed with different track radii and traffic loads. The relationship between HC growth and rail wear is also investigated.

### 3.3.1. HC GROWTH RATE VERSUS TRACK RADIUS

Fig. 3.4 shows the HC growth rates of R260 rails in relation to the track radius, based on statistical data from all 212 curves measured in 2019. It can be seen that the HC growth rate initially increases from about 1.0 mm/100 MGT for curves with radii of 0-500 m, reaching a peak at 1.5 mm/100 MGT in the 750–1000 m range. Afterwards, the growth rate gradually declines with increasing track radius, and reaches a minimum of about 0.4 mm/100 MGT for curves with radii between 2500-3000 m. Combined with Fig. 3.3b, it is found that curves with radii between 750-1000 m have not only the highest HC growth rates, but also the largest HC occurrence probability (25 %), in contrast to only 6%-11% on the other curves.

The variation trend of HC growth rates with respect to the curve radius can be qualitatively explained by the competing mechanisms between wear and RCF [19, 34, 35]. In curves with relatively smaller radii, the friction energy is generally higher, promoting the development of RCF defects. This explains the overall decline in HC growth rates as the curve radius increases beyond 1000 m. However, on tight curves with very small radii (e.g., below 750 m), wear caused by the friction becomes a more dominant damage mechanism that suppresses the RCF by removing the surface-initiated cracks before they have a chance to grow. This interplay explains the initial rise of the HC growth rate as the radius increases within 750 m.

Overall, the HC growth rates of R260 rails in the Belgian rail network are in the range of 0.4-1.5 mm/100 MGT across the curve radii. These values are generally comparable to, but somewhat lower than, the growth rates reported for the DB network, which ranges from 0.8 to 2.0 mm/100 MGT [21]. Several factors may account for this deviation, including differences in the dataset size (212 curves in the current analysis versus 47 curves in the DB study) and variations in rolling stock characteristics. Belgium started the modernisation of its rolling stock in 2016, whereas Germany began this process several years earlier. In addition, some statistical uncertainty in the growth rate calculations may occur, influenced by factors such as cant deficiency and the accuracy limitations of ECT systems.

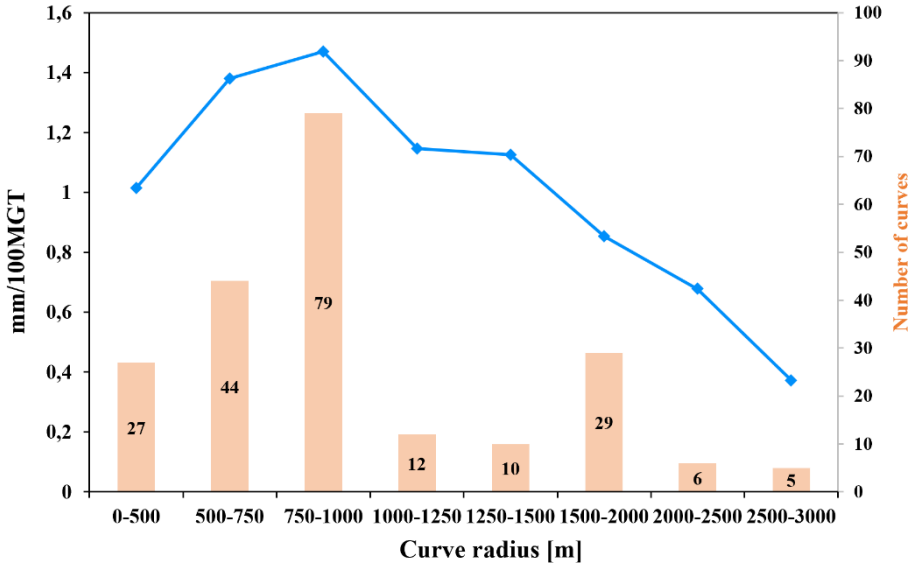


**Fig. 3.4.** HC growth rates of R260 rails as a function of the curve radius measured in 2019.

### 3.3.2. HC GROWTH VERSUS ANNUAL TRAIN LOAD AND UIC CLASS

Fig. 3.5a shows the relationship between the HC growth rates and annual tonnage, based on data from all the 212 curves. The curves were grouped by their crack growth rates per 100 MGT, and the average annual tonnage was then calculated for each group. A counterintuitive trend is observed: HC growth rates are higher on railway lines with lower annual tonnage. This observation provided the basis for further analysis, where the growth rates were subdivided according to the different UIC classes, expressed as a function of annual train load. A similar observation was reported for rail wear in [33], where the wear rates were found to be higher on lower-loaded lines. Since HC growth is expressed in mm/100 MGT, tracks with lower annual tonnage take longer service time to reach the same cumulative load. This suggests that time-related factors, such as fluid pressurisation within cracks [25] or crack-tip corrosion [36], play a significant role in HC development. Therefore, annual train load and the corresponding service time should be considered as a critical factor for HC, together with the cumulative traffic load.

To further investigate this phenomenon, Fig. 5b presents the HC growth rates across different UIC line classes. The results show that HC growth is more pronounced on low-loaded lines. Specifically, the growth rate on UIC4 lines is approximately twice that of UIC3, and about half that of UIC5. These findings highlight the importance of annual load and service time in influencing HC development. In addition, Fig. 3.5b shows that for both UIC3 and UIC4 lines, the fastest HC growth occurs on curves with radii between 750 and 1250 m, consistent with the trends in Fig. 3.4.

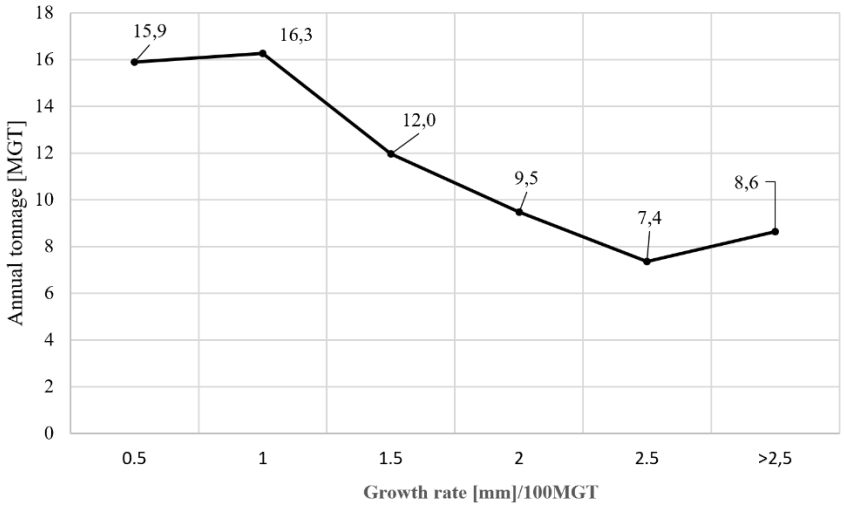


(a)

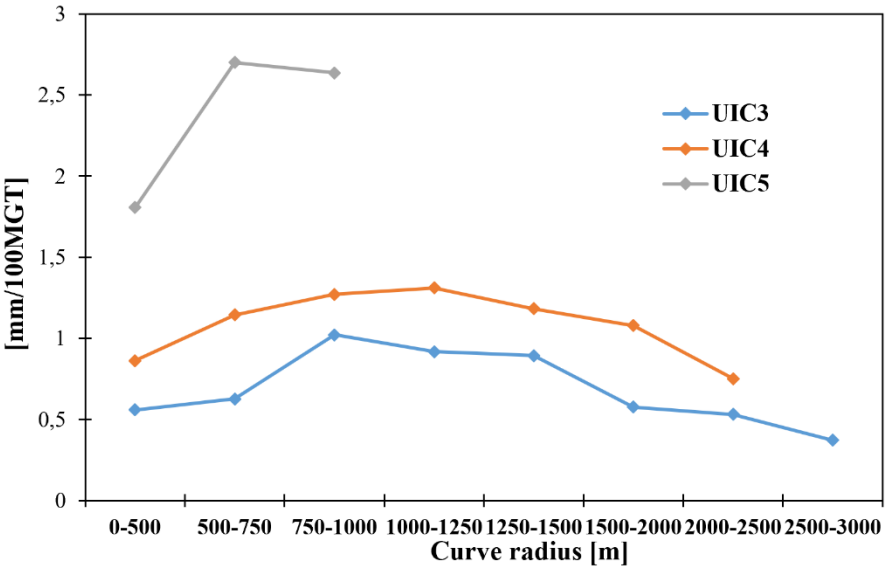


(b)

**Fig. 3.5.** The effect of annual train load on HC growth. (a) HC growth in relation to average annual tonnage; (b) HC growth for UIC3, UIC4 and UIC5 classes.

### 3.3.3. HC GROWTH PER YEAR

In the analyses above, the HC growth rate was expressed in mm/100 MGT, as defined in Equation (3). In this section, the HC growth rate is evaluated in mm/year since the rail installation, based on Equation (4). The wear induced by grinding is not considered in this analysis, as the field measurements indicate that the curves with HCs show an average wear rate similar to that measured in 2012 before the implementation of the preventive grinding strategy. Fig. 3.6 shows the annual HC growth rates per UIC group as a function of curve radius. The overall trend in relation to radius is similar to that observed in mm/100 MGT: annual HC growth rate initially increases with curve radius, reaching a peak in the range of 750–1250 m, and then decreases with further increases in radius.

When evaluated on a time basis (mm/year), HC growth rates increase on higher-loaded lines, in contrast to the trend observed when normalised by tonnage (mm/MGT). Higher daily loads result in greater HC growth per year as expected, but the rate of increase

is not proportional to the increase in daily load. For example, on curves with radii between 750 and 1000 m, the HC growth rate rises only slightly, from 0.14 mm/year on UIC4 lines to 0.16 mm/year on UIC3 lines, despite the nearly doubled daily load. This indicates that traffic load alone does not fully explain the variation in HC growth. Other contributing factors, such as fluid pressurisation within cracks and crack-tip corrosion, as discussed in Section 3.2, likely play a significant role in driving crack development.

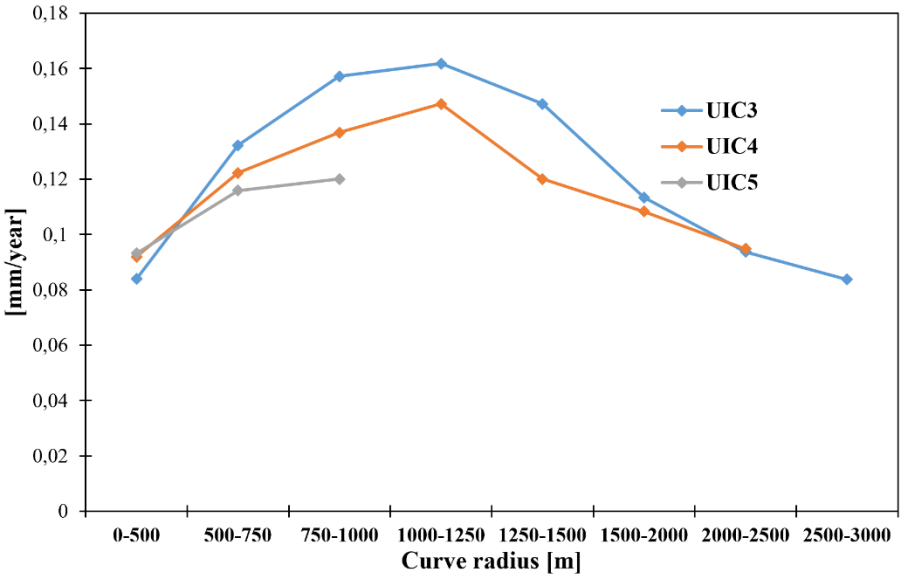


**Fig. 3.6.** HC growth in mm per year as a function of curve radius and track classes.

### 3.3.4. THE RELATIONSHIP BETWEEN HC GROWTH AND RAIL WEAR RATE

This section presents the field statistical data to illustrate the competing mechanisms between rail wear and RCF, as shown in Fig. 3.7. The analysis focuses on rail wear measured at 45° [33], including both the natural wear caused by wheel-rail interaction and corrosion, and the artificial wear from the preventive grinding. Wear rate is calculated as the amount of rail material (in millimetres) removed per 100 MGT of traffic.

Fig. 3.7a shows that the rail wear rate per tonnage for UIC3 and UIC4 lines generally decreases linearly with increasing curve radius. This observation supports the

claim made in Section 3.1 that tighter curves have higher frictional energy. Notably, the wear rate on UIC4 lines is approximately 50% higher than that on UIC3 lines. In curves with radii smaller than 750 m, the average wear rate significantly suppresses the HC development, as material removal prevents crack initiation and growth. In contrast, on curves with radii between 750 m and 1500 m, the average HC growth rate exceeds the average wear rate, indicating that RCF becomes the dominant damage mechanism in this range. By comparing HC and wear rates for curves with radii below 750 m and those between 750 m and 1500 m, it can be seen that artificially increasing the wear rate, e.g., through preventive grinding, can substantially reduce HC growth.

Beyond a radius of 1500 m, the HC growth rate decreases more sharply than the wear rate. This behaviour is likely due to the formation mechanism of HCs, which require wheel–rail contact stresses to exceed a critical threshold that leads to ratcheting and subsequent crack initiation [12]. For example, for UIC3 lines, on curves with radii larger than approximately 1500 m, contact stresses may fall below this threshold, resulting in reduced HC formation. Unlike HC, rail wear does not have a defined initiation threshold and therefore decreases more gradually with increasing radius.

Fig. 3.7b shows the annual rail wear and HC growth rates as a function of curve radius, showing a trend similar to the tonnage-based analysis. It can be seen that the average HC growth rates per year are comparable for UIC3 and UIC4 lines. This suggests that, when considered on a time basis, HC defects on low-loaded tracks can develop at rates similar to those on more high-loaded lines. This finding has important implications for the design of preventive grinding strategies. For low-loaded tracks, the annual increase in wear is less effective in suppressing HCs compared to that in high-loaded lines. As a result, even tight curves on low-loaded tracks may be vulnerable to HC formation. This can be supported by the data in Fig. 3.7b that the HC growth rate for curves with radii below 500 m, is higher on UIC4 than on UIC3 lines.

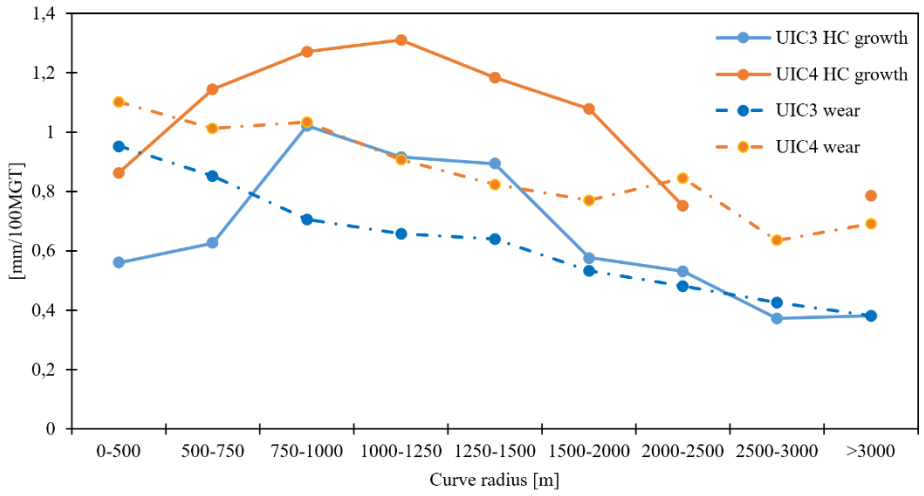


(a)

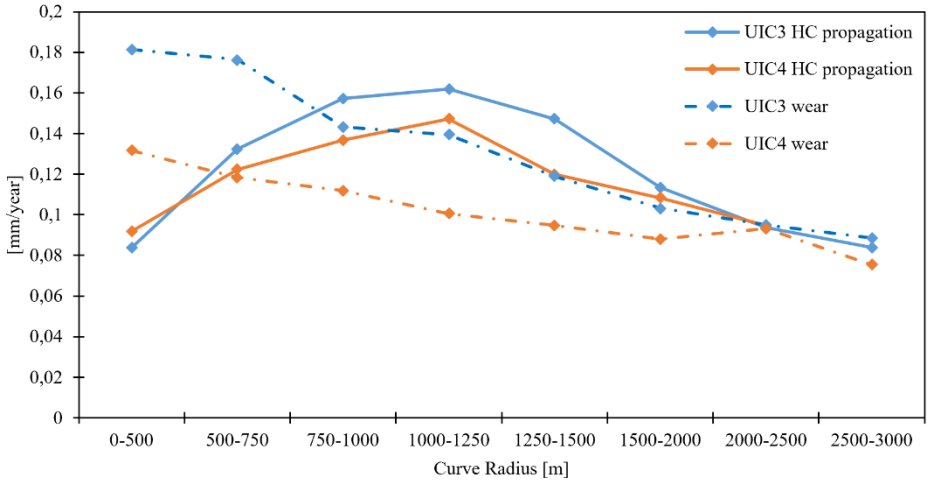


(b)

**Fig. 3.7.** The relationship between HC growth and wear rates. (a) HC growth and rail wear per tonnage as a function of curve radius; (b) HC growth and rail wear per year as a function of curve radius.

## 3.4. ESTIMATION OF MWR FOR HC TREATMENT

Preventive grinding strategies have been implemented across European railway networks to control RCF defects. The intervals between successive grinding campaigns have been typically determined based on cumulative tonnage, with typical values ranging from 15 to 25 MGT. However, as shown in the analysis above, HC growth is influenced not only by cumulative tonnage but also by the annual traffic load and time. In this section, we first evaluate the effectiveness of the current grinding policy in mitigating HC development. Afterwards, we propose a new approach for defining the optimal grinding strategy, referred to as the MWR, which is derived from the statistical data of the natural wear rates and HC growth rates across the Belgian railway network. The analysis focuses on UIC3, UIC4 and UIC5 line classes, which represent the majority of the rail networks in Belgium.

### 3.4.1. EVALUATION OF THE EFFECTIVENESS OF THE CURRENT GRINDING POLICY

In Belgium, Infrabel has implemented a preventive grinding interval of 25 MGT for curves on UIC1-6 lines since 2016. The material removal per grinding campaign is approximately 0.25 mm, corresponding to an artificial wear rate of 1.0 mm/100 MGT. Under this grinding policy, the total wear rates are calculated per UIC-class using the equations below.

$$W_{tot} = W_n + W_a = W_n + 100 G_d / G_i \tag{6}$$

where $W_{tot}$ is the total wear rate in mm/100 MGT; $W_n$ is the natural wear rate caused by traffic load and corrosion; $W_a$ is the artificial wear rate introduced from preventive grinding; $G_d$ is the grinding depth per interval (0.25 mm); $G_i$ is the traffic load every grinding interval (25 MGT). Given that head checks exhibit the fastest growth in curves with radii between 750 m and 1500 m, the calculations in Table 1 are limited to this radius range. The corresponding natural, artificial, and total wear rates for each UIC class are summarised in Table 1.

**Table 3.1.** The wear rate per UIC class based on the current grinding policy. The natural wear data was from [33].

| UIC-Class | Annual load [MGT] | Natural wear at 45° [mm/100MGT] | Artificial wear per grinding interval [mm/25 MGT] | Total wear rate [mm/100 MGT] | Artificial wear/total wear |
|---|---|---|---|---|---|
| **UIC3** | 22 | 0.7 | 0.25 | 1.7 | 142% |
| **UIC4** | 11 | 0.9 | 0.25 | 1.9 | 111% |
| **UIC5** | 4.6 | 2.4 | 0.25 | 3.4 | 42% |

The results in Table 3.1 indicate that natural wear per 100 MGT is significantly higher on annually lower-loaded lines. Since the same grinding interval is applied across all UIC classes based on cumulative tonnage, the proportion of artificial wear relative to total wear is considerably lower for low-loaded lines than for high-loaded ones. For example, artificial wear accounts for approximately 142% of the natural wear on UIC3 lines, while it represents only about 42% on UIC5 lines. When considered from a time-based perspective, this implies that grinding on UIC3 lines occurs roughly once per year (25 MGT/22 MGT≈1), whereas for UIC5 lines, the same grinding interval corresponds to approximately one grinding campaign every five years (25 MGT/4.6 MGT≈5) due to lower annual tonnage.

Statistical data show that in 2016, about 375 km of the Belgian rail network were affected by HCs. By 2023, this number decreased to around 125 km, representing a substantial 70% reduction. This result suggests that the current preventive grinding strategy has been generally effective in reducing the overall extent of HC-affected tracks. However, a more detailed analysis reveals that despite the reduction in affected track length, the average HC growth rates in 2023 have increased compared to 2016, as shown in Table 3.2. While this increase is insignificant for UIC3 (3%), it is very pronounced in low-loaded lines, reaching up to 76% and 200% for UIC4 and UIC5, respectively. These findings indicate that a grinding interval of 25 MGT is sufficient for managing HC development on high-loaded lines like UIC3, but is inadequate for lower-loaded lines like UIC4 and UIC5. Furthermore, the data suggest that when grinding fails to fully remove existing HCs, the remaining defects may grow at an accelerated rate. More field observations and studies could be performed to further verify this finding.

**Table 3.2:** HC growth rate in 2023 with the current grinding policy.

| UIC-Class | Annual load [MGT] | HC growth rate in 2019 without grinding [mm/100MGT] | HC growth rate in 2023 with grinding [mm/100MGT] | Increase in growth rate from 2019 to 2023 |
|---|---|---|---|---|
| UIC3 | 22 | 0.9 | 1.0 | 3% |
| UIC4 | 11 | 1.3 | 2.2 | 76% |
| UIC5 | 4.6 | 2.7 | 8.0 | 200% |

### 3.4.2. MWR FOR HC TREATMENT IN BELGIUM

The current grinding policy, which is solely based on accumulated tonnage, has limitations in effectively mitigating HCs, particularly on lower-loaded lines. This is mainly because it does not account for the influence of annual load and time-related factors on HC growth. Ideally, artificial wear introduced through preventive grinding should be precisely calibrated to remove existing HCs. To achieve this balance, the concept of the MWR is introduced, which defines the optimal amount of material removal required to eliminate HCs without causing unnecessary rail material loss. The MWR can be calculated as the sum of the natural wear rate and HC growth rate, as follows:

$$MWR = W_n + W_a = W_n + \Delta h \tag{7}$$

Where $\Delta h$ is the HC growth rate in mm/100 MGT, which is obtained from the statistical data. Then we can calculate the required grinding interval based on a grinding depth of 0.25 mm as follows,

$$G_i = 100 G_d / \Delta h \tag{8}$$

Table 3.3 summarizes the calculated MWR and the corresponding grinding interval for the UIC3, UIC4, and UIC5 lines. When compared with the values in Table 3.2, it is found that for UIC3, the MWR is slightly lower than the total wear rate, and the proposed grinding interval of 27.8 MGT is higher than the current strategy of 25 MGT. This suggests that the existing grinding policy is adequate for controlling HC growth on UIC3 lines. However, for lower-loaded UIC4 and UIC5 curves, the MWR is significantly larger than the total wear rate, indicating that the current grinding interval of 25 MGT is too large to effectively

manage HC development. Based on the MWR analysis, the optimal grinding intervals should be approximately 19.2 MGT for UIC4 and 9.2 MGT for UIC5. The insufficient grinding frequency on these lines may explain the accelerated HC growth rates observed in Table 3.2. These findings highlight the need for different grinding strategies that consider both cumulative tonnage and annual traffic load, particularly for low-loaded tracks.

**Table 3.3** The calculated MWR as the sum of the natural wear rate and HC growth rate.

| UIC-Class | Annual load [MGT] | Natural wear at 45° [mm/100MGT] | HC growth rate in 2019 without grinding [mm/100MGT] | MWR [mm/100MGT] | Proposed grinding interval [MGT] |
|---|---|---|---|---|---|
| **UIC3** | 22 | 0.7 | 0.9 | 1.6 | 27.8 |
| **UIC4** | 11 | 0.9 | 1.3 | 2.2 | 19.2 |
| **UIC5** | 4.6 | 2.4 | 2.7 | 5.1 | 9.2 |

## 3.5. CONCLUSIONS

This paper investigates the HC growth rate through a statistical analysis of data from the Belgian railway network. Extensive field data were collected and analysed from 212 curved track sections with different track radii and annual traffic loads. Crack depths were mainly measured using the eddy current testing. The HC growth rates were then compared with the corresponding rail wear rates to better understand the interplay between wear and HC. Afterwards, the effectiveness of the current grinding policy in controlling HC development has been evaluated. Based on the measured HC and wear rates, the MWR has been proposed to define the optimal grinding interval for different UIC line classes. The main conclusions are summarized as follows.

(1) The tracks with radii between 750 and 1000 m have the highest HC growth rate, reaching about 1.5 mm/100 MGT, and the largest occurrence probability of around 25%. On curves with radii less than 750 m, the rail wear becomes a more dominant damage mechanism, significantly suppressing HC growth.

(2) A counterintuitive trend is observed that HC growth per tonnage is higher on railway lines with annually lower-loaded lines, consistent with the trend observed in rail

wear rates. This result suggests the importance of time on rail damage development, together with the traffic loads.

(3) In this study, the Magic Wear Rate (MWR) is computed as the sum of the natural wear rate and the head-check (HC) growth rate per UIC class on the Belgian railway network. This formulation is consistent with the commonly adopted definition of MWR as the combined material removal required to control both wear and rolling contact fatigue damage, and is here applied to the available network-specific measurement data. The resulting grinding intervals are 27.8, 19.2, and 9.2 MGT for UIC3, UIC4, and UIC5, respectively.

(4) The current preventive grinding strategy in Belgium, 0.25 mm/25MGT for all UIC curves, has been generally effective in reducing the overall extent of HC-affected tracks. However, it is insufficient for low-loaded tracks, including UIC4 and UIC5, and may accelerate the HC growth rate.

Overall, this work contributes to a better understanding of the HC growth process and provides valuable insights into the predictive maintenance strategies in the treatment of rail RCF defects. In future work, the statistical analysis on other railway networks could be performed, and the corresponding MWR could be obtained and compared to this work. Besides, it is interesting to investigate the acceleration mechanisms for HC crack growth by grinding for low-loaded track in future work.

# REFERENCES



[1] E.E. Magel, Rolling contact fatigue: a comprehensive review, (2011).

[2] Y. Muhamedsalih, S. Hawksbee, G. Tucker, J. Stow, M. Burstow, Squats on the Great Britain rail network: Possible root causes and research recommendations, International Journal of Fatigue, 149 (2021) 106267.

[3] X. Ma, W. Yin, Y. Wang, L. Liu, X. Wang, Y. Qian, Fatigue failure analysis of U75V rail material under Ⅰ + Ⅱ mixed-mode loading: Characterization using peridynamics and experimental verification, International Journal of Fatigue, 185 (2024) 108371.

[4] D. Cannon, K.O. Edel, S. Grassie, K. Sawley, Rail defects: an overview, Fatigue & Fracture of Engineering Materials & Structures, 26 (2003) 865-886.

[5] Y. Zhou, Y. Han, D. Mu, C. Zhang, X. Huang, Prediction of the coexistence of rail head check initiation and wear growth, International Journal of Fatigue, 112 (2018) 289-300.

[6] M. Ph Papaelias, C. Roberts, C.L. Davis, A review on non-destructive evaluation of rails: State-of-the-art and future development, Proceedings of the Institution of Mechanical Engineers, Part F: Journal of Rail and rapid transit, 222 (2008) 367-384.

[7] Y. Zhou, X. Zheng, J. Jiang, D. Kuang, Modeling of rail head checks by X-ray computed tomography scan technology, International Journal of Fatigue, 100 (2017) 21-31.

[8] A. Zoeteman, Life cycle cost analysis for managing rail infrastructure: Concept of a decision support system for railway design and maintenance, European Journal of Transport and Infrastructure Research, 1 (2001).

[9] A. Ekberg, B. Åkesson, E. Kabo, Wheel/rail rolling contact fatigue–Probe, predict, prevent, Wear, 314 (2014) 2-12.

[10] A. Meghoe, A. Jamshidi, R. Loendersloot, T. Tinga, A hybrid predictive methodology for head checks in railway infrastructure, Proceedings of the Institution of Mechanical Engineers, Part F: Journal of Rail and Rapid Transit, 235 (2021) 1312-1322.

[11] R.P. Dollevoet, Design of an Anti Head Check profile based on stress relief, (2010).

[12] R. Dollevoet, Z. Li, O. Arias-Cuevas, A method for the prediction of head checking initiation location and orientation under operational loading conditions, Proceedings of the institution of mechanical engineers, Part F: Journal of Rail and Rapid Transit, 224 (2010) 369-374.

[13] M. Tsujie, M. Miura, H. Chen, Y. Terumichi, A study on the initiation of head check of the low rail using multibody dynamics, Wear, 436 (2019) 202989.

[14] M.S. Nezhad, F. Larsson, E. Kabo, A. Ekberg, Finite element analyses of rail head cracks: Predicting direction and rate of rolling contact fatigue crack growth, Engineering Fracture Mechanics, 310 (2024) 110503.

[15] Y. Xie, H. Ding, Z. Shi, E. Meli, J. Guo, Q. Liu, R. Lewis, W. Wang, A novel prediction method for rolling contact fatigue damage of the pearlite rail materials based on shakedown limits and rough set theory with cloud model, International Journal of Fatigue, 190 (2025) 108654.

[16] M. Takikawa, Y. Iriya, Laboratory simulations with twin-disc machine on head check, Wear, 265 (2008) 1300-1308.

[17] F. Ren, Z. Yang, Z. Li, Experimental and numerical investigation into rolling contact fatigue crack initiation on the V-Track test rig, Engineering Failure Analysis, 170 (2025) 109206.

[18] B.H. Nguyen, A. Al-Juboori, H. Zhu, Q. Zhu, H. Li, K. Tieu, Formation mechanism and evolution of white etching layers on different rail grades, International Journal of Fatigue, 163 (2022) 107100.

[19] M. Hiensch, M. Steenbergen, Rolling Contact Fatigue on premium rail grades: Damage function development from field data, Wear, 394 (2018) 187-194.

[20] Y. Zhou, S. Wang, T. Wang, Y. Xu, Z. Li, Field and laboratory investigation of the relationship between rail head check and wear in a heavy-haul railway, Wear, 315 (2014) 68-77.

[21] R. Heyder, M. Brehmer, Empirical studies of head check propagation on the DB network, Wear, 314 (2014) 36-43.

[22] G. Donzella, M. Faccoli, A. Mazzù, C. Petrogalli, R. Roberti, Progressive damage assessment in the near-surface layer of railway wheel–rail couple under cyclic contact, Wear, 271 (2011) 408-416.

[23] C.L. Pun, Q. Kan, P.J. Mutton, G. Kang, W. Yan, Ratcheting behaviour of high strength rail steels under bi-axial compression–torsion loadings: Experiment and simulation, International journal of fatigue, 66 (2014) 138-154.

[24] S. Bogdański, P. Lewicki, 3D model of liquid entrapment mechanism for rolling contact fatigue cracks in rails, Wear, 265 (2008) 1356-1362.

[25] D. Fletcher, P. Hyde, A. Kapoor, Modelling and full-scale trials to investigate fluid pressurisation of rolling contact fatigue cracks, Wear, 265 (2008) 1317-1324.

[26] S. Zhang, H. Zhao, H. Ding, Q. Lin, W. Wang, J. Guo, P. Wang, Z. Zhou, Effect of vibration amplitude and axle load on the rail rolling contact fatigue under water condition, International Journal of Fatigue, 167 (2023) 107329.

[27] R. Smallwood, J. Sinclair, K. Sawley, An optimization technique to minimize rail contact stresses, Wear, 144 (1991) 373-384.

[28] D. Fletcher, J. Beynon, The effect of intermittent lubrication on the fatigue life of pearlitic rail steel in rolling-sliding contact, Proceedings of the Institution of Mechanical Engineers, Part F: Journal of Rail and Rapid Transit, 214 (2000) 145-158.

[29] S.L. Grassie, Rolling contact fatigue on the British railway system: treatment, Wear, 258 (2005) 1310-1318.

[30] J. Kalousek, Achieveing a balance: The'magic'wear rate, Railway Track & Structures, (1997).

[31] E. Magel, J. Kalousek, P. Sroba, Chasing the magic wear rate, in: Proceedings of the second international conference on railway technology: research, development and maintenance, Paper, 2014.

[32] J. Rajamäki, M. Vippola, A. Nurmikolu, T. Viitala, Limitations of eddy current inspection in railway rail evaluation, Proceedings of the Institution of Mechanical Engineers, Part F: Journal of Rail and Rapid Transit, 232 (2018) 121-129.

[33] T. Vernaillen, L. Wang, A. Núñez, R. Dollevoet, Z. Li, Rail wear rate on the Belgian railway network–a big-data analysis, International Journal of Rail Transportation, (2023) 1-16.

[34] G. Donzella, A. Mazzù, C. Petrogalli, Competition between wear and rolling contact fatigue at the wheel—rail interface: some experimental evidence on rail steel, Proceedings of the Institution of Mechanical Engineers, Part F: Journal of Rail and Rapid Transit, 223 (2009) 31-44.

[35] H. Wang, W. Wang, Z. Han, Y. Wang, H. Ding, R. Lewis, Q. Lin, Q. Liu, Z. Zhou, Wear and rolling contact fatigue competition mechanism of different types of rail steels under various slip ratios, Wear, 522 (2023) 204721.

[36] K. Wang, T. Bai, J. Xu, H. Zhu, Y. Qian, X. Wang, R. Chen, P. Wang, Investigation into the mechanisms of Corrosion-Induced rolling contact fatigue crack initiation and propagation in pearlitic rails, Engineering Failure Analysis, 163 (2024) 108614.

# 4

# GRINDING – GOOD OR BAD FOR REDUCTION OF RCF– OBSERVATIONS FROM IN-SERVICE RAILS WITH WHITE ETCHING LAYER

*Rail grinding has been widely applied in railway networks worldwide to remove or prevent RCF cracks. Yet concerns persist that it may introduce surface damage and shorten rail life. This study assesses its long-term effects on in-service rails, focusing on WELs and RCF cracks. Seven samples from Belgian and Swedish tracks with varying grinding histories, loads and steel grades were examined by hardness testing and optical microscopy. Ground and non-ground rails exhibited similar WELs and microcracks, showing that grinding does not introduce extra defects. Macrocracks occurred only in rails that were never or rarely ground, confirming its mitigating role. Under these conditions, ratcheting—not WEL formation—is the main mechanism of crack initiation.*

Apart from minor updates, this chapter has been published as: Tim Vernaillen, Pan Zhang, Stefan Lundström, Alfredo Núñez, Rolf Dollevoet, Zili Li. Grinding – good or bad for reduction of rolling contact fatigue – observations from in-service rails with white etching layer. Int.J.Fatigue ,Volume 209, August 2026, 109620.

## 4.1. INTRODUCTION

Rolling contact fatigue (RCF) has been a significant and growing problem in rail networks worldwide [1], especially since the early 2000s, largely driven by advancements in modern rolling stock. RCF is induced by repeated high-stress wheel–rail contact, leading to the progressive loss of ductility in rail materials and the initiation of surface or subsurface cracks [2-4]. These cracks may propagate under consecutive cyclic loading, sometimes with fluid entrapment [5, 6], extend deeper into the rail, resulting in catastrophic rail breakage [7, 8]. With increasing axle loads, train speeds and traffic density, the risk posed by RCF continues to rise, becoming a serious threat to rail safety. Therefore, timely and effective measures for RCF mitigation and prevention are essential to ensure safe and reliable railway operations.

Rail grinding has been widely implemented in the railway industry to restore the railhead profile and remove surface defects such as corrugation [9, 10] and RCF cracks [11]. Today, it is globally employed as a standard preventive maintenance practice aimed at mitigating RCF by removing a thin surface layer of material that typically contains plastically deformed microstructures and early-stage cracks [1]. Despite variations in grinding depth and interval across different rail networks, the positive impact of rail grinding on extending rail service life and reducing maintenance costs has been well documented [12-14]. However, concerns have also been raised regarding potential adverse effects on the surface integrity of rails [15], particularly when grinding parameters are not properly controlled [16].

One of the primary concerns regarding rail grinding is its potential to induce initial damage to the rail surface due to the high friction and temperature rise (e.g., above 800 °C [17, 18]). A study of RCF in a head-hardened rail [19] reported that a White Etching Layer (WEL) with a depth up to 8 µm was identified in the low rail after just 1 million gross tonnes (MGT) of service, likely resulting from grinding operations. WEL is a typical microstructural phenomenon in rail steels, characterised by a distinct, hard, and brittle layer [20]. It appears as a white band under optical microscopy due to its resistance to chemical etching. WEL formation in rails is typically attributed to severe plastic deformation and/or

thermal phase transformation resulting from cyclic wheel–rail friction rolling contact [21, 22]. WEL has been considered as a potential initiator of RCF cracks due to its brittle nature [22-25]. Sometimes WEL is present together with a Brown Etching Layer (BEL). The BEL is a more recently identified surface layer [26], which appears brown after etching and is characterised by lower hardness compared to the WEL. The formation mechanism of BEL is not fully clear; it could be considered a tempered pre-existing WEL [22, 27] or a precursor of the WEL [27, 28].

The study in [29] reported that abusive grinding generated WEL on the heat-treated pearlitic rails and causes microcrack initiation under tangential wheel–rail contact stress, which may reduce the normal RCF life. A similar observation was made in [24], where a high density of cracks was found to originate at the interface between the softer pearlite matrix and the harder WEL, which is believed to be a direct consequence of the grinding. In [30], microstructural evolution and damage progression were investigated on a single-track railway line following preventive grinding. The findings indicated that the local damage mechanism is closely associated with the altered surface condition resulting from the grinding process. The work in [31, 32] assessed the impact of grinding on surface quality and crack propagation in both twin-disc and field rail samples. It is found that grinding produced WEL across various rail grades, and harder grades retained larger quantities of WEL due to the smaller hardness gradient between the WEL and bulk material, which could promote the formation of cracks. However, the same study [31] also noted that the number of cracks does not have any significant differences between rail samples with and without WEL/grinding. In [33], the effect of rail grinding on RCF in conventional rail was examined, where it was concluded that grinding not only removes surface fatigue damage caused by repeated wheel–rail interaction but may also reduce subsurface stress concentrations, thereby potentially improving fatigue resistance.

Overall, there seems to be no clear consensus on the impact of grinding on mitigating or accelerating rail RCF. Moreover, most existing studies analyse the transient or short-term effect [29, 34] and provide limited insight into the long-term consequences of grinding on rail degradation in field conditions. Some researchers explored the long-term evolution of rail surface damage after grinding under laboratory conditions [35-37]; they may not fully replicate the complexities of real-world rail operations.

To bridge this gap, the present study investigates the long-term impact of rail grinding on rail material evolution, particularly concerning WEL and RCF. Seven field rail samples with different grinding histories, accumulated tonnages, and steel grades were analysed. The samples were taken from the Belgian and Swedish railway networks; five of them underwent grinding passes according to the EN13231-3 standard series for the acceptance of reprofiling rails in track, while the remaining two were used as reference samples. The analysis includes microstructural characterisation and mechanical properties to assess the evolution of rail damage over time. Compared to the previous research [29-34], this work mainly focuses on the long-term post-grinding effect on in-service rail up to 31 MGT. The structure of this paper is as follows. Section 2 introduces the rail samples and microstructural investigation methods. Section 3 presents the results for six ground and unground samples from the Belgian railway network. Section 4 describes the microstructural findings from a Swedish rail sample after corrective grinding. Section 5 provides a discussion on the influence of grinding on rail damage evolution. Section 6 summarises the main conclusions of the study.

## 4.2. METHODOLOGY

This section provides an overview of the field conditions associated with six rail samples from the Belgian railway network and one sample from the Swedish network. Additionally, the sample preparation procedures and microstructural analysis methods are briefly described.

### 4.2.1. RAIL SAMPLES ON THE BELGIAN RAILWAY NETWORK

Six rail samples were collected from two lines of straight tracks, L130B and L40 (see Fig. 4.1a and 4.1b), on the Belgian railway network, as listed in Table 4.1 and shown in Fig. 4.1c. The first four samples (R1–R4) were taken from Line L130B, with a traffic speed of 100 km/h and annual tonnage of 4 MGT. The remaining two samples (R5 and R6) were taken from Line L40, which has the same train speed but a higher annual load of 8 MGT. Samples R1 and R2 were manufactured from R260 steel grade, while R3 through R6 were made from R350HT. All rails followed the 60 E1 profile and conformed to CEN standard EN 13674-1.

These six rail samples experienced different loading and grinding histories, as detailed in Table 1. R1 was installed in March 2012, ground once in November 2018, and removed from service in December 2020. R2 and R3 were also installed in March 2012 but were never ground before being removed in December 2019. R4, installed in March 2012, underwent one grinding cycle in November 2018 and was removed in December 2019. R5 and R6 were both installed in May 2012. R5 was ground once in June 2015, while R6 was ground once in June 2015 and twice more in November 2018; both were removed from service in December 2019. In Belgium, each grinding cycle consisted of two grinding passes, with a total material removal of approximately 0.25 mm in accordance with EN 13231-3. The resulting longitudinal rail profile satisfied Class 2 requirements (EN 13231-3), while the transverse profile met Class R, Group B criteria with a deviation interval of 0.6 mm. The rail surface was continuously finished without visible bluing marks, and the maximum surface roughness was limited to 10 µm Ra, all acceptance criteria were met in accordance with EN 13231-3. The grinding train was equipped with 48 grinding stones (22-24 Ampère per stone), with the following chemical components of 36% Al2O3, 23% Zr, 4.8% Fe2O3, 4% F, 3.6% S, 1.6 K2O, 1.5% SiO2.

**Table 4.1**: Six field rail samples from the Belgian railway network.

| *Rail sample* | *Line* | *Radius* | *Speed (km/h)* | *Rail profile* | *Steel grade* | *Annual load* | *Installation* | *Grinding* | *Out of track* |
|---|---|---|---|---|---|---|---|---|---|
| R1 | L130B | ∞ | 100 | UIC60E1 | R260 | 4 MGT | 2012-03 | 2018-11 | 2020-12 |
| R2 | L130B | ∞ | 100 | UIC60E1 | R260 | 4 MGT | 2012-03 | none | 2019-12 |
| R3 | L130B | ∞ | 100 | UIC60E1 | R350HT | 4 MGT | 2012-03 | none | 2019-12 |
| R4 | L130B | ∞ | 100 | UIC60E1 | R350HT | 4 MGT | 2012-03 | 2018-11 | 2019-12 |
| R5 | L40 | ∞ | 100 | UIC60E1 | R350HT | 8 MGT | 2012-05 | 2016-05 | 2019-12 |
| R6 | L40 | ∞ | 100 | UIC60E1 | R350HT | 8 MGT | 2012-05 | 2016-05& 2018-11 | 2019-12 |

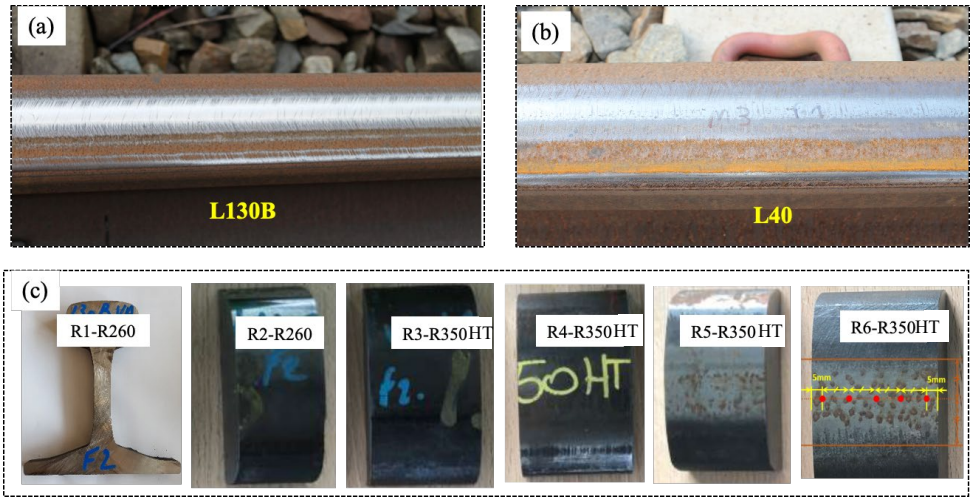


**Fig. 4.1.** Six rail samples taken from two straight lines in Belgium. (a) Track segment on Line 130B after one grinding; (b) track segment on Line 40 after one grinding; (c) six rail samples R1 to R6 in the laboratory. The five red points on R6 indicate the surface hardness measurement locations.

These rail samples were extracted from the field and transferred to Infrabel's laboratory for analysis. For five of the six samples (R2–R6), both longitudinal and transverse cross-sections were prepared and examined using etched optical microscopy (OM). Due to its limited longitudinal thickness, only the transverse section was analysed for Sample R1. All cross-sections were observed around the centre of the running band, corresponding to the primary wheel–rail contact zone. Additionally, surface hardness was measured to support the microstructural evaluation using the Vickers hardness method with a test load of 1 kg, in accordance with NBN EN ISO 6507-1. Five hardness measurements were performed at the middle of the running band along the rolling direction, see an example on R6 in Fig. 4.1c. Overall, this dataset provides a basis for evaluating the long-term impact of rail grinding on material degradation and damage mechanisms. Besides, it allows for the investigation of other relevant influencing factors such as steel grade and traffic load.

### 4.2.2. RAIL SAMPLE ON THE SWEDISH RAILWAY NETWORK

One rail sample was collected from Line 414 of the Swedish railway network with a traffic speed of 180 km/h, as shown in Fig. 4.2a. The rail, made of R260 with a 50 E3 profile, was installed in a curve with a radius of 1000 m in 1974 and has been subjected to an annual traffic load of 13 MGT. In Sweden, standard preventive rail grinding typically involves 4–5 passes, removing 0.3–0.5 mm of material from the rail head. However, in 2020, an extended grinding operation was carried out on Line 414 to reprofile the rail and fully remove head checks. This procedure involved 30–35 grinding passes, resulting in a total material removal of approximately 5–6 mm. This rail sample from the high rail was removed from service in 2021, around one year after the grinding. Taking into account both artificial wear from grinding and natural wear from service, the total vertical wear of the sampled rail reached approximately 11 mm.

A transverse cross-section of the rail was prepared by wet cutting, polishing, and etching for detailed microstructural analysis, as shown in Fig. 4.2b. Based on observations and surface features, the rail head was divided into four distinct zones: 1) the wheel tread–rail head contact zone (Positions A, B), 2) the wheel flange–rail gauge contact zone (Position D), (3) a slight contact region on the rail shoulder (Position C) with residual grinding marks (see Fig. 2a), and (4) a non-contact area (Positions E, F). The examination was conducted using OM and scanning electron microscopy (SEM) at these zones across the rail head. Microhardness tests were performed using Vickers indentation from the rail surface to a depth of 10 mm. The prepared rail sample was used to examine the microstructure at various positions around the rail head and the presence of surface defects, such as WEL or cracks.

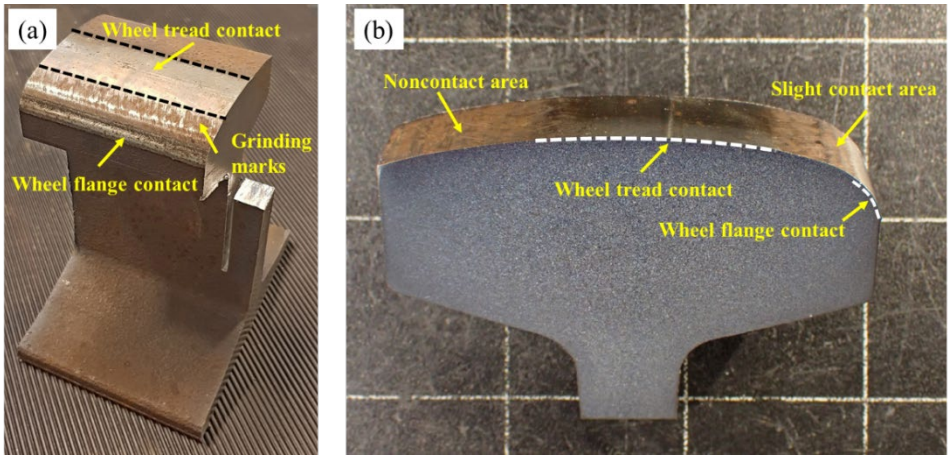


**Fig. 4.2.** The rail samples collected from the Swedish railway network. (a) The targeted rail sample; (b) the prepared cross-section for microstructural analysis.

## 4.3. RESULTS OF BELGIAN RAIL SAMPLES

### 4.3.1. SAMPLE R1-R260 WITH ONE GRINDING CYCLE ON LINE 130B

Fig. 4.3 shows the OM images of the R260 rail microstructure at sample R1 on Line 130B, around 8 MGT after one grinding cycle, which are located approximately in the centre of the running band within the wheel–rail contact zone. The unetched image in Fig. 3a reveals that the rail running surface contains many fine, predominantly vertical cracks. After etching, a distinct layer comprising a mixture of WEL/BEL is observed in the proximity of the rail surface; it has a thickness of about 30 μm, as shown in Fig. 4.3b. Several microcracks are found to originate within this layer, and some are seen to penetrate through it and reach the boundary between the BEL and pearlitic microstructure, see the close-up in Fig. 4.3b. These could be attributed to the brittle nature of the WEL, which makes it prone to cracking under cyclic contact loading. These microcracks are similar to the observations in [25], which show multiple cracks propagating at an angle of ~90◦ to the surface within the WEL region.

The hardness values on the rail surface range from 307 to 389 HV, significantly exceeding the nominal hardness of R260 pearlitic steel, which is approximately 275 HV

[38]. This increase is mainly caused by the work hardening and plastic deformation resulting from repetitive wheel–rail contact as well as rail grinding. They are lower than the typical hardness range reported for WEL/BEL, and likely represent a combined response of the near-surface material, including the rail pearlitic matrix and any thin WEL/BEL present. No pronounced plastic deformation is observed in the subsurface, which may be related to the observation location on a straight track where lateral wheel–rail interaction is limited.

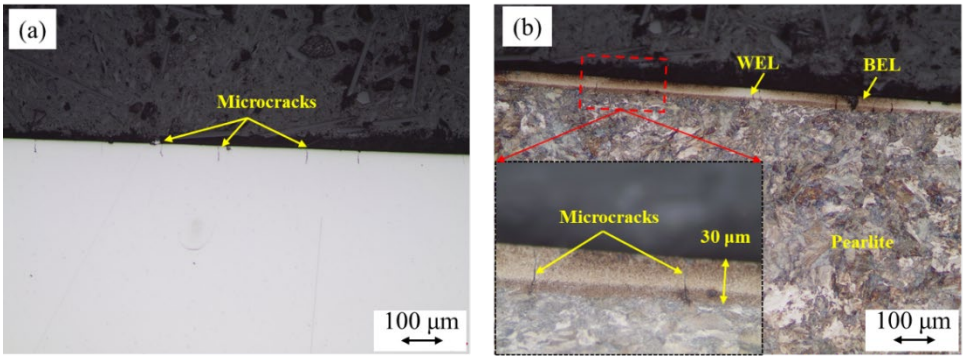


**Fig. 4.3.** The transverse cross-sections of Sample R1, R260 rail on Line 130B after one grinding cycle, (a) before etching, (b) after etching.

### 4.3.2. SAMPLE R2-R260 WITHOUT GRINDING ON LINE 130B

Fig. 4.4 shows OM images of the R260 rail microstructure at Sample R2, which had not undergone any grinding. The unetched image (Figs. 4.4a and 4.4c) reveals an irregular rail head surface characterized by small flaking and surface microcracks. After etching, a WEL layer is observed in the rail materials in Figs. 4.4b and 4.4d, with a thickness ranging from 5 to 77 µm. Additionally, severe plastic deformation is observed in the near-surface region of Fig. 4.4b with depths of approximately 200–300 µm. Given the substantially higher accumulated tonnage (~31 MGT) and the absence of grinding, the WEL is more likely associated with severe plastic deformation–induced microstructural transformation (mechanical WEL) rather than a thermal WEL [22, 39]. The rail surface hardness of R2 ranges from 343 to 394 HV, comparable to and slightly higher than those of Sample R1.

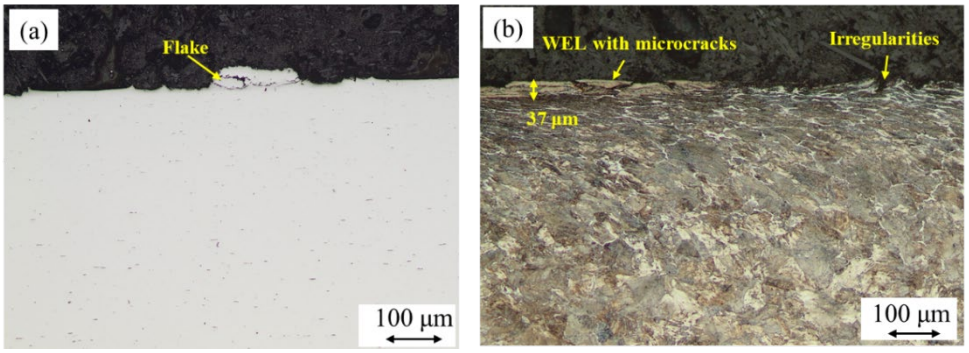


**Fig. 4.4.** The longitudinal cross-sections of Sample R2, R260 rail on Line 130B without grinding, (a) before etching, (b) after etching.

A comparison of Figs. 4.3 and 4.4 indicates that the ground (R1) and unground (R2) samples both have a WEL/BEL layer with thicknesses up to several tens of micrometres, accompanied by microcracks and increased surface hardness. This result suggests that the single grinding cycle performed on R1 did not introduce macrocracks and therefore did not adversely affect the surface integrity during long-term service. In addition, R1 displays a smoother surface than R2, likely as a result of the grinding process. The similar hardness values between R1 and R2 imply that the surface hardening of R260 rail steel may reach a saturation point after approximately two years of service (R1, ~8 MGT). Notably, no macrocracks were observed in the R260 rail (R2) after 7 years and 9 months of service (~31 MGT), indicating good resistance of R260 steel to RCF under the examined conditions. In this work, macrocracks refer to the relatively large cracks that typically propagate into the bulk materials and deeper than 0.1 mm [19].

### 4.3.3. SAMPLE R3-R350HT WITHOUT GRINDING ON LINE 130B

Fig. 4.5 shows OM images of the R350HT rail microstructure at Sample R3, which had not been subjected to grinding. The unetched images (Figs. 4.5a and 4.5c) reveal a highly irregular rail surface with many flakes. Notably, both microcracks and macrocracks are present in this sample. For instance, the crack shown in Fig. 4.5a extends to a depth of 68 µm and a length of 280 µm, oriented at an angle of 11° relative to the rail surface in the

longitudinal cross-section. In Fig. 4.5c, four cracks are visible, with depths reaching up to 133 µm and an orientation angle of approximately 30° in the transverse cross-section.

Post-etching images (Figs. 4.5b and 4.5d) show the presence of a WEL near the rail surface, with thicknesses ranging from 5 to 45 µm. Unlike Samples R1 and R2, where microcracks are confined to the brittle WEL/BEL layer, Sample R3 has macrocracks that propagate deeply into the underlying pearlitic microstructure. Besides, these cracks are observed to initiate at discontinuities in the WEL, either at layer breakages or at the interface between the WEL and the pearlitic material, as highlighted by the red dashed ovals. The surface hardness ranges from 528 to 988 HV, indicating significant surface hardening and confirming the presence of the WEL.

In comparison to Sample R2 (R260 rail), the R350HT rail appears to exhibit lower resistance to RCF under the examined conditions (~31 MGT), as evidenced by the presence of deeper and more severe cracks. Similar observations have been reported in [29, 32].

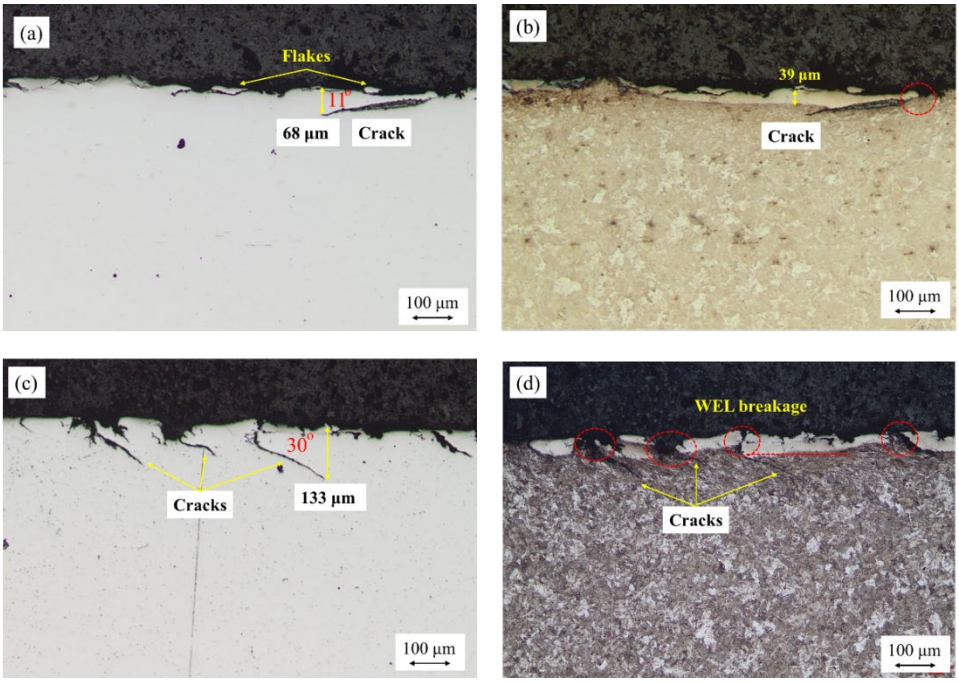

**Fig. 4.5.** The OMs of Sample R3, R350HT rail on Line 130B without grinding. (a) Longitudinal cross-section before etching; (b) longitudinal cross-section after etching; (c) transverse cross-section before etching; (d) transverse cross-section after etching.

### 4.3.4. SAMPLE R4-R350HT WITH ONE GRINDING CYCLE ON LINE 130B

Fig. 4.6 shows OM images of the R350HT rail microstructure at Sample R4, where one grinding cycle had been performed. The unetched image in Fig. 4.6a shows a relatively smooth surface with few microcracks. After etching (Fig. 4.6b), the WEL layer becomes visible, with a thickness ranging from 5 to 35 µm. The underlying pearlitic grains show slight plastic deformation, and no macrocracks are observed. The surface hardness is between 449 and 697 HV, much smaller than that of R3.

In comparison to Sample R3 (unground R350HT), Sample R4, after one year of service following a grinding cycle (~4 MGT), has significantly fewer microcracks, the absence of macrocracks, a smoother surface, and lower surface hardness. These observations suggest that rail grinding has a beneficial effect on the resistance of R350HT rails to RCF by removing the pre-existing plastic deformation layer and initial cracks.

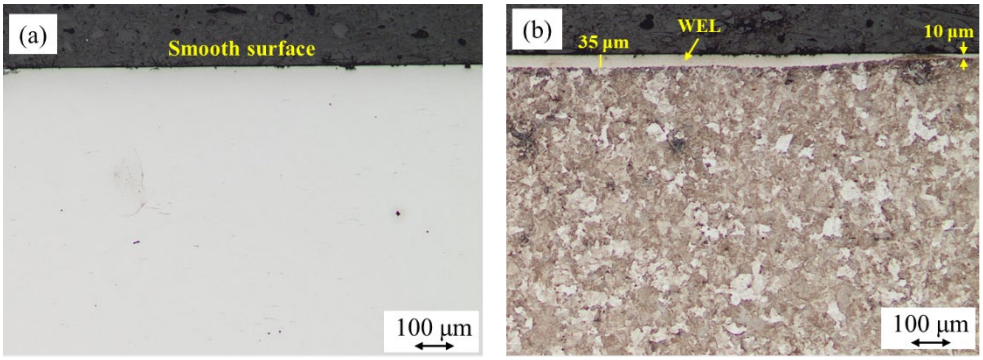


**Fig. 4.6.** The longitudinal cross-sections of Sample R4, R350HT rail on Line 130B after one grinding cycle, (a) before etching, (b) after etching.

### 4.3.5. SAMPLE R5-R350HT WITH ONE GRINDING CYCLE ON LINE 40

Fig. 4.7 presents OM images of the R350HT rail microstructure at Sample R5, taken from the other track, Line 40, after one grinding cycle. The unetched images (Figs. 4.7a and 4.7c)

show numerous microcracks as well as some macrocracks on the running surface. In particular, Fig. 4.7c shows a prominent crack reaching a depth of approximately 200 µm, with an orientation angle of 28° relative to the surface, similar to the angle observed in Sample R3. The grey material observed inside the crack is likely oxide debris formed during repeated crack opening and closing under rolling contact [6], which allows oxygen and moisture to ingress, particularly in an open-track environment.

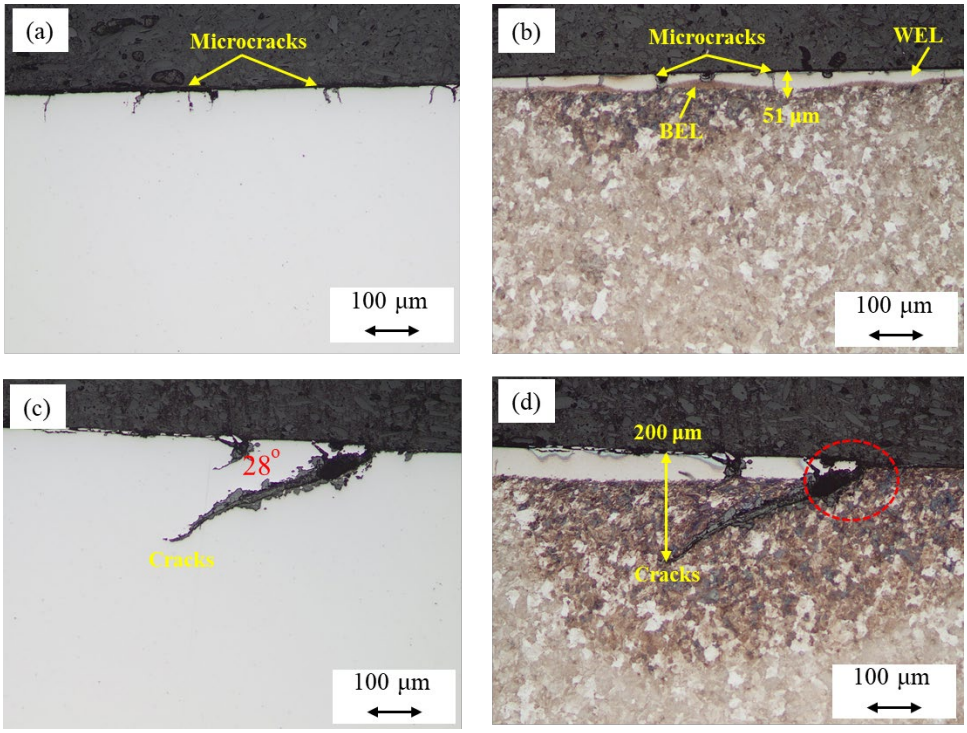


**Fig. 4.7.** The OMs of Sample R5, R350HT rail on Line L40 with one grinding. (a) Longitudinal cross-section before etching; (b) longitudinal cross-section after etching; (c) transverse cross-section before etching; (d) transverse cross-section after etching.

After etching (Figs. 4.7b and 4.7d), a mixture of WEL/BEL is observed, with a thickness ranging from 20 to 80 µm. The microcracks are seen to initiate within this layer and propagate into the interface of the underlying pearlitic structure. The macrocracks are predominantly located at the transition between the WEL and the pearlite. Surface hardness ranges from 470 to 948 HV, which is similar to the values recorded for Sample R3.

Despite differences in railway lines and total accumulated loads (around 61 MGT for R5 and 31 MGT for R3), both the ground Sample R5 and the unground Sample R3 exhibit macroscopic cracks with comparable orientations and similar ranges of surface hardness. A closer analysis reveals that both samples experienced a similar post-grinding load: approximately 29 MGT for R5 and 31 MGT for R3 (without grinding), suggesting that accumulated tonnage after grinding is a more relevant parameter than total service tonnage when assessing RCF development.

### 4.3.6. SAMPLE R6-R350HT WITH TWO GRINDING CYCLES ON LINE 40

Fig. 4.8 shows OM images of the R350HT rail microstructure at Sample R6, which had undergone two grinding cycles. The unetched image (Fig. 4.8a) shows the presence of corrosion products near the surface, along with minor surface flakes and microcracks. After etching (Fig. 4.8b), a BEL is observed in the rail material, with a thickness ranging from 10 to 40 µm. Relatively long cracks are seen to initiate within this layer, either parallel to the surface or propagate with a shallow angle and stop at the interface of the underlying pearlitic microstructure. The surface hardness values range from 564 to 734 HV.

Compared to Sample R5, Sample R6 has no macrocracks penetrating into the pearlite, but some microcracks confined within the WEL/BEL layer. The lower surface hardness suggests reduced accumulated plastic deformation, with the near-surface region being dominated by BEL. These observations indicate that the second grinding cycle performed on R6 had a beneficial effect in removing pre-existing damage layers and enhancing resistance to RCF cracks. Additionally, the surface hardness of R6 is comparable to and slightly higher than that of Sample R4, which may be attributed to their relatively low post-grinding loads, approximately 9 MGT for R6 and 4 MGT for R4, significantly less than the loads for Samples R3 and R5. This further supports the hypothesis that post-grinding load is more relevant in determining surface condition and RCF development.

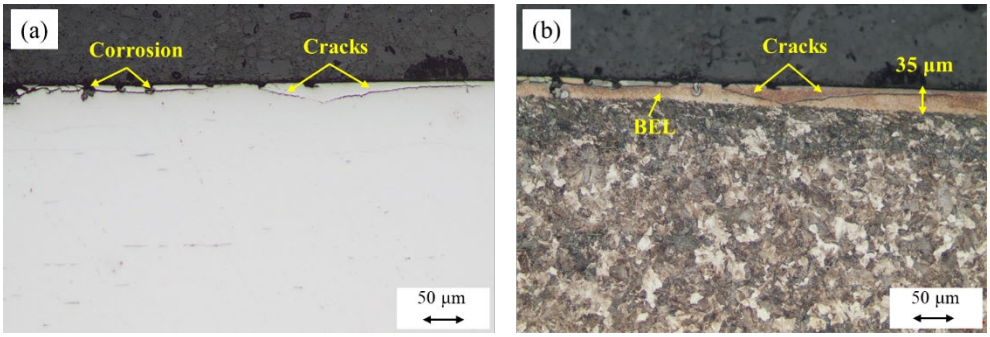


**Fig. 4.8.** The OMs of Sample R6, R350HT rail on Line 40 with two grinding cycles. (a) Longitudinal cross-sections before etching; (b) longitudinal cross-sections after etching.

### 4.3.7. SUMMARY OF SAMPLES R1-R6

Table 4.2 provides a summary of the microstructural observations for all the six rail samples from the Belgian railway network. Regardless of grinding history, all samples show the presence of WEL and/or BEL, accompanied by microcracks and surface flaking. The thickness of these surface layers ranged from 5 to 80 µm, and grinding does not introduce macrocracks and therefore did not adversely affect the surface integrity during long-term service.

A comparison of rail samples (R3–R6) subjected to increasing post-grinding tonnage (4, 9, 29, and 31 MGT) reveals a trend of progressively accelerated damage evolution with increasing service loads. Macrocracks were identified only in Samples R3 and R5, while Samples R4 and R6, which had the same materials and loads but underwent more frequent grinding cycles, present no macrocracks. This suggests that rail grinding enhances the resistance of R350HT to RCF by effectively removing the damaged layers. High surface hardness values were recorded in both R260 and R350HT rail steels, especially in regions containing WEL, confirming the brittle nature. Samples with more grinding cycles generally exhibited lower surface hardness, implying that grinding helps remove the accumulated plastic deformation layers. In addition, ground samples show smoother surfaces in OM images and fewer surface irregularities than unground ones.

**Table 4.2:** Microstructural observations of six field rail samples from the Belgian railway network.

| *Sample* | *Grinding cycles* | *Total load (MGT)* | *Post-grinding load (MGT)* | *WEL/ BEL (μm)* | *Hardness (HV)* | *Micro cracks* | *Macro cracks* | *Surface* |
|---|---|---|---|---|---|---|---|---|
| R1 | 1 | 35 | 8 | 20-40 | 305-379 | Yes | No | Smooth |
| R2 | 0 | 31 | 31 | 5-55 | 343-394 | Yes | No | Irregular |
| R3 | 0 | 31 | 31 | 5-45 | 528-988 | Yes | Yes | Irregular |
| R4 | 1 | 31 | 4 | 5-35 | 449-697 | Yes | No | Smooth |
| R5 | 1 | 61 | 29 | 20-80 | 470-948 | Yes | Yes | Smooth |
| R6 | 2 | 61 | 9 | 10-40 | 564-734 | Yes | No | Smooth |

In addition to microstructural analysis, statistical data from the Belgian rail network further demonstrate the effectiveness of preventive grinding. In 2015, approximately 2,500 ultrasonic defects were detected annually, a number that had declined to around 1,000 by 2023 following the implementation of preventive grinding programs. Similarly, the total length of curved track sections with small RCF defects (<5 mm), as detected via Eddy Current Testing, decreased from 400 km in 2015 to roughly 100 km in 2024 [11]. Across all six test sites, the maximum depth of WEL/BEL layers and associated cracks was less than 0.2 mm. In Belgium, each grinding cycle removes approximately 0.25 mm of material from the rail surface. These routine grinding operations appear to be effective in fully removing early-stage RCF damage and maintaining rail surface integrity.

## 4.4. RESULTS OF THE SWEDISH RAIL SAMPLE

This section presents the microstructural cross-section results of the Swedish rail sample. This sample has undergone a corrective rail grinding with a material removal of 5-6 mm, and was taken from the track after 1 year of service (~11 MGT).

### 4.4.1. MICROSTRUCTURAL FEATURES WITHIN THE WHEEL-RAIL CONTACT ZONE

Fig. 4.9 shows the OM images of the R260 rail microstructure in the wheel tread-rail head contact zone at two positions, A and B (see Fig. 2). It can be seen that a continuous WEL/BEL layer was present at Position A with a thickness of about 20–60 μm, while at Position B the WEL is discontinuous and appears as small patches together with an

underlying BEL. Cracks and voids oriented nearly parallel to the rail surface are also visible, although they do not appear to propagate into the underlying pearlitic structure. The micro-hardness at both locations was about 280-290 HV near the rail surface, and reduced to 235-245 HV at a depth of 10 mm. Within the WEL, localised hardness values reach as high as 830 HV. It is observed that position B contains a thicker BEL and a much thinner WEL compared to position A. Moreover, the cracks at position B are longer and penetrate more deeply, suggesting a larger local wheel-rail contact stress. It is also noted that the boundary between the BEL and the underlying plastic deformation layer cannot be clearly distinguished due to their similar contrast in the current optical micrographs; further analysis using higher magnification or SEM would be required to observe this boundary more clearly.

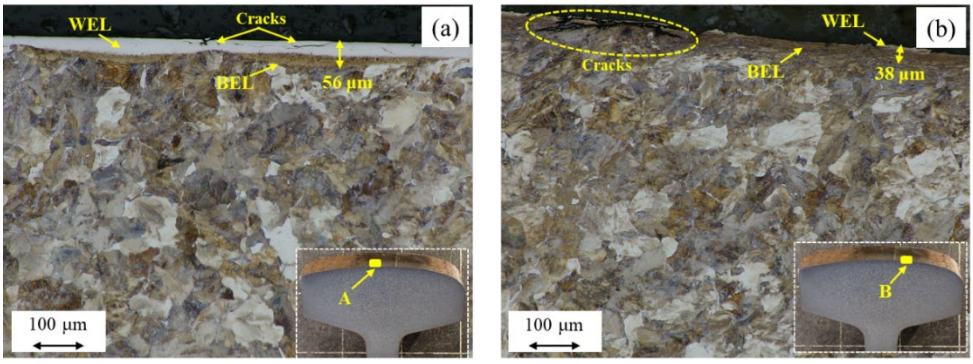


**Fig. 4.9.** The OM images of the Swedish rail sample in wheel tread-rail head contact zone. (a) Position A; (b) Position B.

Fig. 4.10 presents the SEM images of this rail sample at position B for a more detailed examination. It can be seen from Fig. 4.10a that the rail surface shows signs of degradation after around 11 MGT of service, including peeling, spalling and small cracks. These cracks have a depth of dozens of micrometres, are nearly parallel to the surface, and stay within the surface WEL/BEL, as shown in Fig. 4.10b. Notably, no head checks or other defects were observed in this region of the sample, as shown in Fig. 4.2.

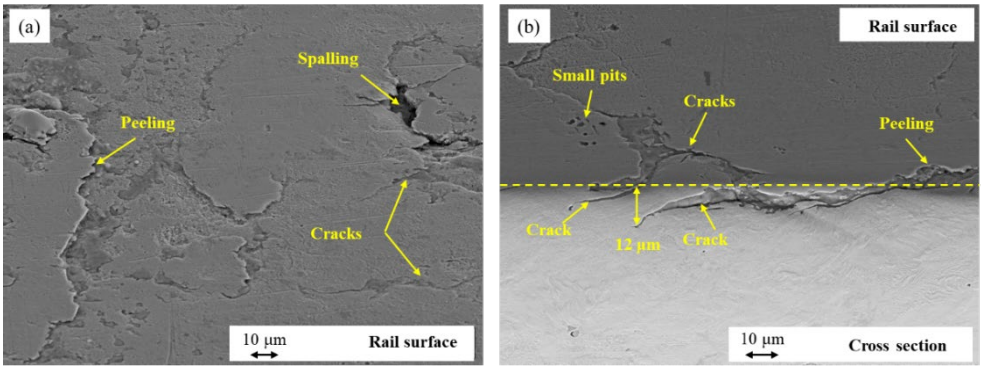


**Fig. 4.10.** The SEM images of the Swedish rail sample at position B. (a) on the rail surface; (b) a combination of the rail surface and cross section.

Fig. 4.11 shows OM images of the R260 rail microstructure at two locations: the slight contact region on the rail shoulder (Position C) and the wheel flange–rail gauge contact zone (Position D). As shown in Fig. 4.11a, the rail surface at Position C contains a thin and discontinuous WEL, with a thickness ranging from 5 to 15 μm. This region also shows signs of slight plastic deformation and an irregular surface profile, probably resulting from the grinding process. In contrast, the microstructure at Position D (Fig. 4.11b) reveals a much smoother surface, which should be caused by more intense and consistent wheel–rail sliding contact. This area shows pronounced plastic deformation, a relatively thick BEL, and only limited WEL presence, similar to the characteristics observed in Fig. 4.9b. A small surface crack is also observed in this region, approximately 43 μm in length. The micro-hardness at both locations was about 285 HV near the rail surface.

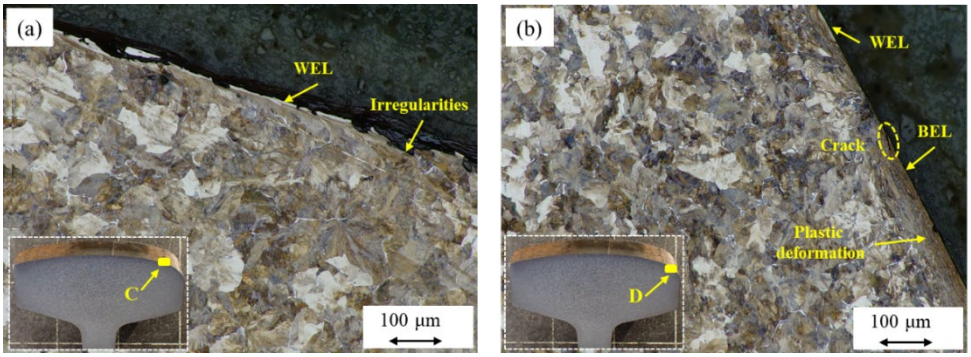


**Fig.4.11.** The OM images of the Swedish rail sample in the wheel flange-rail gauge zone. (a) A slight contact region on the rail shoulder, Position C; (b) the wheel flange–rail gauge contact zone, Position D.

### 4.4.2. MICROSTRUCTURAL FEATURES OF THE NON-CONTACT ZONE

Fig. 4.12 shows the OM images of the R260 rail microstructure in the non-contact zone at two positions, E and F. A discontinuous WEL is observed near the rail surface, with a maximum thickness of approximately 20 μm. In some areas, the WEL is absent, as shown in Fig. 4.12b. The rail surface has some irregularities, similar to those in Fig. 11a, probably introduced by the grinding. Microhardness measurements near the surface at both positions range from 280 to 290 HV, about 15% higher than the hardness measured at a depth of 10 mm, indicating that grinding has induced a certain degree of plastic deformation and surface hardening.

Compared to the contact zones shown in Fig. 4.9, the WEL in the non-contact zone (Fig. 4.12) is thinner, less continuous, and associated with fewer microcracks and a more irregular surface. The overall hardness values are comparable in both cases. Additionally, the microstructural characteristics observed in the slight-contact region (Fig. 4.11a) closely resemble those in Fig. 4.12a, confirming minimal contact in that area.

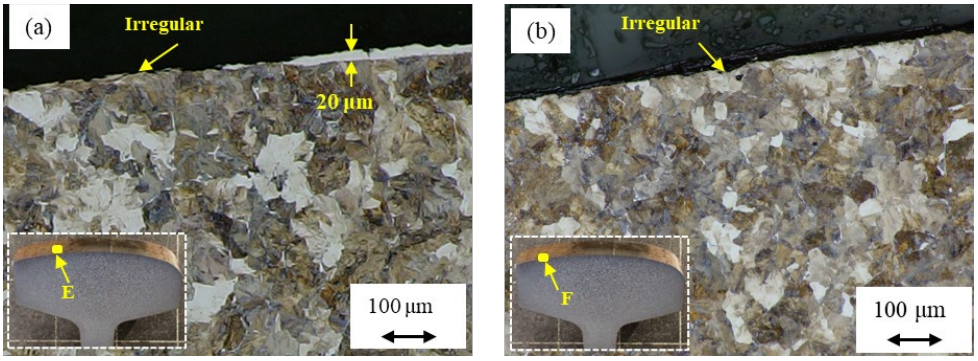


**Fig.4.12.** The OM images of the Swedish rail sample in the non-contact zone. (a) Position E; (b) Position F.

## 4.5. DISCUSSIONS

Two primary mechanisms have been proposed for RCF crack initiation in the rail surface: the ratcheting (I) [40-42] and WEL (II) mechanisms [29, 43]. Crack initiation may occur due to high stress cyclic contact between the wheel and rail, which leads to progressive accumulation of plastic strain or ratcheting (Mechanism I) of rail materials and eventually exhaustion of ductility. Cracks typically initiate at the surface and grow in the direction of maximum shear stress. In this process, the presence of WEL is not necessary [4, 44]. An alternative hypothesis suggests WEL can act as an initiator for rail cracks due to its hard and brittle nature (Mechanism II). WEL is prone to fracturing under wheel–rail contact stresses, and the resulting cracks can then propagate from the WEL into the soft underlying bulk material [43]. Moreover, the significant hardness gradient may promote localised stress concentrations at the interface, which promotes crack initiation [32].

Rail grinding removes the accumulated plastic deformation in the rail materials (see Fig. 4.4b), which may also eliminate early-stage cracks, thereby significantly reducing the likelihood of crack initiation via Mechanism I (ratcheting). However, the grinding process itself can generate the WEL and induce localised plastic deformation due to the high friction and temperature rise, as shown in Fig. 4.12 and reported in [24, 29, 32], which may, in turn, promote crack initiation via Mechanism II.

The comparison among the six rail samples from the Belgian rail network shows that both ground and nonground rail samples exhibit microcracks and WEL/BEL with depths of several tens of micrometres, as listed in Table 4.2. However, macrocracks were observed only in samples that had not been ground (R3) or had undergone fewer grinding cycles (R5). In addition, statistical data from the Belgian network show a significant reduction in the occurrence of RCF cracks following the implementation of preventive grinding. These findings highlight the beneficial role of rail grinding in mitigating RCF crack formation, and support that ratcheting is the dominant crack initiation mechanism under the examined conditions. The presence of WEL may also contribute to crack formation since macrocracks predominantly occur at the transition between the WEL and the pearlite.

In both the ground and nonground samples, many microcracks were observed within the WEL/BEL layers (see Table 4.2), a feature also identified in newly ground rails, as shown in Fig.4.12 and [29]. Statistical data presented in [19] indicate that most microcracks do not evolve into macrocracks, likely due to the protective compressive stresses and their subsequent removal by wear. Therefore, grinding-induced microcracks may also be worn away before sufficient plastic deformation accumulates from wheel passages to drive further crack propagation. This could also explain why the R350HT exhibits lower RCF resistance than R260 under identical loading conditions in this work. R350HT material is harder and more wear-resistant than R260, which inhibits the removal of surface-initiated cracks. Similar findings have been reported in [32], where harder rails may be more susceptible to RCF damage.

In this work, all seven rail samples exhibit either WEL, BEL, or a combination of both (often referred to as a stratified layer in the literature). The formation mechanisms of WEL have been extensively studied and are generally attributed to mechanical or thermo-mechanical loading [21, 25, 45]. Recently, increasing attention has also been given to the formation mechanism of BEL. For example, the BEL in a pearlitic R350HT rail from service has been investigated in [28], which suggested a correlation between cementite decomposition and BEL formation. Detailed characterisation of the WEL and the BEL in a pearlitic rail steel has been carried out from micrometer to atomic scale in [27], and it is reported that BEL could be considered a tempered pre-existing WEL or a precursor of the

WEL, depending on the time and peak temperature. Under well-controlled laboratory conditions, WEL/BEL have also been reproduced using defined mechanical loading combined with successive two thermal inputs [25, 46], and it is found that the initial deformation state plays a critical role in determining the resulting microstructural characteristics of thermally induced WELs. While the present work is not intended to identify the formation mechanisms of WEL or BEL, some insights can be drawn from the field observations. In the investigated samples, predominantly WEL was observed in rails without grinding (Samples R2 and R3) or in non-contact zones subjected only to grinding (Swedish sample), whereas BEL was mainly observed in regions exposed to the combined effect of subsequent wheel–rail contact loading and grinding. Further studies could be performed to fully clarify these observations.

Rail grinding introduces initial surface roughness by residual grinding marks, which are gradually smoothed out through wheel–rail interaction over time [34, 47]. This explains the smoother surface observed in the OM images of the ground rail samples than in the unground ones in Section 3. However, if pre-existing cracks are too deep to be fully removed by grinding, the resulting surface roughness and local high contact stresses may accelerate crack growth, as reported in [11]. Therefore, it is essential to optimise grinding operations, such as selecting appropriate grinding stone materials and minimising friction during grinding, to reduce initial surface roughness and limit the formation of WEL/BEL and plastic deformation. It is worth noting that the results obtained in this study are achieved by grinding in certain methods and the influence of grinding parameters needs to be further investigated.

## 4.6. CONCLUSIONS



This study evaluates the long-term effects of grinding on rail material degradation through microstructural analysis of seven in-service rail samples. Six of them were selected from straight track sections of the Belgian rail networks, and the other from the high rail in a 1000 m radius curve in the Swedish railway network. These samples have different grinding operations, steel grades and load histories, and their mechanical and microstructural properties were examined via the hardness test, OM, and SEM. The main findings have been summarised as follows.

(1) WEL and microcracks were observed in both ground and non-ground rails among the seven investigated samples, suggesting that rail grinding may not introduce additional defects or adversely affect the rail surface after long-term service.

(2) With identical materials and loads, macrocracks were observed only in rail samples that had undergone zero or a single grinding cycle in accordance with EN 13231 standard series. Besides, the statistical data show a considerable reduction in cracks of the Belgian railway network after the implementation of preventive grinding. These results confirm the beneficial role of rail grinding in mitigating RCF crack formation by removing the accumulated plastic deformation.

(3) Ratcheting is the dominant crack initiation mechanism under the examined conditions, while WEL may also contribute to crack formation, given that macrocracks predominantly occur at the transition between the WEL and the pearlite.

(4) Despite the initial WEL and local deformation, rail samples with more grinding cycles generally exhibited lower surface hardness after long-term service.

(5) Rail grinding introduces initial surface roughness, which is gradually smoothed out through wheel–rail dynamic interaction over time [34, 47], causing a smoother surface than in unground ones.

(6) Post-grinding load is more relevant than the total accumulated load in determining the rail surface condition and RCF development.

(7) Under the examined service conditions, R260 steel demonstrated better resistance to RCF than R350HT, likely due to its higher wear rate, which facilitates the removal of early-stage surface cracks before they further grow.

Overall, this research provides valuable insights into the formation mechanism and prevention of RCF cracks in rails. It should be noted that the conclusions are based on a limited number of rail samples and certain grinding methods, and a broader dataset would help to validate and strengthen these findings. Besides, it is observed that BEL only occurs in some samples and not others, which could be further investigated in future studies. Moreover, further research could be performed to optimise grinding operations to avoid aggressive grinding and minimise initial surface damage and roughness.

**Acknowledgments**

This work is partly supported by Infrabel and Trafikverket. The authors thank Dr. Fang Ren for the helpful discussion about the crack initiation mechanism in Section 5.

# REFERENCES



[1] E.E. Magel, Rolling contact fatigue: a comprehensive review, (2011).

[2] A. Ekberg, B. Åkesson, E. Kabo, Wheel/rail rolling contact fatigue–Probe, predict, prevent, Wear, 314 (2014) 2-12.

[3] X. Deng, Z. Qian, Z. Li, R. Dollevoet, Investigation of the formation of corrugation-induced rail squats based on extensive field monitoring, International Journal of Fatigue, 112 (2018) 94-105.

[4] F. Ren, Z. Yang, Z. Li, Experimental and numerical investigation into rolling contact fatigue crack initiation on the V-Track test rig, Engineering Failure Analysis, 170 (2025) 109206.

[5] S. Bogdański, P. Lewicki, 3D model of liquid entrapment mechanism for rolling contact fatigue cracks in rails, Wear, 265 (2008) 1356-1362.

[6] A. Al-Juboori, H. Zhu, H. Li, J. McLeod, S. Pannila, J. Barnes, Microstructural investigation on a rail fracture failure associated with squat defects, Engineering Failure Analysis, 151 (2023) 107411.

[7] Al-Juboori, A., et al., Microstructural investigation on a rail fracture failure associated with squat defects. Engineering Failure Analysis, 2023. 151: p. 107411.

[8] Y. Zhou, X. Zheng, J. Jiang, D. Kuang, Modeling of rail head checks by X-ray computed tomography scan technology, International Journal of Fatigue, 100 (2017) 21-31.

[9] Shen, Y., et al., Evolution and formation mechanism of rail corrugation in high-speed railways involving the longitudinal wheel-track coupling relationship. Science China Technological Sciences, 2024. 67(11): p. 3612-3625.

[10] Zhang, P., et al., Parametric investigation of railway fastenings into the formation and mitigation of short pitch corrugation. Railway Engineering Science, 2024.

[11] Vernaillen, T., et al., Statistical analysis and treatment method of head checks on the Belgian railway network. International Journal of Fatigue, 2025: p. 109349.

[12] G. Chattopadhyay, V. Reddy, P.O. Larsson ‐ Kråik, Decision on economical rail grinding interval for controlling rolling contact fatigue, International Transactions in Operational Research, 12 (2005) 545-558.

[13] S.L. Grassie, Rolling contact fatigue on the British railway system: treatment, Wear, 258 (2005) 1310-1318.

[14] A. Zoeteman, R. Dollevoet, Z. Li, Dutch research results on wheel/rail interface management: 2001–2013 and beyond, Proceedings of the Institution of Mechanical Engineers, Part F: Journal of Rail and Rapid Transit, 228 (2014) 642-651.

[15] M. Mesaritis, J. Santa, A. Toro, R. Lewis, Rail Surface Integrity Analysis in Laboratory, Procedia CIRP, 123 (2024) 83-88.

[16] B. Lin, K. Zhou, J. Guo, Q. Liu, W. Wang, Influence of grinding parameters on surface temperature and burn behaviors of grinding rail, Tribology International, 122 (2018) 151-162.

[17] Z. Zhang, W. Shang, H. Ding, J. Guo, H. Wang, Q. Liu, W. Wang, Thermal model and temperature field in rail grinding process based on a moving heat source, Applied Thermal Engineering, 106 (2016) 855-864.

[18] He, C., et al., *Infrared temperature measurement of wheel-rail frictional rolling contact with high slip ratios.* Case Studies in Thermal Engineering, 2025. **73**: p. 106642.

[19] V. Dikshit, P. Clayton, D. Christensen, Investigation of rolling contact fatigue in a head-hardened rail, Wear, 144 (1991) 89-102.

[20] H.W. Zhang, S. Ohsaki, S. Mitao, M. Ohnuma, K. Hono, Microstructural investigation of white etching layer on pearlite steel rail, Materials Science and Engineering: A, 421 (2006) 191-199.

[21] J. Wu, R.H. Petrov, M. Naeimi, Z. Li, R. Dollevoet, J. Sietsma, Laboratory simulation of martensite formation of white etching layer in rail steel, International Journal of Fatigue, 91 (2016) 11-20.

[22] B.H. Nguyen, E.T. Camacho, A. Al-Juboori, Y. Ma, H. Li, H. Zhu, Tribological behaviors of two distinct classes of white etching layers on rail surface, Wear, 532 (2023) 205097.

[23] J. Seo, S. Kwon, H. Jun, D. Lee, Numerical stress analysis and rolling contact fatigue of White Etching Layer on rail steel, International Journal of Fatigue, 33 (2011) 203-211.

[24] C.J. Rasmussen, S. Fæster, S. Dhar, J.V. Quaade, M. Bini, H.K. Danielsen, Surface crack formation on rails at grinding induced martensite white etching layers, Wear, 384 (2017) 8-14.

[25] Freisinger, M., et al., Fatigue crack initiation in the presence of stratified surface layers on rail wheels. International Journal of Fatigue, 2023. 177: p. 107958.

[26] S. Li, J. Wu, R.H. Petrov, Z. Li, R. Dollevoet, J. Sietsma, "Brown etching layer": A possible new insight into the crack initiation of rolling contact fatigue in rail steels?, Engineering Failure Analysis, 66 (2016) 8-18.

[27] A. Kumar, G. Agarwal, R. Petrov, S. Goto, J. Sietsma, M. Herbig, Microstructural evolution of white and brown etching layers in pearlitic rail steels, Acta Materialia, 171 (2019) 48-64.

[28] P.-Y. Tung, X. Zhou, L. Morsdorf, M. Herbig, Formation mechanism of brown etching layers in pearlitic rail steel, Materialia, 26 (2022) 101625.

[29] M. Steenbergen, Rolling contact fatigue in relation to rail grinding, Wear, 356 (2016) 110-121.

[30] B. Schotsman, J. Huisman, M. Santofimia, R. Petrov, J. Sietsma, T.M.S. Navarro, Microstructure evolution and damage development in the rails of a single-track railway line after preventive grinding, Wear, 576 (2025) 206101.

[31] M. Mesaritis, M. Shamsa, P. Cuervo, J. Santa, A. Toro, M. Marshall, R. Lewis, A laboratory demonstration of rail grinding and analysis of running roughness and wear, Wear, 456 (2020) 203379.

[32] M. Mesaritis, J. Santa, L. Molina, M. Palacio, A. Toro, R. Lewis, Post-field grinding evaluation of different rail grades in full-scale wheel/rail laboratory tests, Tribology International, 177 (2023) 107980.

[33] Y. Satoh, K. Iwafuchi, Effect of rail grinding on rolling contact fatigue in railway rail used in conventional line in Japan, Wear, 265 (2008) 1342-1348.

[34] W. Edjeou, O. Moström, M. Asplund, P.-O. Larsson-Kråik, F. Peréz-Ràfols, R. Larsson, A. Almqvist, Evaluating the impact of rail surface roughness post-grinding: An experimental and elastoplastic modelling approach, Tribology International, 201 (2025) 110270.

[35] R. Wang, K. Zhou, J. Yang, H. Ding, W. Wang, J. Guo, Q. Liu, Effects of abrasive material and hardness of grinding wheel on rail grinding behaviors, Wear, 454 (2020) 203332.

[36] M. Mesaritis, P. Cuervo, J. Santa, A. Toro, R. Lewis, Assessment of rail grinding maintenance surface quality and damage propagation in subsequent loading cycles for premium rail grades, Wear, 530 (2023) 205051.

[37] E. Uhlmann, P. Lypovka, L. Hochschild, N. Schröer, Influence of rail grinding process parameters on rail surface roughness and surface layer hardness, Wear, 366 (2016) 287-293.

[38] P. Zhang, S. Li, F. Ren, O. Hajizad, R. Dollevoet, Z. Li, Microstructural investigation into the damage mechanism of short pitch rail corrugation, Engineering Failure Analysis, 174 (2025) 109512.

[39] Freisinger, M., et al., Severe plastic deformed zones and white etching layers formed during service of railway wheels. Metallography, Microstructure, and Analysis, 2023. 12(3): p. 515-527.

[40] W. Tyfour, J. Beynon, A. Kapoor, Deterioration of rolling contact fatigue life of pearlitic rail steel due to dry-wet rolling-sliding line contact, Wear, 197 (1996) 255-265.

[41] F. Franklin, J. Garnham, D. Fletcher, C. Davis, A. Kapoor, Modelling rail steel microstructure and its effect on crack initiation, Wear, 265 (2008) 1332-1341.

[42] F. Ren, Z. Yang, Z. Li, An efficient 3D finite element procedure for simulating wheel–rail cyclic contact and ratcheting, Tribology International, (2024) 109878.

[43] A. Al-Juboori, D. Wexler, H. Li, H. Zhu, C. Lu, A. McCusker, J. McLeod, S. Pannil, Z. Wang, Squat formation and the occurrence of two distinct classes of white etching layer on the surface of rail steel, International Journal of Fatigue, 104 (2017) 52-60.

[44] S. Pal, W.J. Daniel, M. Farjoo, Early stages of rail squat formation and the role of a white etching layer, International Journal of Fatigue, 52 (2013) 144-156.

[45] Nguyen, B.H., et al., Fracture mechanisms in rails with mechanically and thermomechanically-induced white etching layers under three-point bending. Engineering Failure Analysis, 2022. 131: p. 105813.

[46] Freisinger, M., et al., Comparative study on the influence of initial deformation and temperature of thermally induced white etching layers on rail wheels. Tribology International, 2023. 177: p. 107990.

[47] P. Zhang, Z. Li, The development of short pitch rail corrugation: extensive field monitoring and validation of numerical predictions, Tribology International, (2025) 110821.

4

# 5

# CONCLUSIONS AND RECOMMENDATIONS

*This chapter concludes the scientific and technical implications for society of the research findings in this dissertation*

# 5.1. CONCLUSIONS



Railway infrastructure forms the backbone of modern sustainable transportation. Within this infrastructure, the rail itself serves as the critical component ensuring safe, efficient, and uninterrupted train operations. The rail's operational longevity, however, is compromised by two primary degradation mechanisms: wear and rolling contact fatigue (RCF). This dissertation set out to investigate, through a multidisciplinary lens, the complex interplay between rail wear and RCF, aiming to optimise preventive maintenance strategies in the Belgian railway network, with particular emphasis on grinding interventions.

This chapter integrates the findings of three key research components, drawing conclusions on the mechanisms governing wear and fatigue, the effectiveness of current maintenance practices, and the material and operational variables that modulate degradation. It further outlines actionable recommendations for infrastructure managers, offers strategic guidance for policy refinement, and identifies future research avenues that can enhance understanding and practice in the rail industry.

**Response to the Main Research Question:**

***"How can the relationship between rail wear rate and rolling contact fatigue (RCF) be quantified and understood through big data analysis encompassing an entire country's rail infrastructure, combined with laboratory research on rails?"***

The relationship between rail wear rate and rolling contact fatigue (RCF) can be systematically quantified and understood by integrating macro-scale big data analysis with microstructural laboratory investigation. This dissertation demonstrates that wear and RCF are not independent phenomena but rather competitive and interdependent degradation mechanisms influenced by traffic load, track geometry, material properties, and environmental exposure.

Through a comprehensive big data analysis of the Belgian railway network, wear and RCF were shown to exhibit distinct but interacting behaviours depending on the curve radius, steel grade, and load classification (UIC class). High wear rates in tight curves were found to mitigate RCF by removing surface-initiated cracks, whereas in moderately curved

tracks with lower wear, RCF defects, particularly head checks, were more likely to develop and propagate.

Laboratory analysis of rail samples complemented these network-wide observations by confirming the presence of White Etching Layers. Importantly, in both ground and unground rails, suggesting that cyclic mechanical loading by trains plays a more critical role than grinding-induced thermal effects in their formation.

By combining these empirical findings, the thesis used the concept of the Magic Wear Rate (MWR),an optimal rate of material removal through grinding that balances wear and RCF mitigation. The MWR derived from the analyses does not appear to be a fixed value but depends on the loading conditions of the railway line. This implies that grinding strategies based on cumulative tonnage are insufficient. This integrative approach, presented across Chapters 2 to 4, offers infrastructure managers a robust, data-driven framework for predictive maintenance planning.

**Response to Sub-Research Questions**

**Sub-question 1:**

***"What are the key parameters influencing rail wear rates, and how can a big data-validated model be developed to predict this phenomenon?"***

This sub-question is addressed in Chapter 2 and identifies key parameters influencing rail wear rates, including curve radius, steel grade (R200 vs. R260), annual and accumulated tonnage (UIC class), and preventive grinding practices. A statistically validated big-data model, based on over 5,000 km of measurement data, revealed that wear rates follow an approximately log-linear relationship with curve radius and are significantly higher for R200 rails. Wear rates differ significantly between heavily and lightly loaded tracks. Heavily loaded lines exhibit lower wear rates per tonnage but higher annual wear rates compared to lightly loaded lines, suggesting that time plays a larger role in wear progression on low-tonnage tracks. Corrosion is thus identified as another important factor, that governs this time effect. This chapter demonstrates how big data, when properly filtered and segmented by track characteristics, can yield predictive models that guide rail renewal and

grinding schedules. The model serves as a foundational tool for network-wide wear prediction and prioritization of maintenance interventions.

**Sub-question 2:**

***"How can the analysis of head check growth, considering factors such as wear development, curve radius, annual train traffic, and accumulated tonnage, inform the optimization of preventive rail maintenance strategies, including the determination of an ideal "magic wear rate"?"***

Chapter 3 deals with this sub-question and presents an extensive statistical analysis of head check (HC) development on 212 curves across the Belgian rail network. The analysis revealed that HC growth is highest in curves with radii between 750–1000 meters and on tracks with lower annual tonnage. This counterintuitive result underscores the importance of fluid-assisted crack growth and time-dependent mechanisms, such as corrosion, in RCF evolution. By comparing HC growth rates and wear rates across different UIC classes and curve geometries, the chapter discusses the Magic Wear Rate (MWR), a target wear rate that minimizes RCF damage without excessive grinding. The thesis calculates optimal grinding intervals per UIC class, demonstrating that a one-size-fits-all approach is insufficient. This chapter provides a quantitative and operationally relevant framework for designing targeted grinding strategies based on annual tonnage rather than cumulative tonnage.

**Sub-question 3:**

***"Is the artificial wear by grinding to remove RCF beneficial to rail service life, and what is the impact of white etching layers on rail performance and durability?"***

This sub-question is examined in Chapter 4 and addresses whether artificial wear by grinding improves rail service life, based on microstructural analysis of both ground and unground rail samples that had been in service for at least six months. The comparative analysis of these samples shows that White Etching Layers (WELs) and associated microcracks develop in both conditions and exhibit similar features, indicating that grinding does not generate additional defects nor adversely affect the rail surface. Instead, the findings demonstrate that preventive grinding is beneficial, as macrocracks were observed only in rails that had not been ground or had undergone fewer grinding cycles. This

confirms that grinding effectively mitigates RCF by removing accumulated plastic deformation and early-stage cracks. Under the examined conditions, ratcheting, not WEL formation, is the dominant mechanism initiating surface cracking, suggesting that WELs have a limited detrimental effect on long-term durability. Furthermore, rails subjected to more frequent grinding cycles showed lower surface hardness after prolonged service and developed smoother running surfaces over time. Overall, the study demonstrates that controlled grinding improves rail performance and durability, provided that post-grinding loading conditions remain favourable.

## 5.2. SYNTHESIS OF PRINCIPAL FINDINGS

### 5.2.1. RAIL WEAR AND INFLUENCING FACTORS (CHAPTER 2)

This study provides one of the most comprehensive long-term evaluations of rail wear across a national railway network, drawing on over 5,000 km of monitored track during two large-scale measurement campaigns on the Belgian network. The analysis demonstrates that rail wear is governed by a complex interplay of operational loading, curvature, environmental conditions, and material selection. Wear rates, expressed in mm per 100 MGT, increase sharply with decreasing curve radius and follow an approximately linear trend on a logarithmic scale. Steel grade emerges as a critical parameter, with R200 rails exhibiting 34% higher wear rate than R260 under comparable traffic conditions, confirming the superior performance of modern steels in service.

The introduction of systematic preventive grinding since 2012 has imposed measurable artificial wear, modifying natural wear patterns and influencing the interpretation of wear–radius relationships. When wear is assessed per year rather than per tonnage, heavily loaded lines display higher total wear despite lower wear per 100 MGT, underscoring the importance of annual traffic intensity. A counterintuitive finding is that low-traffic lines show disproportionately high wear rates per 100 MGT, suggesting that time-dependent processes, particularly corrosion, may dominate in these environments. These insights collectively challenge the use of cumulative tonnage as the sole metric for wear assessment

and highlight the need to incorporate steel grade, environmental exposure, and maintenance history into predictive models.

Overall, this work provides a robust empirical foundation for understanding network-wide wear behaviour and emphasises the importance of curve-specific, traffic-class-specific, and material-specific wear laws. Future research should integrate dynamic contact simulations with long-term field measurements to develop more accurate predictive models and to support the optimisation of grinding intervals, intervention depths, and rail replacement strategies.

### 5.2.2. HEAD CHECK GROWTH AND GRINDING STRATEGY (CHAPTER 3)

In Chapter 3, a comprehensive statistical analysis of head check (HC) defects across 212 curved track segments highlighted the complex behaviour of rolling contact fatigue (RCF). The results reveal a clear dependence of HC growth on curve radius, with the highest growth rates and occurrence probabilities concentrated in curves between 750 and 1000 m. This confirms the existence of a geometric vulnerability window in which loading conditions and contact stresses are particularly favourable for RCF crack propagation. Annual traffic load emerged as a stronger predictor of HC growth than cumulative tonnage, emphasising the influence of dwell time and time-dependent mechanisms such as corrosion and fluid-assisted crack propagation.

A key finding is the competitive interaction between wear and fatigue. On tight curves, high wear rates suppress HC development by removing early-stage cracks, whereas in moderately curved sections where wear is insufficient, RCF becomes the dominant degradation mechanism. By systematically comparing HC growth with natural wear rates, the study quantifies the Magic Wear Rate (MWR), the optimal level of material removal through grinding that limits crack propagation without causing excessive rail loss. The resulting optimal grinding intervals, 27.8 MGT for UIC3, 19.2 MGT for UIC4, and 9.2 MGT for UIC5, demonstrate that the uniform grinding intervals currently applied in Belgium, while suitable for heavily loaded lines, are not optimal for low-traffic lines where cracks grow faster relative to wear. In some cases, the present approach may even accelerate HC propagation.

Overall, the findings provide a refined, data-driven framework for optimising grinding interventions and improving the management of RCF defects. Future work should assess whether these trends persist in other networks and further investigate the mechanisms by which grinding influences crack growth under low annual loading conditions, thereby supporting more effective predictive maintenance strategies.

### 5.2.3. MICROSTRUCTURAL ANALYSIS OF RAIL SURFACES (CHAPTER 4)

Chapter 4 evaluates the long-term effects of grinding on rail material degradation through microstructural analysis of seven in-service rail samples. Six were obtained from straight track sections of the Belgian railway network, and one from a 1000 m radius curve in the Swedish network. These samples represented varying grinding histories, steel grades, and load conditions, and their mechanical and microstructural properties were assessed using hardness testing, optical microscopy, and scanning electron microscopy. The results demonstrated that White Etching Layers and microcracks were consistently observed in both ground and unground rails, indicating that grinding itself does not generate additional defects or adversely affect the surface. Importantly, macrocracks were found only in rails that had not been ground or had undergone fewer grinding cycles, and statistical data from the Belgian network confirmed a substantial reduction in (macro) cracks following the systematic introduction of preventive grinding. These findings underscore the beneficial role of grinding in mitigating rolling contact fatigue by removing accumulated plastic deformation and damage. Moreover, the analysis highlighted that ratcheting, rather than WEL formation, is the dominant crack initiation mechanism under the studied conditions. Rails subjected to more grinding cycles exhibited lower surface hardness near the running surface after long-term service, suggesting that repeated grinding influences the hardness evolution. Although grinding introduces initial surface roughness, this is progressively smoothed out by wheel–rail dynamic interaction, ultimately resulting in smoother surfaces than unground rails.

In terms of material performance, R260 steel showed superior resistance to RCF compared with R350HT, likely due to its higher wear rate, which promotes the removal of incipient cracks before they can propagate. Brown Etching Layers (BELs), associated with

more brittle cracking, were observed only sporadically, highlighting the need for further research into their formation.

Overall, these results provide valuable insights into the mechanisms driving RCF crack initiation and highlight the preventive role of grinding. Nevertheless, the conclusions are based on a limited number of samples, and expanding the dataset would be essential to validate and generalise these findings. Future work should also focus on optimising grinding strategies to minimise initial surface damage and roughness while maintaining long-term resistance against fatigue.

## 5.3. PRACTICAL RECOMMENDATIONS

### 5.3.1. MAINTENANCE PLANNING AND GRINDING OPTIMIZATION

Based on the findings, several practical implications for rail maintenance can be derived. Variable grinding intervals should be implemented according to MGT-based thresholds, differentiated by track category (UIC class) and curvature, to ensure that interventions are both effective and cost-efficient. Moreover, annual load, combined with environmental exposure, should be incorporated as a key trigger in rail degradation models, as it provides a more reliable predictor of defect evolution than cumulative tonnage. Finally, for a grinding interval of 25 MGT, as is the case for the rails analysed in this study, a standardised grinding depth of 0.25 mm per campaign is recommended to ensure the consistent removal of microcracks while avoiding unnecessary material loss, thereby extending rail service life.

### 5.3.2. ASSET MANAGEMENT AND PROCUREMENT

In terms of material strategy, steel grade selection emerges as a decisive factor in rail longevity. It is recommended to prioritise the deployment of R260 or higher-grade pearlitic steels in high-stress environments, while gradually phasing out R200 rails in curves or high-speed sections where their performance proves insufficient. In addition, further testing of premium steels, such as bainitic or heat-treated grades, under Belgian operating conditions is advised, particularly on high-load freight corridors, to assess their potential benefits in mitigating wear and rolling contact fatigue. Despite the heavy loading of the Belgian

railway network, most rails are replaced due to RCF rather than wear. Increasing rail hardness is therefore not the primary requirement; instead, the priority is to select rail grades in which RCF defects are less likely to develop.

### 5.3.3. DATA AND TECHNOLOGY INTEGRATION

The integration of advanced digital technologies offers further potential for optimising rail maintenance. Leveraging Infrabel's existing monitoring infrastructure, big data analytics and artificial intelligence algorithms can be developed to improve the prediction of wear and rolling contact fatigue, thereby enabling more proactive and cost-effective interventions.

At the same time, and perhaps even more importantly, advancements in measurement systems, particularly those capable of detecting shallow RCF crack depths, are essential to enable timely adaptations in grinding strategies before macrocracks initiate and propagate beyond 0.25 mm, at which point they can no longer be removed preventively under the current Belgian grinding regime. Moreover, such high-resolution measurement data would also enhance the reliability of predictive models.

## 5.4. IMPLICATIONS FOR INFRABEL AND EUROPEAN RAIL NETWORKS

The findings of this dissertation provide significant value for Infrabel and other European infrastructure managers. As regulatory frameworks and traffic demands continue to evolve, maintenance strategies must be adapted to balance the mechanical realities of rail degradation with the financial constraints of infrastructure management. Strategic investment is particularly relevant: with annual expenditures of approximately €55 million (200km of double rails in 2024) in Belgium on rail renewal, extending rail service life through optimised grinding strategies and iormed material selection offers a substantial opportunity for cost savings. Furthermore, the insights into head check growth and wear mechanisms contribute to harmonisation with EU safety directives and UIC maintenance guidelines. Finally, the collaboration between Infrabel and TU Delft exemplifies the potential of joint academic–industry research initiatives to address complex infrastructural challenges in a scientifically rigorous and practically relevant manner.

### 5.4.1. FUTURE RESEARCH DIRECTIONS

Advancing the understanding of rail degradation mechanisms requires an integrated research approach that combines material science, tribology, and systems engineering.

Although the study investigates whether white etching layers are present, the fundamental question regarding their underlying cause remains unresolved. It is a core issue that requires very specialized expertise for further investigation .

Further investigation is needed into the formation and propagation mechanisms of brown etching layers (BELs), with particular emphasis on their relationship to thermomechanical loading conditions and the chemical composition of the steel. In parallel, long-term studies should address the stability of white etching layers following rail grinding operations. A critical aspect is establishing the correct grinding conditions, specifically the appropriate pressures, stone hardness, and grinding speeds for each steel grade, since these parameters can have important implications for the effectiveness of the intervention, namely whether the grinding operation prevents defects or, conversely, generates additional surface damage.

The complex interaction between corrosion, mechanical wear, and fatigue remains insufficiently quantified. Future research should aim to determine the extent to which corrosion contributes to overall rail degradation, especially in low-traffic environments characterised by high humidity and frequent wetting-drying cycles. The development and standardisation of electrochemical and tribocorrosion testing protocols is essential to simulate material degradation under field-representative environmental and mechanical conditions.

The development of multiscale numerical models that couple dynamic loading, contact mechanics, and microstructural degradation processes holds significant potential for predictive maintenance. These models should be capable of capturing both short-term damage evolution and long-term fatigue behaviour. Moreover, the implementation of digital twin frameworks for high-risk track sections would enable real-time monitoring and simulation of degradation scenarios, providing a foundation for condition-based decision-making and risk-informed asset management.

As environmental considerations become increasingly central in infrastructure management, future research should focus on assessing the environmental impact of rail maintenance strategies. This includes evaluating the carbon footprint and material efficiency of grinding intervals, renewal strategies, and different rail steel grades. Integrating lifecycle cost and carbon impact assessments into rail asset management platforms will support the development of sustainable, economically viable maintenance policies aligned with climate targets and resource efficiency goals. Infrabel recovers used rails that are still in relatively good condition, i.e., free of ultrasonic defects and with at least 3 mm of wear margin remaining before reaching the wear limit, despite having exceeded their theoretical service life. These rails are subsequently reinstalled in sidings and, potentially in the future, on low-traffic main lines. Scrap rails are also recycled for the production of new rails, effectively closing the material loop and enabling full reuse in theory. Grinding residues are likewise collected as much as possible and reused in the manufacturing of new grinding stones.

## 5.5. FINAL REFLECTIONS

The interplay between rail wear and rolling contact fatigue represents a multidimensional challenge for modern railway infrastructure. This dissertation has shown that, by combining empirical observation, big-data analytics, and microstructural insights, it is possible to formulate more intelligent and responsive maintenance strategies. These strategies not only reduce long-term costs and enhance safety but also support the transition toward more sustainable, data-informed infrastructure management.

The concept of the Magic Wear Rate stands out as a particularly valuable contribution, bridging the gap between engineering mechanics and practical scheduling. It exemplifies how fundamental research can be translated into operational policy. This dissertation demonstrates that there is no single Magic Wear Rate (MWR); rather, it must be calculated as a function of the annual traffic load. The lower the annual train tonnage, the more artificial wear must be generated per passing ton.

Although the Belgian railway network is subject to high traffic loads, rail replacement is predominantly driven by rolling contact fatigue rather than by wear.

Consequently, enhancing rail hardness alone is not the key objective; greater emphasis should be placed on selecting rail grades with an improved resistance to the initiation and propagation of RCF defects.

Advancements in measurement systems, particularly those capable of detecting shallow RCF crack depths and early-stage defects such as squats, are crucial to enable timely adaptations in grinding strategies before microcracks propagate beyond 0.25 mm, at which point preventive removal is no longer possible. Without such high-resolution monitoring systems, maintenance strategies cannot be fully optimized or condition-based. In addition to guiding grinding interventions, the data obtained from these advanced systems would significantly improve the accuracy and reliability of predictive models, supporting more informed decision-making for rail infrastructure management.

As the Belgian rail network continues to modernize, and as European rail systems contend with growing traffic and budget pressures, the insights offered by this dissertation will remain highly relevant. Sustaining rail assets in the 21st century demands precisely the kind of interdisciplinary, evidence-based approach that this research has sought to embody.

# ACKNOWLEDGMENTS

My Ph.D. journey has been much like baking a layered cake, with each stage adding a distinct ingredient to the mix. Some layers were sweet and rewarding, while others were more challenging or required extra care to perfect. The icing on the cake, the completion of this journey, would not have been possible without the support of many incredible people. I am profoundly grateful for their encouragement, guidance, and inspiration throughout this process. While I hope to thank everyone personally, I apologize if anyone is inadvertently omitted here due to space constraints.

First and foremost, I would like to express my deepest gratitude to my promotor, Prof. Dr. Rolf Dollevoet. Meeting him in Ängelholm, Sweden, in 2008 during the UIC Rail Defects Meeting, and nearly ten years later sharing my interest in working with him, was one of the most significant opportunities of my academic life. My Ph.D. officially began in March 2017, and since then, his guidance, constructive suggestions, and unwavering support have been invaluable.

I would also like to express my sincere appreciation to my promotor, Prof. Dr. Zili Li, whose dedication and expertise have greatly shaped my work. Despite managing numerous projects, his tireless commitment to students and colleagues is truly admirable. They exemplify the high standards of professionalism expected from world-class researchers and have remained a constant source of inspiration throughout this journey.

Next, I would like to extend my heartfelt gratitude to my promotor and daily supervisor, Assoc. Prof. Dr. Alfredo Núñez Vicencio. There were moments during this journey when I questioned my abilities and my suitability for this degree. I can confidently say that this accomplishment would not have been possible without his scientific guidance and personal support. Our frequent discussions, often extending beyond strictly academic topics, revealed his kindness and inspired me to become more supportive and collaborative in return.

I am also sincerely thankful to the members of my doctoral committee : Prof. Dr. Rolf Dollevoet, Prof. Dr. Zili Li, and Assoc. Prof. Dr. Alfredo Núñez Vicencio, Prof. Dr. M . Veljkovic, Prof. Dr. H. Li, Prof. Dr. D.J. Fletcher, Dr. ir. B. Schotsman for dedicating their time and expertise to reviewing my dissertation. Their critical feedback has significantly improved the quality of this work, and their participation in the defense ceremony contributed greatly to its overall success.

I am deeply grateful to Infrabel and to those who made it possible for me to undertake this research, particularly José Agache and Kurt Demeersseman. Their invaluable guidance and support during my early years as a young and inexperienced rail engineer were instrumental in shaping both my professional and personal growth.

I would also like to thank Dr. Pan Zhan and Dr. Li Wang for their collaboration in writing journal papers and for their exceptional assistance throughout the research process. Their hard work and dedication were crucial to the completion of this work.

Finally, my heartfelt gratitude goes to my family and friends. Their unwavering support and encouragement have been essential in helping me reach this significant milestone in my academic journey.

I sincerely hope to continue collaborating with Infrabel and TU Delft in the future, contributing to making railway infrastructure more reliable and cost-efficient in maintenance for the decades to come.

Tim Vernaillen

12 March 2026

Delft, The Netherlands

# CURRICULUM VITAE

## Tim Vernaillen

**Mar. 9, 1981** — **Born in Aalst, Belgium**

### EDUCATION

**Mar. 2017 – Apr. 2026** — **Ph.D. Researcher (0.2 fte)**
Section of Railway Engineering
Delft University of Technology, Delft, The Netherlands

**Sep. 2017 – Sep. 2019** — **Master of Science in Management**
Free University Brussels, Belgium

**Sep. 2003 – June 2005** — **Master of Science in Electrical Engineering**
Free University Brussels, Belgium

**Sep. 1999 – June 2003** — **Master of Science in Industrial Engineering**
Free University Brussels, Belgium

### EMPLOYMENT

**Feb. 2006 – Present** — **1e Engineer, Rail Maintenance & Inspection**
Infrabel, Brussels, Belgium

**Aug. 2005 – Feb. 2006** — **Young Potential, Project New Sorting Centers**
Bpost, Brussels, Belgium

# LIST OF PUBLICATIONS

## JOURNAL PAPERS

1. **T. Vernaillen**, L. Wang, A. Núñez, Z. Li, R. Dollevoet, Rail wear rate on the Belgian railway network – a big-data analysis, Journal Of Rail Transportation 2024, Vol.12, NO.5, 765-780

2. **T. Vernaillen**, P. Zhang, A. Núñez, Z. Li, R. Dollevoet, Statistical analysis and treatment method of head checks on the Belgian railway network, International Journal of Fatigue, Volume 203, February 2026, 109349.

3. **T. Vernaillen**, P. Zhang, A. Núñez, Z. Li, R. Dollevoet, grinding – good or bad for reduction of rolling contact fatigue – observations from in-service rails with white etching layer, International Journal of Fatigue, Volume 209, August 2026, 109620.

## CONFERENCE PAPERS

1. **T. Vernaillen**, P. Zhang, A. Núñez, Z. Li, R. Dollevoet, Evaluating the effect of rail grinding on white etching layer and rolling contact fatigue in the Belgian railway network, in the 13$^{th}$ International Conference on Contact Mechanics and Wear of Rail/Wheel Systems (CM2025), Tokyo, Japan, September 22-26, 2025

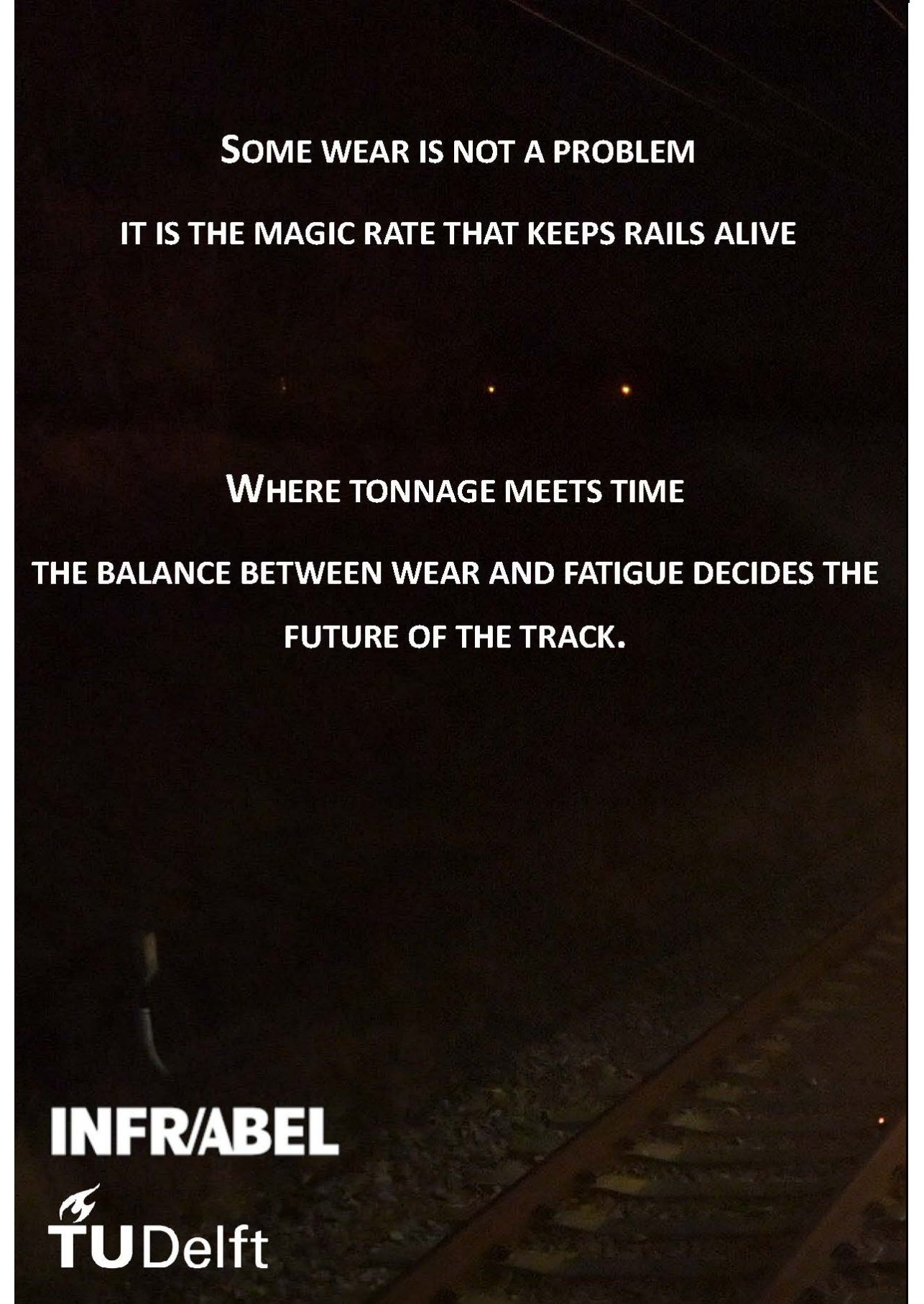
SOME WEAR IS NOT A PROBLEM
IT IS THE MAGIC RATE THAT KEEPS RAILS ALIVE
WHERE TONNAGE MEETS TIME
THE BALANCE BETWEEN WEAR AND FATIGUE DECIDES THE FUTURE OF THE TRACK.
INFRABEL
TU Delft